The expression of miRNA in Oral Lichen Planus

Heba Mousa Ali

BDS, MSc

A thesis submitted in partial fulfilment of requirements for the degree of Doctor of Philosophy

Biosciences Institute and Oral Medicine Department,

School of Dental Sciences

Newcastle University, UK

March 2022

Declaration

I declare that this thesis titled “The role of miRNA in OLP pathogenesis” is my own work that has not been submitted for any degree or examination in university, and that material have been acknowledged and referenced.

Abstract

Oral lichen planus (OLP) is a chronic T-cell-mediated immune disease of unknown aetiology. Micro-RNA (miRNAs) are short non-coding RNAs capable of regulating mRNA that are closely correlated with cytokines in various inflammatory diseases. The aim of this study was to investigate the profile of miRNAs in a cohort of OLP patients and their interaction with potential target genes.

Oral biopsy specimens were taken from a total of 32 patients: 24 patients, 12 females, , with an average age of 57.37 had been diagnosed with OLP whereas 8 patients, 5 females with an average age of 57.55 affected by oral disorders different from OLP causing white patches, were used as the control group. All experimental procedures were approved by the NRES Committee North East - Newcastle & North Tyneside (13/NE/0368) and the enrolled patients gave their informed written consent. Total RNA was extracted from fresh frozen biopsies and the paraffined tissues were used for immunohistochemical studies. The Nano string nCounter Analysis System was used to analyse total RNA samples and the raw data was processed using the nSolver software version 4.0. Nano String expression was confirmed by RT-qPCR analysis. Genes targeting up and down regulated miRNAs were identified using the following four tools: Target Scan human (www.targetscan.org), DIANA (www.diana.imis.athenainnovation.gr/DianaTools), Exiqon (www.exiqon.com/miRSearch) and mirTarBase (www.mirtarbase.mbc.nctu.edu.tw). Predicted target genes were further narrowed down to focus on genes that influence signalling pathways in OLP. RT-qPCR was employed to investigate the expression of target genes in OLP and controls. Non parametric statistical tests were employed to analyse the results. Probability values <0.05 were considered statistically significant.

The results reveal that OLP is mainly a T-cell mediated disease characterized by overexpression of IFN-γ and TNF-α and apoptosis markers. NanoString analysis showed that the following 9 miRNAs were upregulated in OLP tissues: miR-155, miR-146a, miR-3195, miR-342, miR-4516, miR-21, miR-29a, miR-193, and miR-222. Contrarily, the following 9 miRNAs: miR-221, let-7, miR-23b, miR-200b, miR-149, miR-205, miR-23a, miR-27b, miR-95, were downregulated in OLP tissues. Two upregulated, namely miR-4516 and miR-222 and 2 downregulated miRNAs, miR-149, miR-95, were novel discoveries, whilst the remaining miRNAs were confirmation of previous findings. NanoString findings have been confirmed by RT-qPCR results for the following 5

upregulated miRNAs, miR-155, miR-146a, miR-29a, miR-222 and miR-342 and two downregulated miRNAs, namely miR-205 and miR23b.

The expression of three target genes, namely MYC for miR-29a, interleukin-24 (IL-24) and MMP1 for miR-205 was found to have a negative correlation with the respective miRNA. This, suggests that MYC, IL-24 and MMP1 could be regulated by the above miRNAs in OLP.

In conclusion, the work presented in this thesis suggests that miRNAs could be involved in both the immunopathogenesis and malignant transformation of OLP.

Acknowledgement

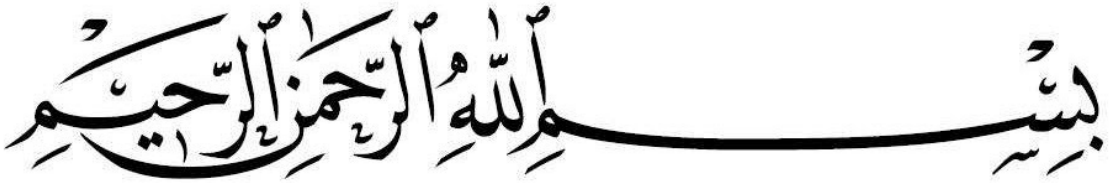

IN THE NAME OF ALLAH AND WITH HIS BLESSING, THE ALL-KNOWING, THE MOST-WISE

First and foremost, I thank God for my health and wellness and I thank God for extending my life so that I could complete my PhD study.

I want to thank my supervisors, Professor Marco Carrozzo and Dr. Andreas Werner, for their unwavering support. Marco and Andi, the conversations we have had, the freedom you have given me, your enthusiasm and encouragement over the last five years have all helped me to reach this point; without you, this project would not have been possible. I could not have asked for anything more and am grateful for your assistance.

I am using this opportunity to express my gratitude to everyone who supported me throughout my work. I would like to acknowledge and thank Dr. Max Robinson, Department of Oral Biology. Faculty of Dentistry Newcastle University for carrying out immunohistochemistry work in Cellular Pathology at the Royal Vitoria Infirmary. I also acknowledge the kind help from Miss Anastasia Resteu, a research assistant in the Human Dendritic Cell Lab for working on Nano String Technology.

I would like to thank Miss Rowen Coulthard, Department of Cellular Pathology, for her essential contribution to the processing, sectioning and immunostaining of human tissue during this project. I am also grateful to Maxine Geggie for giving me the opportunity to work in the cell culture lab at the Institute for Cell and Molecular Bioscience.

This acknowledgement would not be complete without expressing my deepest gratitude to my beloved husband Dr. Mahmoud Aleraig who supported and encouraged me from the first day to the last, for his sustained support when I was experiencing problems with my health. To my lovely kids (Jenan, Abdulrauf, Arwa and Roaa), thank you for your patience and love.

I would also like to convey my gratitude to the soul of my late father, Prof. Mousa M Mousa, for his support and encouragement; I wish he could be with me at this moment. Also, I must thank my wonderful mother, Mrs. Halima Mousa for her love and inspiring me throughout my life, my brothers and sisters for the ongoing moral support that has helped me believe in myself; your encouragement has been a source of inspiration during the tough times.

List of Abbreviations

ΔΔCT	Double Delta Cycle Threshold
ΔCT	Delta Cycle Threshold
µg	Micrograms
µl	Microliters
APCs	Antigen Presenting Cells
BCL2	B-cell lymphoma 2
bp	base pair
CA12	Carbonic anhydrase 12
CCND1	Cyclin D1
CDK6	Cyclin-dependent kinase 6
cGVHD	chronic Graft Versus Host Diseases
DNA	Deoxyribo Nucleic Acid
dNTP	Deoxynucleotide tri phosphate
FFPE	Formalin Fixed Paraffin Embedded
HCV	Hepatitis C
HEK239	Human Embryonic Kidney cell line
HIPK2	Homeodomain-Interacting Protein Kinase 2
HMGA1	High Mobility Group Protein A1
IHC	Immunohistochemistry

IL-24	Interleukin-24
INF-γ	Interferon gamma
INF-λ3 (IL28B)	Interferon Lambda 3 (Interleukin 28b)
LP	Lichen Planus
miRNA	microRNA
ml	Millilitres
MMP1	Matrix metalloproteinase-1
mRNA	messenger Ribonucleic Acid
MYC	Myelocytomatosis
NF-kB	Nuclear Factor kappa- B
ng	Nano grams
NSAIDs	Non Steroid Anti-Inflammatory Drugs
OKF6	Oral Keratinocyte Cell line
OLCLs	Oral Lichenoid Contact Lesions
OLDRs	Oral Lichenoid Drug Reactions
OLP	Oral Lichen Planus
OSSC	Oral Squamous Cell Carcinoma
PBMC	Peripheral Blood Mononuclear Cells
QC	Quality Control
qPCR	quantitative Polymerase Chain Reaction
RNA	Ribonucleic Acid
rpm	Revolutions per minutes

RT-PCR	Reverse Transcription- Polymerase Chain Reaction
STAT3	Signal transducer and activator of transcription 3
Smad4	SMAD Family Member 4
TAB2	TGF-beta activated kinase binding protein 2
TRAF6	TNF Receptor Associated Factor 6
Th	T helper cell
TNF-α	Tumour Necrosis Factor alpha
UTR	Untranslated Region
WHO	World Health Organization
β-actin	beta actin

Table of contents

List of Tables

List of figures

Chapter 1. Literature review

1.1 Introduction

Oral lichen planus (OLP) is a chronic disease that mainly affects the immune system, involving the oral mucosa, that features recurrence and remission. OLP was classified as a potentially cancerous oral ailment by the World Health Organisation in 2005 (Van der Meij and Van der Waal, 2005). Therefore, it is critical to comprehend the causes of and remedies for OLP; in addition, the significance of micro RNAs (mirRNAs) in OLP has drawn growing interest. It is crucial to recognise the function of miRNAs in OLP as a pre-cancer condition since they play a crucial role in cancer.

A number of miRNAs also exhibit altered expression in OLP. Therefore, the function of miRNA as a diagnostic and prognostic biomarker should also not be disregarded due to its participation in the pathogenesis of OLP.

1.2 Oral lichen planus overview

Oral lichen planus (OLP) is considered the oral variant of LP. It is a chronic inflammatory oral mucosal disease frequently, of unknown cause. The clinical management of OLP may pose considerable difficulties to the dermatologist and the oral physician (Lodi et al., 2005a).

In actual fact, OLP can also be potentially malignant cause of morbidity, especially when erosive/ulcerative or erythematous lesions are present (Thongprasom, Prapinjumrune et al. 2013). Mucosal lesions, unlike skin lesions, have a long-term course. The oral lesions have been reported to last for up to 25 years. In adults, the condition affects 1-2 % of the population. It is more common in females and the middle-aged than in males (ratio 1.4:1). However, there have been reports of OLP in children and young adults (Chitturi, Pandian Sindhuja et al., 2015).

1.2.1 Oral Manifestations and diagnosis

Generally, OLP lesions have recognisable and distinctive clinical features and show a characteristic distribution. OLP lesions primarily affect the posterior buccal mucosa, tongue and gingiva, while lesions of the palate are exceptionally rare. Other uncommon

sites of involvement are the floor of the mouth and the upper lip. Interestingly, around 10% of patients with OLP have the disease restricted to the gingiva. The lesions are typically bilateral and may affect several parts of the oral cavity (Eisen, Carrozzo et al. 2005).

Uncommonly, the lesions are restricted to one area in the oral cavity. There are six clinical subtypes of OLP which can occur individually or in combination: papular, reticular, plaque-like, atrophic, erosive/ulcerative and bullous. Classification is determined by the worst presenting form; thus, a patient presenting with reticular and erosive changes would be best classified as having erosive OLP (Carrozzo and Thorpe, 2009). The elemental lesion is a white papule that is a small white patch. Isolated papular lesions are uncommon as papules coalesce and form lines known as Wickham's striae (Carrozzo and Thorpe, 2009).

In 1978, the World Health Organization (WHO) published a set of clinic-pathological diagnostic criteria, which was updated in 2003 (Van der Meij and Van der Waal, 2003). To make an OLP diagnosis, both clinical and histological criteria must be met. The presence of bilateral, more or less symmetrical lesions, as well as a lace-like network of slightly elevated grey-white lines, is required by the modified WHO clinical criteria. In addition, in cases when the lesion is similar to OLP, the term "clinically compatible with" should be used, because the erosive, atrophic, bullous, and plaque-like lesion is only acknowledged as a subtype in the presence of a reticular lesion. The histopathological features of OLP include orthokeratosis or parakeratosis, a band like infiltration confined to the superficial part of the connective tissue, principally of lymphocytes and also the vacuolar degeneration of the basal cell layer of keratinocytes besides the absence of epithelium dysplasia (Van der Meij and Van der Waal 2003)

1.3 Oral lichenoid lesions

Oral lichenoid reactions or lesions (OLLs) are terms used to describe lesions that clinically and histologically resemble OLP but have an identifiable aetiology (Gandolfo, Richiardi et al. 2004). However, several authors suggest the use of these terms in the case of an inconclusive diagnosis of OLP in the presence of the clinical or histological features of the condition. In addition, the OLL term is frequently employed as negative terminology to refute certain hypotheses detailing the premalignant nature of OLP or its aetiologic associations (Gandolfo, Richiardi et al., 2004)

In 2006, during the fourth World Workshop on Oral Medicine, there was an attempt to classify OLLs oral lichenoid lesions in the mouth as OLP, oral lichenoid drug reactions (OLDRs) caused by systemic drug exposure (primarily beta blockers, non-steroidal anti-inflammatory drugs (NSAIDs), allopurinol, anti-malarial, angiotensin-converting enzyme inhibitors), oral lichenoid contact lesions (OLCLs) triggered by a local hypersensitive reaction to dental materials, particularly amalgam and OLLs of graft-versus-host disease (oGVHD) (Al-Hashimi, Schifter et al., 2007). Regrettably, apart from oGVHD, whose clinical features are often sufficient in the diagnosis of OLL–cGVHD together with the history of allogeneic bone marrow transplant, this consensus paper fails to provide reliable clinical and histological criteria to properly differentiate OLLs from OLP.

A recent authoritative paper has introduced a new classification of OLLs that includes OLP, OLCLs, OLDRs, oral lichenoid lesions of graft vs. host disease but also discoid and systemic lupus erythematosus, lichen planus-like variant of paraneoplastic pemphigus/paraneoplastic autoimmune multi-organ syndrome, chronic ulcerative stomatitis, lichen planus pemphigoids, solitary fixed drug eruptions, and lichen sclerosis (Carrozzo, Porter et al. 2019). The same Authors have also suggested diagnostic criteria to help to distinguish between the different OLLs that include clinical, pathological and immunological tests (Carrozzo, Porter et al. 2019).

1.3.1 Genetic Background

Most idiopathic cutaneous LP world-wide is related to the HLA-DR1 (DRB1*0101 allele), whereas in Italy, HCV- related OLP appears to be particularly associated with the HLA class II allele HLA-DR6. Moreover, a significant association was found between erosive OLP and HLA-DR3 allele (Jontell et al., 1987; Carrozzo et al., 2001). A key,

early event in LP is the genetically induced increased production of Th1 cytokines, particularly interferon gamma (IFN-γ) and tumour necrosis factor alpha (TNF-α) (Carrozzo et al., 2004). Cytokine polymorphisms appear to govern whether lesions develop in the mouth in isolation (IFN-γ associated) or in conjunction with skin lesions (TNF-α associated) (Carrozzo et al., 2004). A recent meta-analysis has confirmed the association between the 308 G/A polymorphism in the TNF-α gene and OLP (Jin et al, 2012).

1.4 Aetiology and associations

Oral LP is unlikely to be caused by a single precipitating factor. Studies of T-cell receptor variable region genes from OLP lesion have not revealed the use of a restricted number of different variable region genes (Thomas et al., 1997). OLP is likely to be the common outcome of the influence of a limited combination of extrinsic antigens, altered self-antigens or super antigens. In a minority of patients, precipitating factors have been identified including dental materials, drugs, stress, trauma and infectious agents (Scully, Eisen et al. 2000).

Dental restorative materials thought to cause OLP/OLL include amalgam, composite resin, cobalt and gold (Issa et al., 2004). When OLP lesions are confined to the mucosa in close contact with- or in proximity to the restoration these reactions should be suspected. They are generally, but not invariably, unilateral. Primarily, mercury in amalgams is supposed to trigger a delayed hypersensitivity reaction (Coombs and Gell classification: type IV; (McParland and Warnakulasuriya, 2012)). also, the drugs inducing OLP/OLL are historically reported to be mostly NSAIDs and angiotensin-converting enzyme inhibitors (Robertson and Wray 1992). There is currently no specific test for OLDRs. Although withdrawal and re-introduction of the drug is the most reliable method of diagnosing a drug reaction based on resolution or re-activation of the lesion. However, it is still unclear whether observed psychologic alterations constitute a direct aetiological factor or are just a consequence of OLP. Indeed, the chronic discomfort that can afflict patients with OLP can itself be a stressing factor and may partially explain any documented association (Alrashdan, Cirillo et al., 2016).

Several infectious agents, including Helicobacter pylori and a number of viruses have been implicated in the precipitation of the cell mediated reaction that results in OLP. However, frequently on the basis of equivocal Human herpes viruses (Herpes simplex

virus 1, Epstein–Barr virus, cytomegalovirus, human herpes virus [HHV] -6 and HHV-7), involvement in the pathogenesis of OLP is uncertain and maybe occurs as a secondary infection to oral erosive lichen planus type lesions (Shimoyama, Horie et al., 2000)

The relationship between oral lichen planus, diabetes mellitus (DM) and hypertension was first described by Grinspan in a small group of seven patients in 1966 and named 'Grinspan syndrome'. This association could be simply a result of anti-diabetic and anti-hypertensive medication (Alrashdan, Cirillo et al., 2016).

The best available evidence of the involvement of a virus in the pathogenesis of OLP pathogenesis concerns the hepatotropic hepatitis C virus (HCV). Four meta-analyses have shown that OLP is associated with HCV (Shengyuan et al., 2009; Lodi et al., 2010; Petti et al., 2011; Alaizari, Al-Maweri et al., 2016).

Notably, HCV may also replicate in the oral mucosa (Arrieta, Rodriguez-Iñigo et al. 2000) and (Carrozzo et al., 2002) and may attract specific T cells (Pilli, Penna et al. 2002). In fact, a study confirmed that HCV specific CD4+ and/or CD8+ T lymphocytes can be found in the oral mucosa of patients with chronic hepatitis C and OLP (Pilli, Penna et al. 2002). In addition, CD4+ polyclonal T-cell lines were generated more efficiently from lichen infiltrating lympho-mononuclear cells than from peripheral blood mononuclear cells from the same patients, suggesting a higher frequency of HCV-specific T cells in the oral compartment. Intra lesion HCV-specific T cells were in the majority, CD69+ positive showing the phenotype of recently activated T cells. They were also able to produce IFN-γ but displayed poor expansion capability, all distinctive features of terminally differentiated effector cells. OLP can be caused by direct immune aggression against epithelial cells that carry HCV antigens, or it can be sustained by a cytokine milieu that promotes the initiation and maintenance of autoimmune reactions. (Pilli, Penna et al., 2002).

1.5 OLP malignant potential

Since the first report of the malignant transformation of OLP in 1910, the progression of OLP to oral squamous cell carcinoma (OSCC) has generated a longstanding controversy, and different research groups have proposed distinct approaches and interpretations (Scully and Carrozzo, 2008). Recent meta-analysis reported that a small subset of OLP patients (around 1.1%) develop OSCC (Giuliani, Troiano et al. 2019) and (Aghbari,

Abushouk et al. 2017). Therefore, regular follow-up is recommended for these particular patients, where the epithelial precancerous lesions morphologically changed tissue in which cancer is more likely to form than in its normal mucosae, typically lead to oral squamous cell carcinoma (OSCC). The development of cancer is indicated by the presence of epithelial oral dysplasia (OD) in precancerous lesions. Thus, early detection of such lesions may help to stop the onset of OSCC.

Smokers, alcoholics, and HCV-infected patients had a greater rate of malignant transformation; however, these links need be further investigated (Aghbari, Abushouk et al., 2017). Contrarily, the likelihood of malignant transformation appears to be unaffected by the clinical type of OLP or the application of topical and systemic steroid therapy (Gandolfo, Richiardi et al., 2004).

1.6 Pathogenesis of oral lichen planus

A strong body of evidence suggests that lichen planus (LP) is a T-cell-mediated disease. When autoreactive T-cells were injected into the footpads of syngeneic mice, they produced a histopathological picture indistinguishable from that of LP (Saito, Tamura et al. 1986). Moreover, patients with chronic graft-versus-host disease (cGVHD) may develop cutaneous and oral lesions clinically and histopathologically indistinguishable from those of OLP (Farmer, 1985; Boyd and Neldner, 1991; Treister, Schawinski et al., 2012). The lymphocytic infiltrate in OLP is composed almost exclusively of T-cells. Most lymphocytes in the lamina propria are CD4+ and the majority of T-lymphocytes within the epithelium are activated CD8+ lymphocytes (Matthews, Scully et al. 1984), (Kilpi, Rich et al. 1988) and (Farthing and Cruchley 1989). Conversely, B-cells or plasma cells are scarce in OLP lesions that also contain few and minimal deposits of immunoglobulin or complement. Moreover, only a minor fraction (<2 %) of CD3+ cells in OLP co-expressed the CD94 marker, indicating that they are NK cells (Parolini, Santoro et al., 2007).

In OLP inflammatory infiltrate there is an enrichment of CD45RO memory T cells that predominantly express Th1 cytokines (Walton, Handfield et al., 1998). The absence of eosinophils in OLP inflammatory cell infiltrate indirectly confirms the dominance of the Th1 cytokine pattern. However, recently, it has been suggested that some of the Th1 T-cells in OLP could in reality be Th0 lymphocytes, as they appear to produce Th2-type cytokines, such as IL-4, IL-5 and IL13, together with IFN-γ (Piccinni, Lombardelli et al.

2014). The same study also suggested a possible role for Th17 lymphocytes in erosive OLP. CD4+CD25+ Fork head box protein 3 (Foxp3+) regulatory T cells are possibly also important in OLP (Tao, Cheng et al. 2017) and (Shen, Gao et al., 2014).

The genetically driven enhanced production of Th1 cytokines is a critical early event in OLP (Carrozzo et al., 2004). Another important event in OLP pathogenesis is the migration of distinct subsets of dendritic cells (DCs), such as Langerhans cells, myeloid, and plasmacytoid DCs, perhaps through endothelial cells lining blood arteries expressing the chemotacting agonist chemerin (Parolini, Santoro et al., 2007).

In 2002, Sugerman and colleagues suggested a unifying model of OLP pathogenesis, which was further refined in 2005 (Lodi, Scully et al., 2005). As a result, viral infection (e.g., HCV), systemic medications, contact sensitivity (e.g., amalgam), or an unexplained factor "activate" antigen presentation cells (APCs), which can be either stromal dendritic cells or epidermal Langerhans cells, and basal keratinocytes (Lodi, Scully et al. 2005). CXCR3/CCL20/CCR6 (Ichimura, Casais et al., 2006) is a chemokine secreted by activated APCs and keratinocytes that attract lymphocytes to the growing OLP lesion. IFN-producing plasmacytoid dendritic cells could increase the activating impact of such stimuli (Santoro, Majorana et al., 2005). CD4+ T lymphocytes are presented with antigen linked with MHC class II by activated APCs. CD4+ T lymphocytes are presented with antigen linked with MHC class II by activated APCs. CD81 T cells are presented with antigen linked with MHC class I by activated basal keratinocytes. T helper-1 (Th1) CD4+ T-cell response is promoted by co-stimulatory signals such as CD40 and CD80 co-expression and IL-12 secretion by MHC class II dendritic APCs, as well as binding to CD154, CD28, and IL-12R on the CD4+ T-cell. Th1 CD4+ helper T-cells produce IL-2 and IFN-gamma, which bind to CD8+ T-cell receptors figure 1.1

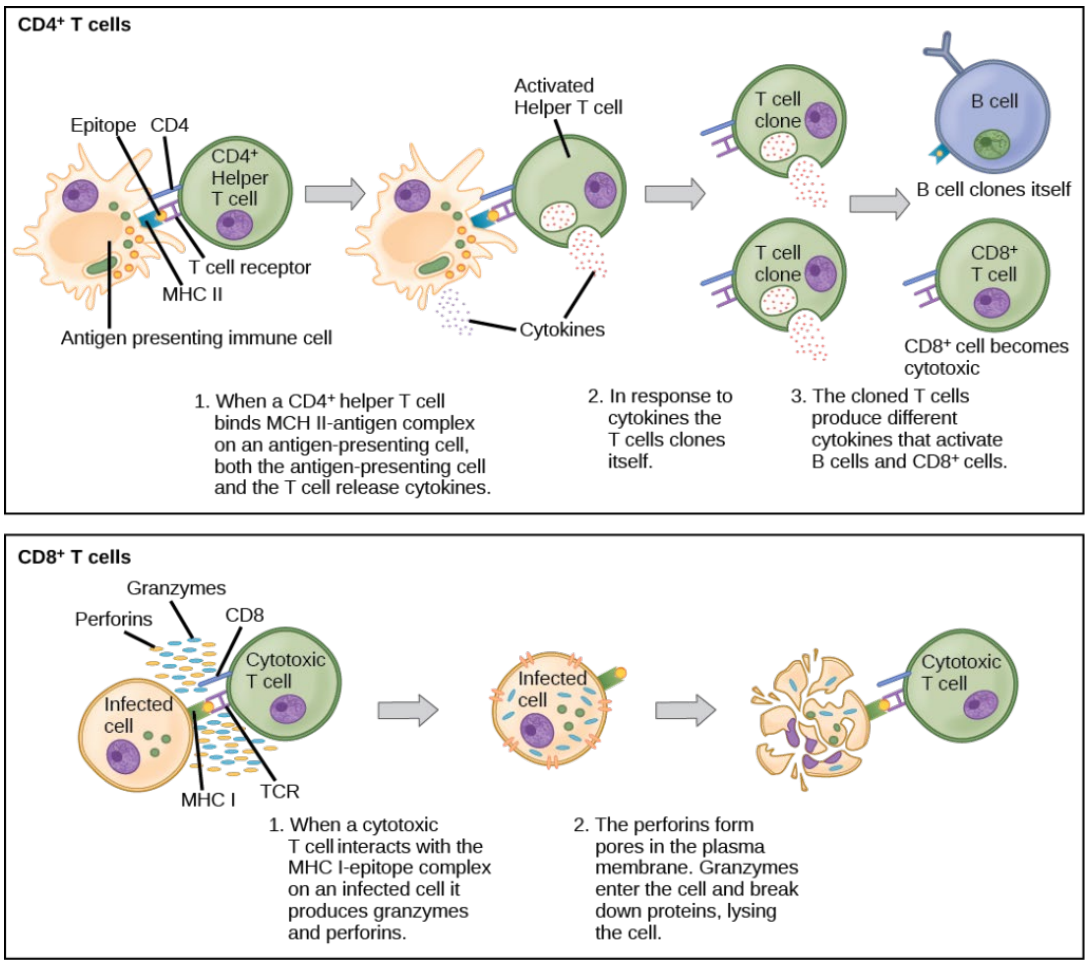

Figure1.1 CD4+ T cells engage MHC II molecules on antigen-presenting cells (APCs) and become activated. Clones of the activated helper T cell, in turn, activate B cells and CD8+ T cells, which become cytotoxic T cells. Cytotoxic T cells kill infected cells. Image available at courses.lumenlearning.com

It's possible that the newly discovered Th0 and/or Th-17 cells are also involved, particularly in erosive OLP. Antigen-specific CD8+ cytotoxic T cells that have been activated produce FASL or release granzyme B or TNF-, which cause basal keratinocyte death. The basal cell layer apoptosis in OLP could be mediated by cytotoxic and pro-apoptotic mediators/stimuli generated by fully activated cytotoxic CD8 T lymphocytes, such as granzyme and perforin FAS ligand. In OLP lesions, the pro-inflammatory environment associated with degranulated mast cells may play a role in assisting T cells in breaching the epidermal basement barrier.

1.7 Essential cytokines involved in OLP

Numerous cytokines are involved in the pathogenesis of OLP including TNF-α, IFN-γ, IL-10, IL-17, and IL-22. TNF-α, the most extensively studied cytokine in OLP, has been

reported to play a key role in the immune regulation of OLP (Pezelj-Ribaric, Prso et al., 2004).The presence of TNF-α exhibited positive relationship to clinical forms of OLP, as it is significantly higher in the erosive/atrophic subgroup than in the reticular subgroup of the disease. In addition, typical features of OLP lesions such as apoptosis of basal epithelial cells and activation of Langerhans cells, have also been reported to be triggered by TNF-α (Sugerman et al., 1996).

IFN-γ is the characteristic cytokine produced by type 1 T-helper (Th1) cells and some studies suggest that certain IFN- gene polymorphisms affect disease susceptibility and progression of OLP (Bai, Lin et al., 2008) and (Carrozzo, Dametto et al. 2004). IL-10 is the principal cytokine produced by Th2 cells and because OLP is a T-cell–mediated disease characterised by Th1/Th2 imbalance, IFN-γ and IL-10 have been extensively studied in patients with OLP.

IFN-γ has been confirmed to be involved in the activation of CD8+ T cells and to maintain the expression of major histocompatibility class II molecules in keratinocytes (Zhou, Chen et al., 2013). Recent studies have revealed that the expression of IFN-γ has also been located in CD4+Th cells in OLP lesions.

The expression levels of IFN-γ are mainly increased in erosive OLP lesions, (Lu, Zhang et al., 2015). IL-10 has important anti-inflammatory functions and several studies investigated the levels or production of IL-10 in peripheral blood in OLP, but the results varied. The reason behind the diversity of IL-10 expression patterns in patients with OLP may be due to different regulatory mechanisms, including effects from other inflammatory mediators and the various genetic tendencies of this disease (Lu, Zhang et al., 2015). Recent studies have also demonstrated altered levels of IL-17 and IL-22 in OLP.

IL-17 triggers the expression of numerous inflammatory mediators to bridge adaptive immunity and innate immunity (Yu, Ruddy et al., 2007). IL-22, in contrast strengthens the epithelial barrier function and balances tissue repair and wound healing (Chen, Feng et al., 2013). In the context of OLP, IL-17 plays a potential role in the local inflammatory environment of lesions where CD4+ T cells (Th17 cells) are also present. Moreover, IL-22 may be involved in the defence against oral microbiota and tissue antigens in OLP. The Table 1.1 shows the summary of expression patterns and gene polymorphisms of cytokines in OLP.

Table 1-1 Summary of expression patterns and gene polymorphism of cytokines in oral lichen planus, (modified from Carrozzo, 2014)

Cytokine	Cell Source	Lesion	Serum	Saliva	Gene Polymorphism
IL-1	Keratinocyte, TIMC	Unclear	Unclear	Increased	No association found
IL-2	TIMC	No difference	Inconsistent	Unclear	No association found
IL-4	TIMC	Inconsistent	Inconsistent	Inconsistent	Higher frequencies of -590 C/C and – 1098 G/G genotypes
IL-5	Unclear	Increased	No difference	Unclear	Unclear
IL-6	T cells, Keratinocyte, TIMC	Increased	Increased	Increased	Higher frequencies of -174 G/G genotype
IL-8	Not detected	Not detected	Increased	Inconsistent	Lower frequencies of -251AA genotype and -251 A/+ 781 C haplotype
IL-10	TIMC	Increased	Inconsistent	Unclear	Higher frequencies of -1082A/-819T/-592A haplotype
IL-12	Epithelial cell	Increased	Unclear	Unclear	No Association found
IL-17	CD4+ T cell	Increased	Inconsistent	Unclear	Unclear
IL-18	Unclear	No difference	Increased	Increased	Higher frequencies of -607 C/C genotype
TGF-β	Sub-epithelial infiltrate	Decreased	Inconsistent	Unclear	No association
IFN-Y	Sub-epithelial infiltrate, CD4+Th1 cell and CD8+Tcell	Increased	Inconsistent	Inconsistent	Higher frequencies of UTR 5644 T/T genotype and +874 T/T genotype
TNF-α	Keratinocytes, mast cells and CD4+Tcell	Increased	Inconsistent	Increased	Higher frequencies of -308 G/A polymorphism

1.8 MicroRNAs overview

MicroRNAs (miRNAs) are 20–22 nucleotide long non-coding RNA molecules that were first discovered in 1993. The main function of miRNAs is the post-transcriptional regulation of complementary messenger RNAs (mRNAs) by binding to their 3′ untranslated region (UTR) through at least 6- to 8-nucleotide-long complementary sequences (Pauley, Cha et al. 2009). miRNAs generally cause gene silencing through

degradation of target mRNAs or inhibition of translation (Makeyev and Maniatis 2008). To date, the miRNA sequence database, miRBase (http://www.mirbase.org/index.shtml), includes over 8000 predicted miRNAs in numerous species in plants, animals and viruses.

In humans, the expression of miRNAs is often tissue specific and developmentally controlled, and in the human genome there are more than 1400 different miRNAs (Bartel 2009) and (Tomankova, Petrek et al. 2012). The importance of miRNA regulation to cellular functions is becoming increasingly clear as new miRNA targets are revealed.

1.8.1 microRNA biological functions

Genetic and molecular studies in mammals have identified the biological functions of several mammalian miRNAs (John, Sander et al. 2006). Currently, miRNAs are known to regulate biological processes, such as cell division, cell differentiation, angiogenesis, migration, apoptosis and oncogenesis (Hwang and Mendell 2006) and (Peláez and Carthew 2012).

The regulation of genes by miRNAs generally involves the modulation of multiple mRNAs by a given miRNA (" multiplicity") and cooperative interactions of multiple miRNAs (" cooperativity") to regulate a given gene (John, Sander et al. 2006). The molecular mechanisms underlining miRNA-mediated gene regulation is still not completely known, but experimentally verified miRNA target sites indicate that the 5′ end of the miRNA tends to have more bases complementary to the target than its 3′ end (John, Sander et al. 2006). The 5′-end of the microRNA (the so- called 'seed region') is most important for the binding to the mRNA targets. The target sites can be further divided into three main classes, according to degree and localisation of the complementarity (Stark, Brennecke et al. 2005) the dominant seed site targets (5′ seed-only), the 5′ dominant canonical seed site targets (5′ dominant) and the 3′ complementary seed site targets (3′ canonical).

1.8.2 Prediction of microRNA targets

Whereas in plants miRNA and target mRNA are often nearly perfectly complementary, animal miRNAs are generally not completely complementary to their targets (Stark, Brennecke et al. 2005). As a result of this very short complementarity to the target mRNA in humans, a particular miRNA can have hundreds of target genes and it has been suggested that as much as one-third of all mRNAs in human may be regulated by miRNAs (Farh, Grimson et al. 2005)

To overcome the above described limitations in identifying specific targets for miRNAs, several computational or bioinformatics methods were developed to predict animal miRNA target sites (Lindow 2011). Several algorithms have been developed to include a set of features known to modulate the interaction between miRNA and their cognate mRNA in addition to the essential Watson-Crick pairings (Peterson, Thompson et al. 2014).

This resulted in the creation of more than 187 target prediction tools all of which have their strengths and weaknesses (Quillet, Saad et al. 2020).

However, most target prediction methods provide hundreds of possible targets for a single miRNA and their accuracy and sensitivity is generally poor as revealed by experimental data (Quillet, Saad et al. 2020). Because no single method consistently outperforms others, it is usually accepted that databases content combination is an efficient way to improve prediction relevance. Moreover, the application of external biological knowledge can lead to a more refined and testable list of targets (Lindow 2011).

1.8.3 microRNAs involvement in cancer

Normal cells undergo genetic modifications that cause them to progress from pre-malignant states (initiation) into invasive cancer (progression), which has the potential to spread throughout the body (metastasis). The resulting altered cellular phenotype has a number of distinctive features that allow cells to multiply excessively and on their own. For example, cancer cells are able to multiply without the aid of growth signals, are unresponsive to signals that would normally inhibit growth, avoid intrinsic cell replication limits, induce and maintain angiogenesis, and form new colonies that are unrelated to the original tumor. (Matson, House et al. 2019)

Cancer development and progression are linked to the deregulation of genes involved in cell proliferation, differentiation, and/or death. Oncogenes and tumor suppressors are terms used to describe genes associated with the development of cancer. Based on their function, oncogene products can be divided into six groups: signal transducers, chromatin remodelers, apoptotic regulators, transcription factors, growth factors, and growth factor receptors(Liu 1990). When these gene products are overexpressed, they offer selective growth benefits that may promote the growth of tumors. Oncogenes can be made more active by genetic changes that either amplify the gene, change the promoters or enhancers

to increase gene expression, or change the structure of a protein to make it permanently active. (Hartl and Bister 2013)

Changes in genomic miRNA copy numbers and gene positions are frequently implicated as the cause of abnormal miRNA expression in malignant cells relative to normal cells (amplification, deletion or translocation). The loss of the miR-15a/16-1 cluster gene at chromosome 13q14, which is frequently seen in people with B-cell chronic lymphocytic leukaemia, is the earliest identification of a miRNA gene position alteration (Lovat, Fassan et al. 2018). In contrast, miR-17-92 cluster gene amplification was seen in B-cell lymphomas, lung cancers, and T-cell acute lymphoblastic leukemia, leading to overexpression of these miRNAs in these cancers. Lung cancer frequently has deletions of the 5q33 region harbouring miR-143 and miR-145, which results in decreased expression of both miRNAs (Dwivedi, Purohit et al. 2019).

(Aradhya and Cherry 2007) revealed that high-resolution array-based comparative genomic hybridization on 227 specimens from human ovarian cancer, breast cancer, and melanoma confirmed the high frequency of genomic changes in miRNA loci. Additional genome-wide analyses showed that many miRNA genes are situated in genomic areas linked to cancer. A minimal zone of loss of heterozygosity, which may contain tumor suppressor genes, a minimal region of amplification, which may contain oncogenes, fragile sites, or common breakpoint regions are some examples of these regions. Overall, these results imply that particular genomic areas enclosing miRNA genes may be amplified or deleted, leading to aberrant miRNA expression in malignant cells. (Zhu, Skogerbø et al. 2012).

(Hanahan and Weinberg 2011) According to Hanahan and Weinberg, six biological abilities acquired during tumors development, including maintaining proliferative signaling, evading growth suppressors, resisting cell death, enabling replicative immortality, activating invasion and metastasis, and inducing angiogenesis, are the hallmarks of human cancer. It is thought that the dysregulated miRNAs could disrupt one or more of the cancer hallmarks for tumors initiation and development because malignancies have aberrant miRNA expression. Mirna may occasionally act as an oncogene or a tumors suppressor, depending on the genes they target.

The most significant characteristic of cancer is cell proliferation, and aberrant cell proliferation is the main factor in carcinogenesis. In order to achieve a balance between encouraging and restraining cell proliferation, the progression of the cell cycle is

specifically regulated by internal programmers and external signal molecules. When cell growth or division is out of control, cells might develop cancer (Feitelson, Arzumanyan et al. 2015). After years of research, it has become clear that some miRNAs functionally integrate into numerous important cell proliferation pathways, and that dysregulation of these miRNAs is what allows cancer cells to evade growth inhibitors and maintain proliferative signaling (Peng and Croce 2016).

Another important indicator of tumors growth that is thought to be controlled by miRNAs is the evasion of apoptosis. 81,82 Tumor cells use a variety of mechanisms to prevent or delay apoptosis. The most frequent one of these is the loss of p53 tumors suppressor activity. Upregulating anti-apoptotic regulators, suppressing pro-apoptotic factors, and inhibiting the death pathway brought on by extrinsic ligands are some alternate methods of avoiding apoptosis. MiRNAs have a broad inhibitory or activating effect on anti-apoptotic factors (Portt, Norman et al. 2011).

Shenouda and Alahari (2009) revealed that under specific conditions, miRNA can act as an oncogene or a tumour suppressor. Despite the fact that miRNAs have numerous targets, their role in carcinogenesis may be attributable to the regulation of a few particular targets. Finding the crucial miRNA targets involved in cancer and determining their role in malignant transformation will therefore be a future challenge.

Notably, it has been shown that 50% of miRNA genes may be located in cancer-associated genomic regions or in fragile sites (Smolarz, Durczyński et al. 2022). Altered expression of individual miRNAs has been shown in numerous cancers, including head and neck squamous cell carcinoma (HNSCC), which may indicate the oncogenic or suppressor potential of miRNAs (Smolarz, Durczyński et al. 2022). miRNA expression in HNSCC cancer has been investigated using microarray analysis, qRT-PCR methods, and RNA sequencing (Vahabi, Blandino et al. 2021). One of the most commonly deregulated miRNA in HNSCC, is miR-21, that regulates the expression of numerous target genes such as phosphatase and tensin homolog (PTEN) and programmed cell death protein 4(PDCD4) and these findings support the role of miR-21 as an oncomiR (Liu, Zhang et al. 2017). TP53 tumour suppressor gene is the most frequently genetic alteration (about 70–80%) found in HNSCC (Vahabi, Blandino et al. 2021). though, the overexpression of two miRNAs, namely miR-96-5p and miR-205-5p, have been involved in the expression of mutant p53 proteins (Vahabi, Pulito et al. 2019) and (Valenti, Deiana et al. 2019).

In contrast, some other miRNAs, as for example Let-7 family and miR-145 are downregulated in HNSCC and work as tumour suppressing genes by targeting oncogenes (Johnson, Grosshans et al. 2005) and (Gao, Zhang et al. 2019).

1.8.4 microRNAs regulation of inflammation

More recently, miRNAs have been recognised as important players in normal immune function and inflammation. miRNAs are involved in the control of both innate and adaptive immunity (Rebane and Akdis 2013). For example, the central pathway in innate immunity is the nuclear factor κB (NF- κB) pathway and miR-146a is a NF- κB dependent miRNA (Taganov, Boldin et al. 2006). Another miRNA, miR-155 strongly influences macrophages and dendritic cell functions (O'Connell, Taganov et al. 2007).

Interestingly, miRNA is also involved in the development and function of mainly T lymphocytes in adaptive immunity. Both miR-181 and miR-150 are important for early T cell development (Mehta and Baltimore 2016). Conversely, miR-146a deficient mice develop spontaneous autoimmunity (Boldin, Taganov et al. 2011) whilst miR-155 has been reported to inhibit IFN-γ signalling in CD4+ T cells (Hu, Zhang et al. 2015). However, over-expression of miR-155 in activated CD4+ T cells promoted Th1 differentiation (Hu, Zhang et al. 2015). On the other hand, the absence of miR-155 of T cells allows the activated CD4 + T cells to exhibit a Th2 bias in vitro (Ji, Wrzesinski et al. 2015). Further to Th1 cells , miR-155 positively regulated the secretion of IL-17A by Th17 cells (Yao, Ma et al. 2012). miR-29 also regulates Th1 differentiation by targeting transcription factors and cytokines such as IFN-γ ((Wissink, Smith et al. 2015). miR-17-92 plays critical roles in the immune tolerance mechanism and the overexpression of these miRNA clusters results in lymphoproliferative disease and autoimmunity (Lai and Xiao 2015) and (Simpson and Ansel 2015).

1.8.5 Cytokine targeting by miRNAs

Recent studies have suggested possible roles for miRNA regulation in a number of T cell-related autoimmune diseases, including systemic lupus erythematosus (SLE), rheumatoid arthritis (RA), multiple sclerosis (MS), inflammatory bowel disease (IBD), Sjogren's syndrome(SS), and Type-I diabetes mellitus (T1MD) (Esmailzadeh, Mansoori et al. 2017).

The four primary ways that miRNAs control cytokine levels are listed in figure 1.2. It is possible for regulation to be "direct"—affecting the target cytokine—or "indirect," where

a specific miRNA post-transcriptionally controls the expression of a protein, which in turn affects the cytokine's level. Targeting of cytokine mRNA, which results in decreased cytokine levels, and stimulation of TLR7/8, which results in increased cytokine levels, are both examples of "direct" regulation. If one miRNA targets a cytokine activator, "indirect" regulation predicts that the level of the cytokine will drop. In contrast, cytokine levels rise when a repressor is targeted (Salvi, Gianello et al. 2019). The level of the studied miRNA in the particular disease also influences the final result in terms of cytokine production (increased or decreased in respect to healthy individuals). The terms "repressor" and "activator" are used with a more general definition, and depending on the cytokine under investigation, a single protein may be regarded either a repressor or an activator.

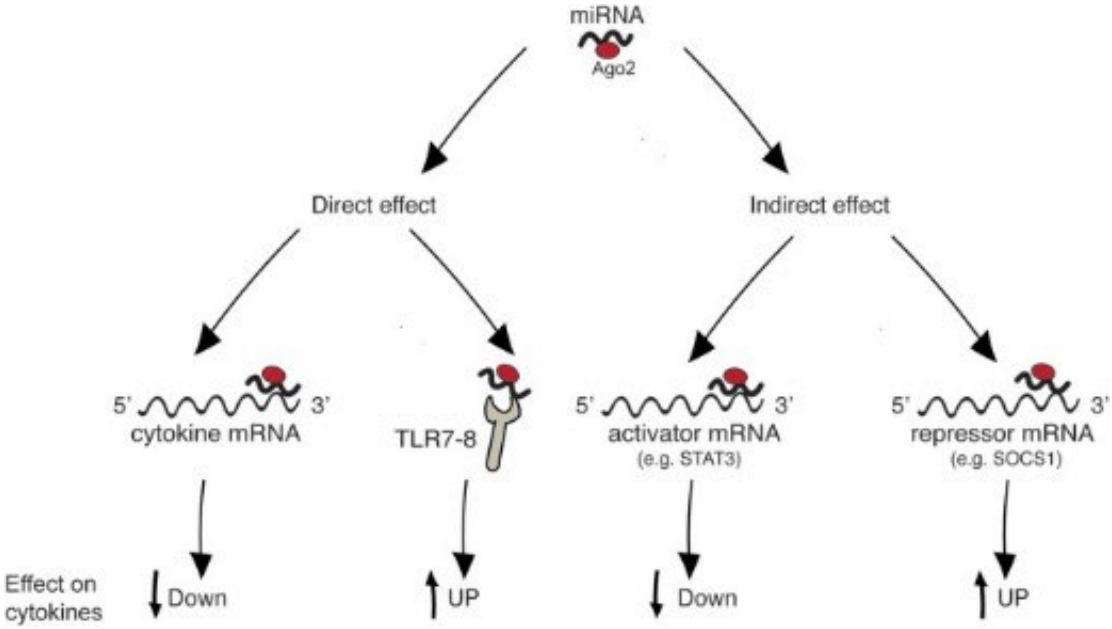

Figure 1.2 Mechanisms by which miRNAs regulate cytokines. Targeting of cytokine mRNA and activation of innate immune receptors that produce cytokines are examples of "direct" regulation. Targeting molecules that function as inducers or inhibitors of a particular cytokine is referred to as "indirect" regulation. Image from Salvi et al. (Salvi, Gianello et al. 2019).

1.8.5..1 The primary pro-inflammatory cytokines TNF-, IL-1, and IL-6

Lately, compelling evidence has revealed that the nuclear Factor-B (NF-B) signalling pathway contributes significantly to the development of various cancers, including head and neck cancer, breast cancer, hepatocellular carcinoma, gastric cancer, and others (Papoutsopoulou and Campbell 2021). A growing body of research suggests that patients with oral premalignant lesions have higher amounts of NF-B-dependent cytokines in both saliva and tissue samples. Moreover, several cytokines can be used as diagnostic tests to

find precancerous and cancerous tumours and diseases in the mouth. Patients with oral cancer had significantly higher levels of interleukin (IL-6).

It has become clear that many cytokines, the most prevalent of which are tumour necrosis factor alpha (TNF-), IL-1, IL-6, and IL-8 (Jang, Lee et al. 2021) are expressed by malignant cells. Studies on the functions of TNF-, IL-6, and IL-8 in oral precancerous and cancer are scarce (Balkwill 2009). The local and systemic character of these responses raises the possibility that precancers and malignancies release cytokines with proinflammatory and proangiogenic activity, which may play a role in the pathogenesis of oral malignancy. In this investigation, we anticipated that oral precancerous lesions and circumstances could result in higher salivary and serum TNF-, IL-6, and IL-8 levels. This study used serum and saliva samples to examine the levels of TNF-, IL-6, and IL-8 in oral precancerous in an effort to test this concept (Ghalwash 2020).

Fekete et al. have shown that human primary plasmacytoid dendritic cells (pDCs) activated with exosomes obtained from plasma of SLE patients generate TNF- and IL-6 (Fekete, Sütö et al. 2018). This result is dependent on exosome-associated miRNAs activating TLR7. The team discovered that a number of miRNAs abundant in guanosine and uridine can act as mediators for TLR7 triggering. This is consistent with recent structural investigations showing that TLR7 functions as a dual sensor for ssRNAs containing guanosine and uridine by binding with RNA breakdown products rather than detecting particular RNA sequences. Comparing RA patients with healthy controls, miR-155 levels were shown to be higher in peripheral blood mononuclear cells (PBMCs) (Kolarz, Ciesla et al. 2020). peripheral blood monocytes, and synovial macrophages and monocytes Increased miR-155 may target Suppressor of cytokine signalling 1 (SOCS1), which may enhance the expression of pro-inflammatory cytokines (Hart, Ahern et al. 1993).

Two more miRNAs, miR-140 and miR-22, which were also down-regulated in synovial tissue samples from RA patients, were also found to increase the production of IL-6. When miR-140 was involved, a large increase in TLR4, its direct target, caused IL-6 overexpression (Dang, Zhao et al. 2015).

Lin et al. discovered that Cyr61, a secreted extracellular matrix protein that encourages synoviocyte proliferation with fibroblastic characteristics, and miR-22 expression did not correlate favourably (Lin, Huo et al. 2014). As a result, there was an increase in IL-6 production and Th17 differentiation.

Persistent and excessive cytokine production is a hallmark of autoimmune diseases and may play a role in disease pathogenesis and amplification. Increased knowledge about the key role of deregulated cytokine production in autoimmunity allow the development of drugs called biologicals that target specific cytokine productions leading to major successes in the treatment of diseases such as, for example, RA and psoriasis (Salvi, Gianello et al. 2019). Substantial evidence suggest that altered miRNA levels observed in most autoimmune diseases impact the production of pathogenic cytokines. In table 1.2, we have summarized the main interactions between miRNAs and primary pro-inflammatory cytokines.

As OLP is a T-cell mediated localized autoimmune disorder characterized by altered expression of cytokine such as IL-10, IL-17, IFN-γ, TNF-α, TGF-β and IL-6 (Carrozzo, 2014) there is a substantial possibility that miRNAs may be involved in the pathogenesis of OLP.

Table 1-2 Summary of some regulations of cytokine productions by miRNAs

Cytokine	MiRNA	Action	Reference
IL-10	let-7e	Upregulation of let-7e directly decreases IL-10	(Guan, Fan et al. 2013)
	miR-233	Increased levels of miR-223 areimplicated in decreased production of IL-10	(Lu, Yu et al. 2014)
	miR-21	Silencing of miR-21 decreased IL-10 production by T cells	(Stagakis, Bertsias et al. 2011)
IL-6	miR-146	Lack of miR-146 leads to excessive production of IL-6	(Chen et al, 2018)
	let-7b	Overexpression of Let-7b is capable of inducing IL-6	(Kim et al, 2016)
TGF-β	miR-210	Increased expression of miR-210 enhance production of TGF-β	Wu et al, 2018
IL-17	miR-155	Inhibition of miR-155 reduces production of IL-17	(Zhang, Wang et al. 2017)
	miR-21	Lack of miR-21 reduces production of IL-17	(Murugaiyan, Da Cunha et al. 2015)
	miR-146	Absence of miR-146 can increase IL-17 production	(Li et al, 2017)

	miR-132 and miR-26°	Upregulation of miR-132 and miR26a is to increased expression of IL-17	(Abou-Zeid and Ben-Akiva 2011)
TNF-α	miR-146	Lack of miR-146 leads to excessive production of TNF-α	(Chen et al, 2018)
	let-7b	Overexpression of Let-7b is capable of inducing TNF-α	(Kim et al, 2016)
	let-7a and let-7e	Upregulation of let-7a and let-7e increases the production of TNF-α	(Liu et al, 2015)
	miR-132 and miR-26a	Upregulation of miR-132 and miR26a is to increased expression of TNF-α	(Abou-Zeid and Ben-Akiva 2011)
IFN-ϒ	miR-210	Increased expression of miR-210 enhance production of IFN-ϒ	Wu et al, 2018
	miR-29	miR-29 suppressed IFN-γ production	Ma et al, 2011

1.9 OLP relation with MicroRNAS

MicroRNAs (miRNAs) have been recognised as novel players in normal immune function and inflammation. For example, miR-29 has been identified to regulate innate and adaptive immune responses to intracellular bacterial infection. Likewise, miR-155 has been reported to inhibit IFN-γ signalling in CD4+ T cells (Ma, Xu et al., 2011) miRNAs are known to regulate the expression of inflammation-related cytokines. Therefore, miRNA–mRNA–cytokine regulation pathways may be associated with the pathologic features of OLP (Arão, Guimarães et al., 2012). Even though, in depth studies of miRNAs in OLP are scarce, studies of patients with OLP revealed that both miR146a and miR-155 are de-regulated in PBMCs and oral lesions. Consequently, microRNA–messenger RNA (miRNA–mRNA) networks have been proposed to be involved in the development of OLP (Gassling, Hampe et al., 2013).

As the function of specific miRNAs is to regulate the expression of inflammation-related cytokines, miRNA-mRNA-cytokine pathways may impact on the pathological features

of OLP. Accordingly, various cytokines involved in OLP, for instance IL-10, IL-17, IFN-γ, IL-22, and TNF-α, TGF-β and IL-6 are possibly regulated by miRNAs (Carrozzo, Dametto et al., 2007). For example, miR-155 exhibits a stimulatory effect on Natural killer NK cell proliferation, development and effector functions. Moreover, miRNA-155 promotes the production of IFN- γ in natural killer NK cells (Tao, Ai et al., 2019). Likewise, miR-146a stimulates T helper 1 cells but not T helper 2 cells. These findings indicate that miR-146a could have role in the differentiation of simple T cells into Th1 effector cells. Furthermore, miRNA-146a decreases IFN-γ mediated activation of regulatory T cells.

1.10 Previous studies of miRNAs in OLP

A literature searches on microRNA (miRNA) expression in oral lichen planus (OLP) was performed in PubMed-Medline and Scopus databases using the following MESH terms: ("microRNAs" [Mesh] and ("oral lichen planus" [Mesh]) or ("oral lichenoid" [Mesh]). Studies in which OLP/OLL diagnosis that were not made according to clinical-pathological assessment as defined by Carrozzo et al. (2019), were excluded as well as duplicated studies. To summarise the results, miRNA expression analysed by microarray and RNA sequencing (RNA-Seq) and by real-time polymerase chain reaction (RTq-PCR) were separately considered, as shown in Tables 3.1 and 3.2. Seven studies (Zhang, Liu et al., 2012; Gassling, Hampe et al., 2013; Shi, Yang et al., 2015; Chen, Du et al., 2017; Ahmadi-Motamayel1 et al., 2017; Wang et al., 2019; Di Stasio et al., 2019) reported abnormal mRNAs expression in OLP by microarray/RNA-Seq (Table 1.3). Most of the studies investigated miRNA expression in lesion tissues but saliva and peripheral mononuclear blood cells (PBMC) were also used as a source of samples. Whilst for other systemic immunological-mediated diseases for example systemic lupus (SLE) or graft-versus-host disease, PBMC could represent a sound source of material, in a localised auto-immune condition such as OLP, the use of PBMC and even saliva remains controversial when it comes to investigating the pathogenesis of the disorder.

The majority of studies used healthy patients as controls and sample size ranged from 3 to 40 OLP patients. Overall, 125 miRNAs were abnormally expressed in OLP: 65 miRNAs were upregulated and 55 downregulated (appendix). Five miRNAs (miR-455-5 p, miR-375, miR-923, miR-210 and miR-203) were determined to be both up-and down-regulated in different studies (Table 1.3). Only six miRNAs (miR-423-3p, miR-203 a-3p, miR-155, miR-133, Let-7i and miR-21-5p) were found upregulated in different studies,

whereas 3 miRNAs (miR-204, miR-205 and miR-199 a-5p) have been shown to be downregulated in more than one study (Table 1.3). Sporadically, qPCR or other techniques jointly confirmed microarray/RNA-Seq findings (Table 1.4). Moreover, validation of the miRNAs results within a second independent population was seldom performed. Upregulation of 7 miRNAs (miR-203, miR-142-3p, miR-146a, miR-155, miR-21, miR-31 and miR-206) with microarray/RNA Seq was confirmed by qPCR studies, whilst only one miRNA, namely miR-200a and -b, was recognised as downregulated. One study employed NanoString technology to assess miRNA expression in 8 patients with OLP and 17 with oral squamous cell carcinoma (OSCC). Nevertheless, it did not detail the results of OLP compared to healthy controls but just with OSCC, showing down regulation of miR-146a, miR-US-2, mirR-223 and miR-29a (Momen-Heravi, Trachtenberg et al., 2014).

Table 1-3: Summary of abnormal miRNAs expression in OLP analysed by microarray/RNA-seq

MiRNA	Upregulated	Downregulated
miR-146a	(Chen, Du et al., 2017) (Ahmadi-Motamayel1 et al., 2017)	
miR-155	(Chen, Du et al., 2017) (Ahmadi-Motamayel1 et al., 2017) (Wang et al., 2019) (Gassling, Hampe et al., 2013)	
miR-205	(Shi, Yang et al. 2015)	(Chen, Du et al., 2017) (Gassling, Hampe et al., 2013)
miR-133	(Chen, Du et al., 2017 Wang et al., 2019)	
miR-21	(Shi, Yang et al. 2015) (Di Stasio et al., 2019)	

miR-135	(Chen, Du et al., 2017) (Shi, Yang et al. 2015)	
miR-210	(Shi, Yang et al. 2015)	(Zhang, Liu et al., 2012)
miR-199		(Chen, Du et al., 2017 Wang et al., 2019)
miR-30b		(Gassling, Hampe et al., 2013) (Shi, Yang et al. 2015)
Let-7i	(Chen, Du et al., 2017) (Gassling, Hampe et al., 2013)	
miR-204	(Chen, Du et al., 2017)	(Zhang, Liu et al., 2012)
miR-923	(Zhang, Liu et al., 2012)	(Gassling, Hampe et al., 2013)
miR-27a	(Chen, Du et al., 2017)	(Zhang, Liu et al., 2012)

Table 1-4 Summary of abnormal miRNAs tested by qPCR in OLP patients

MiRNAs	qRT-PCR results	Sources	Country	Reference
miR-7	Increased	Tissue	India	(Chattopadhyay et al., 2016)
miR-203	Increased	Tissue	Sweden	(Danielsson, Ebrahimi et al. 2012)
miR-142-3p	Increased	Tissue	China	(Meng et al., 2021)
miR-146a	Increased	Tissue, PBMC PBMC Tissue	Brazil China China	(Arão, Guimarães et al., 2012) (Wang et al., 2018) (Wang et al., 2016)
miR-155	Increased	Tissue; PBMC PBMC	Brazil	(Arão, Guimarães et al., 2012) (Hu et al., 2015)
miR-1290	Increased	Saliva	South Korea	(Byun, Hong et al., 2015)
miR-4484	Increased	Saliva	South Korea	(Byun, Hong et al., 2015)
miR-1246	Increased	Saliva	South Korea	(Byun, Hong et al., 2015)
miR-21	Increased	Tissue Saliva	Sweden	(Danielsson, Ebrahimi et al., 2012) (Uma Maheswari et al., 2020)
miR-31	Increased	Saliva	India	(Uma Maheswari et al., 2020)

		Tissue	India	(Chattopadhyay et al., 2016)
miR-204	Increased	Tissue	India	(Chattopadhyay et al., 2016)
miR-206	Increased	Tissue	India	(Chattopadhyay et al., 2016)
miR-1293	Increased	Tissue	India	(Chattopadhyay et al., 2016)
miR-200a,b	Decreased	Tissue	China	(Zhang, Liu et al., 2012)
miR-214	Decreased	Tissue	China	(Zeng and Li., 2018)
miR-216 a	Decreased	Tissue	China	(Zeng and Li., 2018)
miR-216 b	Decreased	Tissue	China	(Zeng and Li., 2018)
miR-375	Decreased	Tissue	China	(Shi, Yang et al., 2015)
miR-138	Decreased	Tissue	Egypt	(Ghallab et al., 2017)
miR-27b	Decreased	Tissue Tissue, Saliva	China Egypt	(Zhang, Liu et al., 2012) (Aghbari et al., 2018)
miR-635	Decreased	Tissue	China	(Shen et al., 2016)
miR-578	Decreased	Tissue	China	(Shen et al., 2016)

Hypothesis

This study will test the hypotheses that:

1. miRNAs may be abnormally regulated in UK patients with OLP.

2. miRNAs may be involved in the immunopathogenesis of OLP.

1.11 Aims of the project

(i) To conduct a literature search to compile a list of cytokines that are expressed in oral mucosa and are linked to OLP and may potentially be influenced by miRNAs.

(ii) To determine the expression patterns for the established list of cytokines in human immortalized oral keratinocyte cell line (OKF6). For these analyses, quantitative Real Time-PCR (qRT-PCR) will be used

(iii) To investigate miRNAs profile in OLP patients and controls with other diseases causing oral white patches. Genomic-wide analysis of miRNAs will be performed using multiplexed NanoString nCounter miRNA expression assay (NanoString Technologies, Seattle, WA, USA.

(iv) To confirm the NanoString findings, differentially expressed miRNAs expression will be assessed using qRT-PCR.

(v) To conduct a bioinformatics search of potential targets for the confirmed differentially expressed miRNAs and assess the potential link with miRNAs using qRT-PCR

(vi) To investigate with immunohistochemistry (IHC) the expression of relevant cytokines and potential target genes of miRNAs in OLP and controls tissue

Chapter 2. NanoString miRNA analysis

2.1 Introduction

The NanoString technology permits digital examination of multiple genetic materials either RNA or DNA in a single tube (Wallden, Storhoff et al., 2015). NanoString nCounter technology detects target molecules using colour-coded molecular barcodes, providing a digital count of the number of target molecules. This is achieved by allocating fluorescently categorised probes to genes of interest. Probes that have bound to a molecule of interest can be counted by a computerised optical lens. The barcodes consist of a chain of 7 fluorescent tags coupled to a biotin-containing oligonucleotide complementary to a 100bp region of the 3' end of a gene of interest. The coloured tags act as barcodes and indicate which gene the complementary oligonucleotide refers to

NanoString technology can provide digital statistics of comparative gene expression from hundreds of cDNA, mRNA and miRNA fragments from extracted nucleic acids, whole cell lysate and Formalin-Fixed Paraffin-Embedded (FFPE) material. Significantly, the methodology does not require any enzymatic reactions that may introduce error in the results (Waggott, Chu et al., 2012)

The benefits of using the Nano String nCounter Platform is the capability to measure up to 800 genes in one single reaction, with fully computerised and digital mode to detect and evaluate samples, without need for amplification or polymerase step and great flexibility of sample input Moreover, for a future classification of cancer patients and therapeutic response prediction using NanoString-based cancer expression panels are anticipated to play more significant roles in improving individualised therapeutic care. However, since the Nano String uses about 800 preselected genes that were chosen based on published data, it is not appropriate for biomarker discovery. It is an exclusive platform with little flexibility. Other disadvantages are, the requirement for more input nucleic acids than some other methods and the inability to detect novel gene fusion variants.

2.2 The nCounter NanoString technology:

The NanoString nCounter Assay System allows the quantification of hundreds of genes in a single reaction without amplification and a high degree of flexibility in sample input (Kulkarni, 2011). The fact that the process is fully automated and the detection and analysis is digitalised minimises user error, increasing reproducibility and sensitivity (Geiss, Bumgarner et al., 2008). The nCounter system has demonstrated that it is more sensitive than microarrays and similar in sensitivity to real-time PCR (Geiss, Bumgarner et al., 2008).

Each target gene is detected using a pair of reporter and capture probes carrying 35- to 50-base target-specific sequences. The capture probe (Figure 2.1), contains a sequence complementary to a particular target gene plus a short common sequence coupled to an affinity tag such as biotin. The reporter probe (Figure 2.1) contains a second sequence complementary to the same target gene but coupled to a colour-coded label that provides a detection signal. All probes are mixed together in a single hybridisation reaction that precedes in solution.

Hybridisation produces three-component structures, each comprised of a target gene bound to its specific reporter and capture probes. Excess probes are then removed and the probe/target complexes are aligned and immobilised in the n Counter cartridge, which is subsequently placed in a digital analyser for imaging and data processing (Figure 2.1). Each target molecule of interest is identified by the colour code generated by the ordered fluorescent segments present on the reporter probe. The expression level of a gene is measured by counting the number of times the colour-coded barcode for that gene is detected (Geiss, Bumgarner et al., 2008).

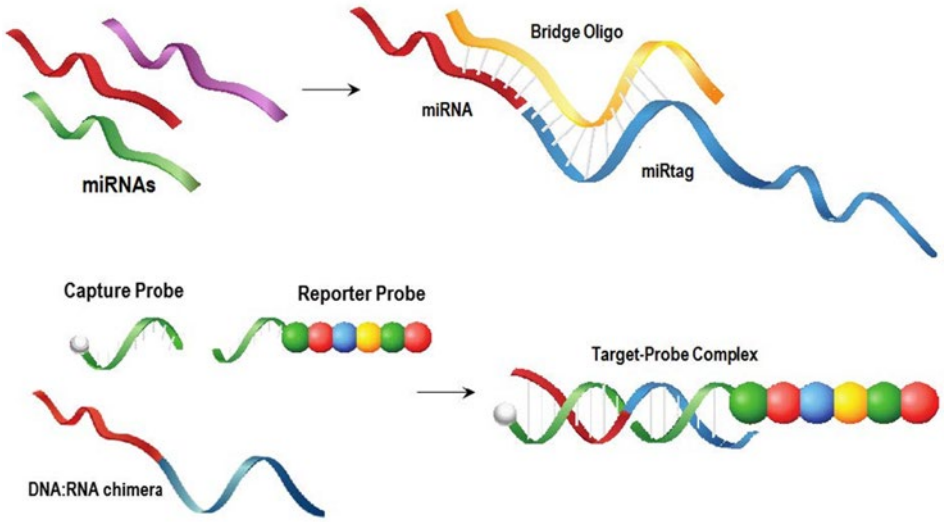

Figure2-1 miRNA-specific preparation to utilise the general nCounter technology pipeline. NanoString's technology is based on the direct molecular barcoding and digital detection of target molecules using a color-coded probe pair. The probe pair consists of a Reporter Probe, which carries the signal on its 5' end, and a Capture Probe, which carries a biotin moiety on its 3' end. The complexity of the colour codes, comprised of four colours in six positions, allows a large diversity of targets present in the same sample to be individually resolved and identified during data collection.

2.3 Aim

To perform a genomic-wide analysis of miRNAs profile in OLP patients and controls with other diseases causing oral white patches.

2.4 Materials and Methods

2.4.1 Sample Collection

Oral mucosa biopsy specimens were collected from patients who had been clinically and pathologically diagnosed with OLP according to the 2003 World Health Organisation diagnostic criteria at the Department of Oral Medicine, Newcastle Dental Hospital between March 2014 and February 2018.

OLP clinical criteria included the presence of bilateral, mostly symmetrical lesions, with the appearance of a lacelike network of slightly raised white lines in a reticular pattern accompanied or not with erosive, atrophic, bullous and plaque-type lesions. Histological inclusion criteria where the presence of well-defined band like zones of cellular infiltration confined to the superficial part of the connective tissue, consist primarily of lymphocytes, signs of ''liquefactive degeneration'' in the basal cell layer and the absence

of epithelial dysplasia. Also, patients with white lesions in close contact to oral amalgam restorations that may represent “oral lichenoid contact lesions” as well as patients with unilateral lesions who have started new medications in the previous 6 months that could have theoretically triggered so-called “oral lichenoid drug reactions” were excluded.

Other oral lichenoid disorders diagnosed according to Carrozzo et al (2019) were also excluded. As a control group patient matches for age and gender with OLP and affected by other oral disorders causing white patches and diagnosed according to clinical pathological standard criteria were enrolled. Moreover, 2 samples representing the OKF6 cell line were included in the analysis. All samples were suspended in RNA later and immediately transferred into liquid nitrogen until RNA extraction. All experimental procedures were approved by the NRES Committee North East - Newcastle & North Tyneside (13/NE/0368). The enrolled patients gave their informed written consent.

2.4.2 RNA Extraction

Total RNA including miRNAs was extracted from fresh frozen biopsies by using an RNesay Mini Kit from QIAGEN. RNA was extracted from each tissue sample according to the manufacturer’s protocol. First, the fresh frozen tissue was removed from the container and placed in a new clean universal tube. Tissue samples were homogenised in 600ml of RLT buffer with a Tissue Ruptor II (Qiagen) and then processed according to the manufacturer’s guidelines.

In brief, the samples were centrifuged for 3 minutes at 10000 rpm in a table top centrifuge to clear the lysate. The supernatant was collected and mixed with 600ml of 70% of ethanol. The ethanol/lysate mixture was then transferred into spin columns and centrifuged for 15 seconds at 10000rpm at 4°C. The flow-through was discarded. Subsequently, samples were washed with 700µl of RW1 buffer and centrifuged (15sec, 10000 rpm at 4°C). Once gain the flow through was discarded. As a last step, 500 µl of RPE buffer was added to the spin column followed by centrifugation as above. This step was repeated twice. The flow was discarded after each centrifugation step. The RNA was eluted with 50 µl of RNAase-free water and stored at -20 °C.

The quantity of RNA was determined using Nano drop™ (Thermo Scientific). RNA was further tested using an Agilent Bioanalyzer 2100. Furthermore, the quality of the extracted RNA was analysed by running the RNA sample on a 2% agarose gel in 1x TAE buffer (Tris-Acetate-EDTA).

2.4.3 nCounter specifics

All probe sequences were specifically designed and manufactured by means of NanoString. A number of housekeeping genes are included in each code set to account for variations in RNA input amount and/or quality. Housekeeping genes were chosen from publicly accessible databases for their stability and measurable expression levels in the tissue types of interest. While one Code Set had four housekeeping genes, the others all had at least eight.

The nCounter miRNA expression assay was run on the nCounter Analysis system. The system consists of two instruments, the Prep Station used for post-hybridisation processing and the Digital Analyser used for data collection.

All experiments included twelve samples. The protocol started with diluting the miRNA Assay control and preparation of the annealing master mix followed by the ligation protocol as by the manufacturer's instructions. After adding ligation clean-up enzyme to each reaction they were ready for purification according to the supplier's protocol. At that point, the samples can be stored at -20°C for several weeks, before proceeding with the miRNA CodeSet Hybridisation protocol.

After hybridisation, excess probes were washed away using a two-step magnetic bead-based purification on the nCounter Prep Station. Magnetic beads coupled to short nucleic acid sequences that are complementary to the Capture Probe and the Reporter Probes were used sequentially. The hybridisation mixture containing target/probe complexes was then allowed to bind to magnetic beads complementary to sequences on the Capture Probe.

Wash steps were completed to remove excess Reporter Probes and non-target cellular transcripts. After washing, the Capture Probes and target/probe complexes were eluted off the beads and were hybridised to magnetic beads complementary to sequences on the Reporter Probe. An additional wash was performed to remove excess Capture Probes. Lastly, the purified target/probe complexes were eluted off the beads and immobilised on the cartridge for data collection.

Data Collection was carried out in the nCounter Digital Analyser. Digital images were processed and the barcode counts were arranged in a comma separated value (CSV) format.

2.4.4 NanoString nCounter miRNA assay for miRNA profiling

The multiplexed NanoString nCounter miRNA expression assay (NanoString Technologies, Seattle, WA, USA) was used to profile more than 800 human miRNAs. The assay is performed according to the manufacturer's protocol. A Large quantity of miRNAs can be quantified with the nCounter Prep Station and Digital Analyser (NanoString) via counting individual fluorescent barcodes and quantifying target miRNA molecules present in each sample.

2.4.5 NanoString analysis

The NanoString n Counter Analysis System (NanoString Technologies®, Inc.), was utilised to analyse total RNA samples with a concentration of 30µg/µl. The quantification of the miRNAs was performed in the NanoString facility at Newcastle University Medical School.

2.4.5..1 miRNA sample preparation

Total RNA was used as starting material in the nCounter miRNA expression assay. NanoString protocols recommend using 100 ng of total RNA.

Total RNA samples were prepared using RNAse-free water to dilute the total RNA samples to 33 ng/µl. 3 µl were used to provide 100ng input. Samples were free of organic solvents and any other contaminations. Controls were prepared with 1 µl of miRNA Assay Controls and 499 µl of RNAse-free water.

The third step, sample annealing, involved an annealing master mix, a combination of 13µl of annealing buffer, 26 µl of nCounter miRNA Tag Reagent and 6.5 µl of the miRNA Assay Control generated in the previous step. Afterward, 3.5 µl of the annealing master mix were combined with 3 µl of total RNA (100ng) prior to starting the annealing protocol in a thermocycler.

The next step was to mix the ligation master mix, 19.5 µl PEG and 13 µl ligation buffer in a microfuge tube, mixing thoroughly by pipetting. 2.5 µl of the ligation master mix per tube were then preheated 5 minutes at 48 °C in a thermocycler and 1 µl of ligase added to each tube.

Prior to hybridisation, 1 µl ligation Clean-Up was added to each tube and topped up with 40 µl of RNAse-free water. Reactions were stored at -20 °C prior to hybridisation.

2.4.5..1 miRNA hybridisation protocol

According to the nCounter® miRNA Expression Assay user manual the final hybridisation reaction contained the following components: 10 µl of the reporter CodeSet, 10 µl hybridisation buffer, a 5 µl aliquot from of the prepared miRNA sample and 5 µl of the capture ProbeSet.

First, aliquots of the reporter CodeSet and capture ProbeSet were mixed and collected with a brief spin. Next, hybridisation buffer (130 µl) was added to the tube containing the reporter CodeSet (130 µl) and 20 µl were pipetted into each tube. MiRNA samples were denatured for 5 minutes at 85°C, chilled quickly on ice and a 5 µl aliquot was added to the hybridisation mix. The thermocycler was programmed for a hybridisation at 65 °C for longer than 12 hours followed by a cool down to 4 °C. Before placing the tubes at 65 °C, 5 µl of Capture ProbeSet were added to each tube followed by a quick spin. Hybridisation was performed for at least 12 hours and transferred to the nCounter Prep Station.

2.4.5..2 Purification and immobilisation

After hybridisation, samples were transferred to the nCounter Prep Station where excess probes were removed and probe/target complexes were bound, immobilised and aligned on the nCounter Cartridge. Afterwards, the counting and analysis process was initiated on the nCounter digital analyser for data collection.

The raw data was processed using the nSolver software version 4.0. Counts were normalised to eliminate systematic experimental variability, differing amounts of input RNA, along with variability in the background. The seven steps of a basic analysis are explained in the workflow diagram (Figure 2.2).

Figure 2-2 nSolver work flow

In the first step, the data were imported from the nCounter instrument in the form of RCC files using the RCC Import Wizard.

Subsequently, a new experiment was created and the data were normalised using the geometric mean of the counts observed with the positive controls as well as by using the normalising genes in CodeSet. The expression levels for individual miRNAs was then established and the ratio, i.e., fold change was determined.

2.4.6 Data analysis

The fold change (FC) for each miRNA was determined for the two groups as the ratio of the geometric mean of the normalised counts of the OLP group over the geometric mean of the control group. The FC was also determined for OKF6 cells. Three comparisons were completed, specifically first patient vs. control, second patient vs. OKF6 cells and third, control vs. OKF6 cells.

Differential miRNA expression was quantified using the NanoString nCounter FLEX platform and the data was normalised using n Solver software. Data filtering and analysis were undertaken in R (version 4.1.2) and R Studio using a script provided by Anastasia Resteu, Human Dendritic Cell Lab, Newcastle University.

Standard normalization uses a combination of Positive Control Normalization, which uses synthetic positive control targets, and CodeSet Content Normalization, which uses housekeeping genes, to apply a sample-specific correction factor to all the target probes within that sample lane Normalized.

NanoString gene expression data is most commonly analysed in terms of ratios or fold changes. These calculations are used to determine the relative over- or under-expression of each gene across different sample groups in an experiment.

These expressions can be calculated in either linear or log2 scale. To calculate ratios using a hypothetical experiment with three groups of samples: those in a control group, patients group, and OKF6 group.

Calculating linear ratios for a single gene in this data set overexpressed genes will have ratios >1, but under-expressed genes will have a ratio that ranges in value from 0 – 1 therefore, compressed in the linear scale.

Fold changes are readily calculated from linear ratio data. If the ratio numerator is greater than the ratio denominator (i.e., ratio > 1), then the fold-change is equal to the ratio. If the ratio numerator is less than the ratio denominator (i.e., ratio < 1), then fold-change equals the negative inverse of the ratio: The output of a t-test is a p-value, and the standard convention is to assign significance to all genes with a nominal p-value of less than 0.05 Furthermore, a negative FC indicates down regulation, a positive FC stands for up regulation and the *p* value was calculated for the expression changes and a value of <0.05 were considered significant.

2.5 Results

2.5.1 Patients and controls

Oral biopsy specimens were collected from a total of 32 patients: 24 samples were from patients diagnosed with OLP. Twelve were female and 12 are male with an average of age 57.37. Twelve patients had reticular lesions of OLP, 6 reticular/atrophic, 5 reticular/patch-like and 1 reticular/erosive.

Additionally, 8 samples represented the control group composed of tissue from patients affected by other oral diseases causing white patches and diagnosed according to standard clinical-pathologic criteria. Five were female and three were male with an average of age 57. 55. Four controls patients had a final diagnosis of leukoplakia without dysplasia, two were affected by chronic hyperplastic candidosis (candida leukoplakia), one had leukoplakia with mild dysplasia and the last one was diagnosed with hairy leukoplakia.

2.5.2 Samples and RNA yield

The quality and quantity of RNA extracted from 24 patients with oral lichen planus as well as from 8 controls patients with were determined by running the RNA samples on an agarose gel and using Nano drop as well as the Bioanalyzer 2100. For NanoString analysis, a concentration of approximately 30ng/µl RNA is required. It is also recommended that the RNA integrity (RNA Integrity Number, RIN) was tested using Bioanalyzer. The maximum integrity of RNA is indicated by a reading of 10. The ratio of 28S and 18S rRNA peaks is also given. As RNA degradation becomes more apparent, peak heights for the 28S and 18S rRNA peaks decrease, while smaller or degraded RNA peaks become more prominent (Figure 2.3).

The software also estimates RNA concentration by comparing peak areas of the ladder with RNA fragments of known concentration and peak areas of the unknown samples. In addition, a gel-like image is provided to visualise fragment sizing and distribution as well as a visual representation of the RNA ladder. The RNA concentration and dilution optimisation for both techniques is summarised in Table 2.1.

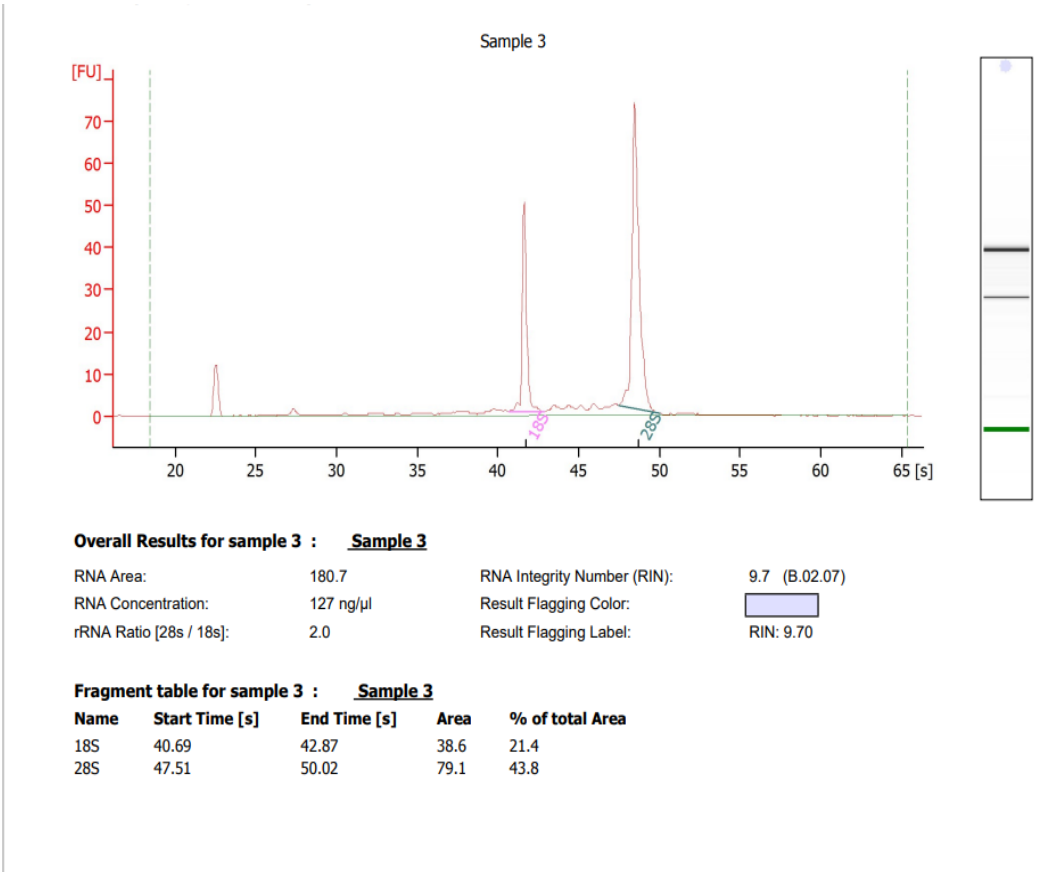

Figure 2-1 Example of a patient sample Bioanalyzer trace with RIN number. The ratio of 28S/18S rRNA is demonstrated too. The gel images from the 2100 Bioanalyzer software are displayed on the right side with the 28S and 18S rRNA bands indicated in dark and light grey, respectively.

Table 2-1 RNA concentration determined by Nano drop and Bioanalyzer

Sample Code	Sample Source	Nano drop con µg/µl	260/280	Final Concentration to send to NanoString	RIN	Bioanalyzer conc.
OKF1	cell line	526.9	1.98	40.1	10	83
OKF2	cell line	376	2.21	38.6	N\A	14
MC23 MRH 0159543A	mucosal biopsy	1017.3	2.27	32.5	8.90	37
MC27 MRH 1567101A	mucosal biopsy	120.9	2.24	40.5	9.70	60
MC28 MRH 91007265	mucosal biopsy	104.8	2.2	31.1	9.70	12
MC29 MRN 0344620X	mucosal biopsy	149.4	2.03	30	9.40	39
MC37 MRN1580008J	mucosal biopsy	129.6	2.18	36.7	3.70	35
MC21 MRN 91258291	mucosal biopsy	21.1	1.2	29.1	10	83
MC38 MRN91333117	mucosal biopsy	301.3	2.11	39.8	7.70	11
MC34 MRN 91326672	mucosal biopsy	285.7	1.99	40.3	7.90	14
MC39 MRN 0644097W	mucosal biopsy	235.4	2.13	36.2	10	15
MC35 MRN 5001069E	mucosal biopsy	165.9	2.07	38.8	8.30	39
MC36 MRH 1312119X	mucosal biopsy	217.5	2.18	33.8	8.90	32
MC15 MRN 2014042G	mucosal biopsy	324.8	2.17	40.4	8.70	18
MC30 MRN0051431X	mucosal biopsy	65.1	2.28	30.6	8.90	82
MC26 MRN 6243305A	mucosal biopsy	511.1	2.1	45.1	10	70
MC54 MRN 0335280J	mucosal biopsy	422.1	2.11	39.8	9.90	71
MC40 MRN 1592426X	mucosal biopsy	185.2	2.04	40.4	9.70	34
MC41 MRN 0144548U	mucosal biopsy	120.2	2.22	30.9	9.50	18
MC43 MRN 1530691R	mucosal biopsy	118.1	2.09	30.6	8.30	63
MC44 MRN 5009286Q	mucosal biopsy	131	2.1	29.9	8.70	47
MC 45 MRN 4000865K	mucosal biopsy	107.3	2.1	32.4	8.80	90
MC 46 MRN 6207249J	mucosal biopsy	100.1	2.19	38.2	9.90	95
MC48 MRN91335126	mucosal biopsy	169.9	2.09	31.1	9.30	45
MC 50 MRN 9135297	mucosal biopsy	114.4	2.22	41.8	9	228
MC52 MRN 0203208E	mucosal biopsy	360	2.11	31.8	9.90	96
MC 53 MRN 0799962H	mucosal biopsy	107.8	2.2	37.3	9.70	87
MC59 MRN 0390156N	mucosal biopsy	265.8	2.13	37	9.70	127

MC 60 MRN 6167945Q	mucosal biopsy	245.1	2.16	33.4	10	138
MC 55 MRN 0411967M	mucosal biopsy	70.9	2.12	29.9	9.90	71
MC 57 MRN 2059521W	mucosal biopsy	147.9	2.08	28.9	9.10	95
MC56 MRN 0380409N	mucosal biopsy	111.7	2.12	34.2	9.10	120

The samples specified in Table 2.1 was analysed by NanoString to profile the expression of 798 miRNAs. Raw counts were normalised using the geometric mean of the top 100 miRNA, housekeeping genes and spike-in probes. Background levels were determined using negative controls and counts below 20 were considered as background and excluded from analysis. Finally, expression of miRNAs was compared in the different groups using R studio.

2.5.3 Hierarchical clustering

The purpose of hierarchical cluster analysis was to create a tree diagram in which the most similar miRNA expression profiles of the participants in the study they are placed on branches that are close together. A dendrogram is presented in Figure 2.4 to illustrate the relationship between patients and controls, as well as the OKF6 cell lines.

The outcome of the hierarchical cluster analysis is shown in Figure 2.4. In this tree, there are 5 clusters that exhibit similar overall expression patterns of the analysed miRNAs, highlighted by different colours. The red cluster represents the OKF6 cell line samples which are clearly separated from the other clusters, as expected. Despite the human origin of OKF6 cells one would expect that the miRNA profile is significantly altered as compared to human oral tissue samples.

Interestingly, the majority of the OLP patient samples are clustered in the green and the yellow group. The yellow cluster (12 samples) contains no controls, whereas the green one comprises 1 control and 6 patient samples. In contrast, most control samples are segregated in the purple cluster (7/9). These results indicate that there may be distinct miRNA signatures detectable in the OLP and control samples. Of note, control sample number 62 has been loaded twice as (62a and 62b) for technical reasons and represent technical replicates.

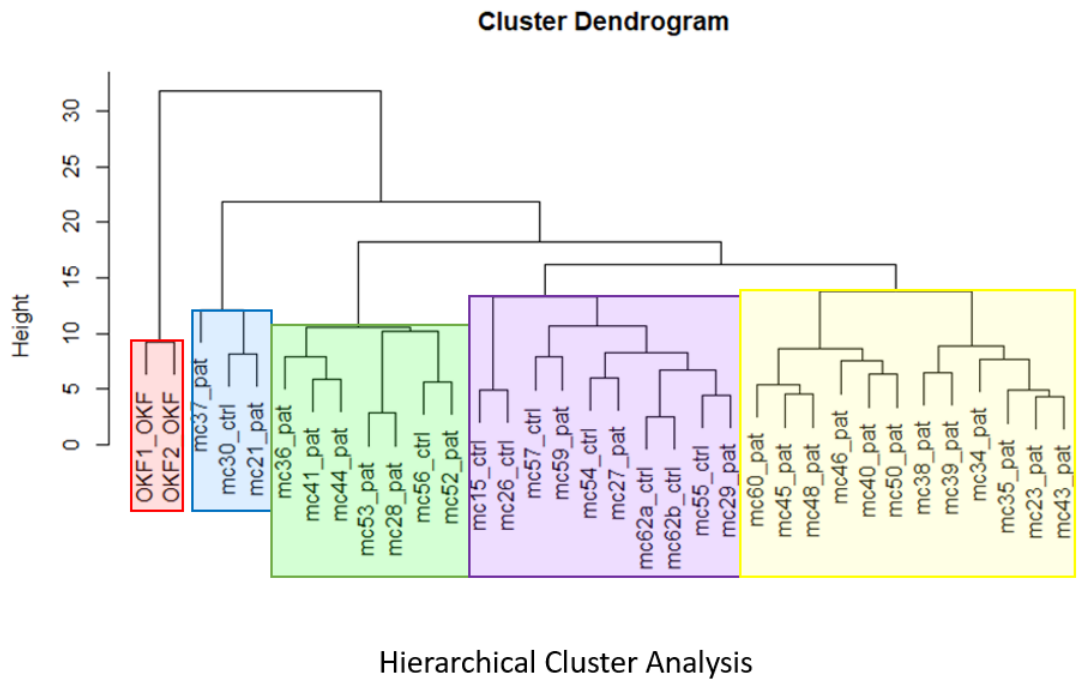

Figure 2-2 Hierarchical clustering or cluster dendrogram of 24 OLP patients and 8 controls and 2 OKF6 samples. The y-axis (the height) are values of the distance in which three groups can split or merge, using the Euclidean distance calculation. pat = patient and ctrl= control.

Next, the expression data were analysed for differentially expressed miRNAs between the OLP patient group and the controls.

The expression profile of 799 host cellular miRNAs was assessed in OLP (n = 24) and control white lesion samples (n=8) as well as OKF6 cell lines (n=2). The results revealed that in OLP patient samples the expression of several miRNAs was differentially regulated. The level of expression in OLP was compared with that in the white lesion control samples. Fold change differences were calculated based on normalisation with internal controls. The fold differences ranged between -2 and -100 fold for different miRNAs. The *p* value of the miRNA was considered in the patient samples to determine if they were upregulated or downregulated.

Among the total 799 miRNAs tested, nine were upregulated by more than 2-fold compared to controls (miR-155, miR-146a, miR-3195, miR-342-3p, miR-4516, miR-21-5p, miR-29a, miR-193a-5p and miR-222-3p) with increased expression levels in patients. In contrast, 9 miRNAs exhibited lower expression in patients (let-7c, miR-23a-3p, miR-23b-3p, miR-200b-3p, miR-1495, miR-205-5p, miR-221, miR-27b and miR-95) (Table 2.2 and Table 2.3).

A heatmap was generated for all identified biomarkers, demonstrating their relative increase (red) or decrease (green) (Figure 2.5).

Heatmap analyses further cluster the miRNA species between the tested groups; these results indicate that fold difference did not necessarily correlate with the differential regulation of miRNAs in multiple donors. OKF6 cells show a distinct over-expression of all highly expressed miRNAs (green column at the top of the figure). Moreover, the OLP patients marked with an arrow (pt43, pt50, pt53 and pt60) show a marked downregulation of the most highly expressed miRNAs. Of note, a group of controls shows a down-regulation of lowly expressed miRNAs. These findings indicate that one or more miRNA signatures may be identified that help identification or classification of OLP.

Table 2-2 Upregulated miRNAs in OLP patients against control group

Upregulated miRNA	Fold Change	Log FC	*p* value
hsa-miR-155-5p	-30.5520249	-1.48504	5.52E-06
hsa-miR-146a-5p	-15.5951659	-1.19299	0.000154
hsa-miR-3195	-8.58281991	-0.93363	0.005895
hsa-miR-342-3p	-5.77005562	-0.76118	0.002252
hsa-miR-4516	-5.69403326	-0.75542	0.007072
hsa-miR-21-5p	-4.10071890	-0.61286	0.032911
hsa-miR-29a-3p	-3.87141742	-0.58787	0.033439
hsa-miR-193a-5p	-3.63011179	-0.55992	0.017599
hsa-miR-222-3p	-2.65411661	-0.42392	0.035582

Table 2-3 Downregulated miRNAs in OLP patients against control group

Downregulated miRNA	Fold Change	Log FC	*p* value
hsa-miR-221-3p	0.143156	0.844195	0.000936
hsa-miR-205-5p	0.162185118	0.789988506	0.010361
hsa-miR-149-5p	0.184614405	0.733734415	0.000984
hsa-miR-200b-3p	0.2452394	0.61040972	0.021430
hsa-miR-23b-3p	0.3217054	0.49254155	0.017914
hsa-let-7c-5p	0.4039610	0.39366049	0.035300
hsa-miR-23a-3p	0.472713	0.336734	0.021654
hsa-miR-27b-3p	0.815157	0.153056	0.007364
hsa-miR-95-3p	0.902863	0.125066	1.51E-05

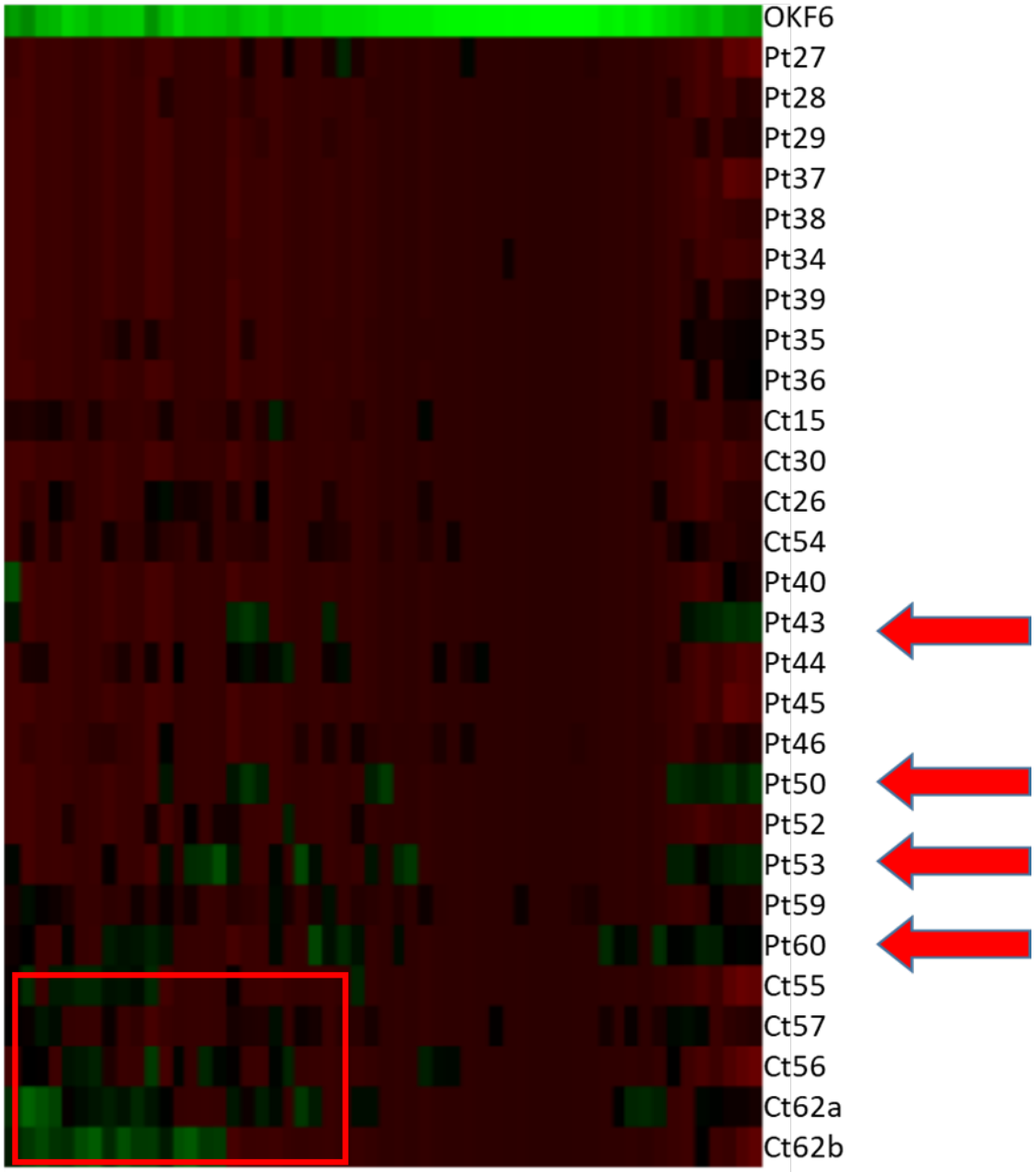

Figure 2-5 The heat map represents the result of the two-way hierarchical clustering of miRNA and samples. Each row represents samples and each column represents the miRNAs tested. The clustering represents the miRNA and samples on the top and sides, respectively. Red represents miRNA with an expression level above the mean, while green represents miRNA with an expression level below the mean/average. A cluster of apparently down regulated mRNAs in controls is circled.

2.6 Discussion

The work presented in this chapter involves the NanoString nCounter technology for the detection of miRNAs associated with OLP patient samples, control the white lesions and the OKF6 cell line. see figures (2-6 A and B)

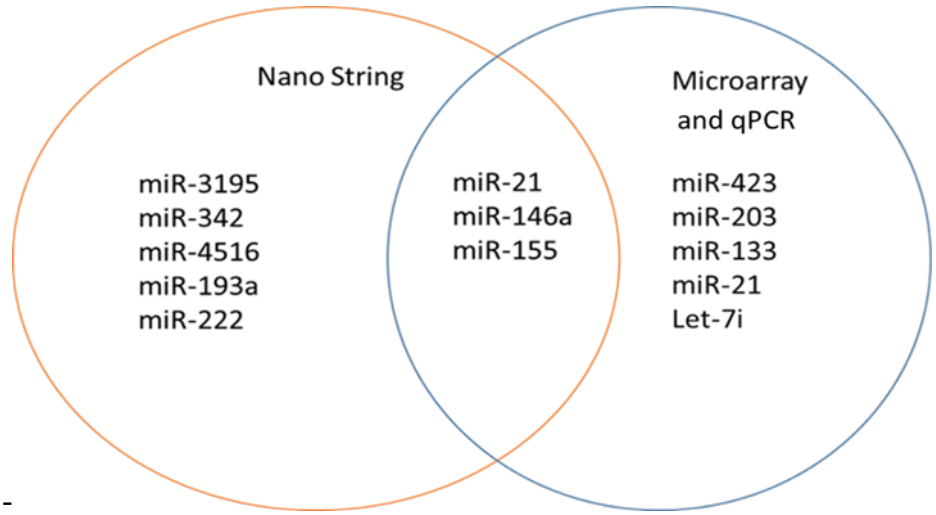

-

figure 2-6 (A) shows the project upregulated miRNAs finding by using Nano String technology and the other lectures reviews finding by using microarray and qPCR also it represents the common miRNAs in both different methods

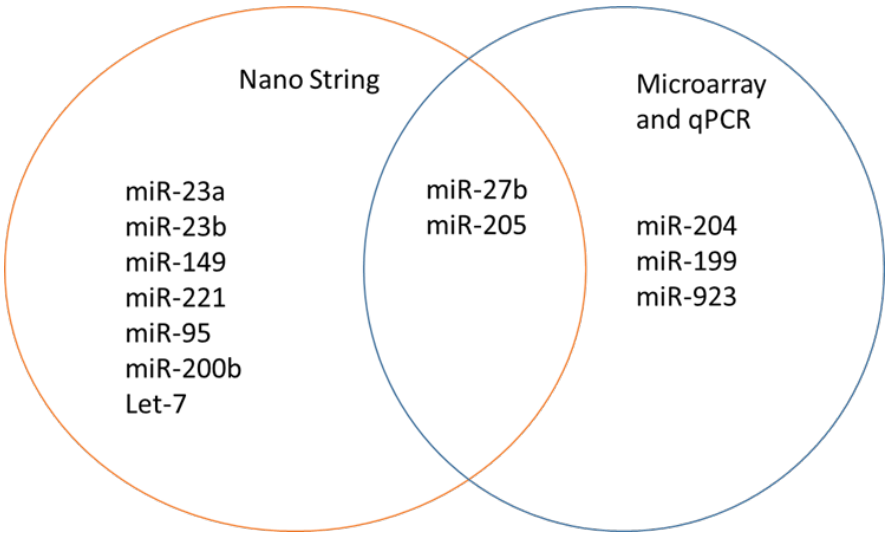

figure 2-6 (B) shows the project downregulated miRNAs finding by using Nano String technology and the other lectures reviews finding by using microarray and qPCR also it represents the common miRNAs in both different methods

MicroRNAs (miRNAs) have emerged as biomarkers in different materials, including plasma, serum, saliva and tissue samples (Yoshizawa and Wong, 2013). In fact, several studies have reported the prognostic value of circulating miRNAs in different disorders. Likewise, it may be also important to identify these markers with predictive power for patient management and therapy. For example, a considerable number of tissue and circulating miRNAs have been proposed as prognostic predictors in oral cancer (Momen-Heravi, Trachtenberg et al., 2014).

This work quantified miRNAs with the nCounter Prep Station and Digital Analyser (NanoString) by way of counting individual fluorescent barcodes and quantifying target miRNA molecules present in each sample. For each assay, a high-density scan (800 fields of view) was performed. Each sample was normalised to the geometric mean of the top 100 most highly expressed miRNAs.

The normalisation is essential in order to minimise the impact of technical variations. This can be undertaken using small RNA controls or the expression of selected miRNAs. The use of synthetic RNA molecules as spike-in controls can correct for extraction efficiency.

The dendogram showed the clustering of two groups that contain patient samples primarily. By narrowing down the group of miRNAs that segregation may be improved. Eventually, a limited selection of miRNAs may be identified that is specific for OLP and may be used for identification or prognostic purposes.

At the end of this stage I was able to determine that 9 miRNAs were upregulated in OLP (miR-155, miR-146a, miR-3195, miR-342, miR-4516, miR-21, miR-29a, miR-193a, and miR-222) and 9 miRNAs were downregulated (let-7, miR-23a, miR-23b, miR-200b, miR-149, miR-205, miR-27b, miR-221, and miR-95). Two upregulated namely (miR-4516 and miR-22) and 2 downregulated miRNAs namely (miR-149 and miR-95) were novel discoveries.

Momen-Heravi and colleagues used NanoString nCounter to screen 734 human RNA samples from saliva of patients with oral squamous cell carcinoma (OSCC), OLP and healthy controls (Momen-Heravi, Trachtenberg et al., 2014). Their results revealed that miR-146a and miR-29a were significantly under expressed in OSCC when compared with OLP. Contrarily, miR-27b was significantly overexpressed in OSCC compared to OLP.

A different study by Liu et al used a microarray approach to assess miRNA expression in OLP. For their experiments, they extracted RNA from plasma and PBMC as starting material (Liu, Wu et al., 2015). Their findings suggest that in plasma miR-155 and miR-146a expression was significantly higher in erosive OLP patients than in the non-erosive OLP group which was itself still higher than the control group. In contrast, there were no significant difference in the expression of miR-155 and miR-146a in the from PBMC patient and healthy control group. Shi et al. utilised the same method to characterise the relationship between miR-21 and OLP and found a significant upregulation of miR-21 in OLP patients compared to control healthy group (Shi, Yang et al., 2015).

Quantitative real-time polymerase chain reaction was used to analyse miRNA expressions in OLP patients by Arão et al. (2012). They investigated the expression of miR-146a and miR-155 in 31 tissue and in blood samples compared to healthy patients. Their results indicated increased expression of miR-146a and miR-155 in OLP lesions compared to the healthy group. Moreover, Danielsson and colleagues found that miR-21 was significantly downregulated in OLP oral mucosa samples in contrast to the healthy control samples (Danielsson, Wahlin et al., 2012).

Chapter 3. Target Genes and miRNAs interaction

3.1 Introduction

There are well established strategies to identify miRNAs that are differentially expressed in certain diseases and that correlate with other disease markers. Numerous computational and experimental approaches concerning miRNA target gene discovery have been developed and tested, which take into account the biological processing and the function of miRNAs, besides the complex target gene-binding parameters and how microRNAs can recognise and regulate their targets (Ørom and Lund, 2010).

Computational approaches to miRNA target identification are strong tools to narrow down the list of supposed targets of miRNA regulation and have contributed significantly to the development of the miRNA field.). The most commonly used algorithms are miRanda, TargetScan and PicTar. All these algorithms are predominantly based on miRNA-target interaction (Lewis, Shih et al. 2003). Notwithstanding, it is still not fully known how miRNAs interact with their targets. (Vella, Reinert et al. 2004).

Although just a prediction, these sites provide a starting point to plan specific experiments to confirm the involvement of specific miRNA in different diseases. However, scrutinising the biological significance of usually long lists of probable candidates is still difficult (Didiano and Hobert, 2006). For example, TargetScan which is the most commonly used prediction algorithm, predicts three validated target genes of let-7 within the top five predictions (HMGA2, LIN28B and TRIM71), whereas the other proven targets of let-7, NRAS and ITGB3 were placed at positions 143 and 393, respectively, in the prediction list (Akbari Moqadam, Pieters et al., 2012).

3.2 Previous studies of cytokine that related to OLP

Several studies have detected cytokines which are involved in the pathogenesis of OLP. The main cytokines in this role include TNF-α, IFN-γ, IL-10, IL-17 and IL-22. In this group, TNF-α is the most widely studied cytokine in OLP and has been confirmed to play an crucial role in the immune regulation of OLP disease (Pezelj-Ribaric, Prso et al., 2004).

Table 3.1 shows a summary of cytokines that are related to OLP and the different tissues that were used to analyse the expression in OLP.

Table 3-1 List of potential target genes related to OLP

Cytokine	Material	Regulation	Reference
TNF-α	Saliva	Increased	(Thongprasom, Dhanuthai et al., 2006)
INF-Ɣ	Blood	Decreased	(Thongprasom, 2017)
BCL-2	Oral mucosa	Increase	(Nafarzadeh, Jafari et al., 2013)
IL-10	Serum	No significant change	(Mohseni, Saleem et al., 2021)
STAT-3	Oral mucosa	Not clear	(Du, Chen et al., 2018)
NOTCH1	Oral mucosa	Increased	(Nowwarote and Osathanon, 2017)
NOTCH3	Oral mucosa	Decreased	(Nowwarote and Osathanon, 2017)
IL22	Oral mucosa	Increased	(Shen, Du et al., 2016)
NF-kappB	Oral mucosa	Increased	(Santoro, Majorana et al., 2004)
TGF-B1	Oral mucosa	Increased	(Georgakopoulou, Troupis et al., 2011)

3.3 Aims

To confirm the NanoString findings and to conduct a bioinformatics search of potential targets for the confirmed differentially expressed miRNAs and assess the potential link with miRNAs

3.4 Material and methods

3.4.1 Sample collection

At the Department of Oral Medicine, Newcastle Dental Hospital, oral mucosa biopsy specimens were taken from patients who had been clinically and pathologically diagnosed with OLP and controls with other diseases causing white patches. Inclusion and exclusion criteria have been described in chapter 2. For this set of experiments, 10 samples of patients with OLP, randomly selected from the 24 original cohort, and 8 of controls were used. The NRES Committee North East - Newcastle & North Tyneside (13/NE/0368) approved all experimental procedures. Additionally, the enrolled patients submitted their informed written consent.

As we intended to use limited biological material (fresh frozen oral tissue) from patients with OLP and oral keratosis in this project, it was essential to establish and test the

methodology for analysis prior to using the patient material in the actual experiment. For that reason, we started to determine the miRNA expression pattern related to an established list of cytokines in a human immortalized oral keratinocyte cell line (OKF6).

3.4.2 Cell line and tissue culture

OKF6 cells were cultured in high DMEM with glutamine (Invitrogen), supplemented with bovine pituitary extract (BPE)/EGF (Invitrogen) and 1% penicillin and streptomycin (Invitrogen) and epidermal growth factor 1%. Cells were incubated in complete media in T-25cm canted neck cell culture flasks at 37°C with 5% CO2 in a sterilised humidified incubator.

The culture medium was changed every 3 days. Confluent monolayers were harvested and transferred to new tissue culture flasks. To achieve that, cells were washed with phosphate buffered saline (PBS). 5 ml trypsin was added and incubated at 37˚C, 5% CO_2 for 4 minutes to detach cells from the base of the flask. They were transferred into a sterile universal tube and a minimum of 20 ml of medium was added. The tubes were centrifuged at 200g; "g is the relative centrifugal force" for 3 minutes (12000 rpm), and the pellet was re-suspended in 10 ml of appropriate medium, then a syringe was used to remove clusters. 20 µl of cell suspension was pipetted into a cell counting chamber and the number of cells was counted using a Cellometer Auto T4 Cell counter (Nexcelom, Bioscience, USA). Suspensions were then diluted and seeded at a concentration of $1x10^6$ cells per flask for stock culture. All tissue culture manipulations were undertaken in a class II laminar flow hood (BioAir, Safe flow).

3.4.3 RNA extraction

RNA was extracted from confluent monolayers using TRIzol® Reagent (Ambion). 1 mL of TRIzol was used per 10 cm2 of culture and cells were lysed by pipetting up and down several times. Chloroform was added to separate the phases (200 µl/1 ml of TRIzol®Reagent). After centrifugation (20,000g, 15 min. 4 ˚C) (14.000 rpm), the upper aqueous phase containing the RNA was transferred to a new tube and precipitated using 100% isopropanol (500 µl/1 ml of Trizol). After centrifugation (as above), the RNA pellet was washed with 1 ml of 75% ethanol, air dried and re-suspended in 20 µl RNase free water. Subsequently, the concentration of the extracted RNA was determined using Nano drop (Thermo scientific) and tested by running on a 2 % Agarose gel (Sigma-Aldrich).

3.4.4 Reverse transcription-PCR (RT-PCR)

For first strand cDNA synthesis the Omni script RT-PCR kit (Qiagen) was used. Random nanomers (2.5 µm) (Sigma-Aldrich) were used in these experiments. The total volume of each reaction was 10 µl composed of: 2 µl RNA template 1 µl of nanomers, 1 µl 10x RT buffer, 1 µl of (5 mM) dNTP mix, 0.5 µl of (40 U/µl) RNase inhibitor, 0.5µl of (4 U/µl) Omni script Reverse Transcriptase and RNAse free water up to the final volume. The reactions were incubated at 37 °C for 1 hour followed by denaturation for 10 minutes at 65 °C. Samples were stored at - 20 °C. PCR reactions were performed using three specific primer pairs synthesised by IDT. The total volume for each reaction was 15 µl: 7.5 µl of red master mix (Rovalab), 6.5 µl H2O and 1 µl of (10µM) primers. The temperatures and cyclic condition were: Initial denaturation (95 °C for 1 minute), subsequent denaturation (96°C for 20 seconds), annealing (55 °C for 30 seconds) and extension (72 °C for 10 seconds). Samples were resolved on 2% agarose/TAE gels stained with SafeView Gel Red, together with a 100bp DNA ladder (Bioline). The sequences of each of the primers are listed in the appendix.

3.4.5 DNA sequencing

DNA sequencing is the process of determining the precise order of nucleotides within a DNA fragment. Sanger sequencing was performed by Source Bioscience (Glasgow).

3.4.6 Extraction of DNA from agarose gels

Extracting DNA bands from an agarose gel is a crucial step because agarose will interfere with further reactions such as DNA sequencing. The DNA band was cut out of the gel using a scalpel while visualising the band on a UV light-box in a dark-room (a trans-illuminator). The excision process should take place quickly because UV causes mutagenesis of the DNA at a measurable rate. The excised band was placed in a 1.5mL microfuge tube.

3.4.7 Purification of PCR fragments

The PCR purification kit from Thermo Scientific was used. In brief, 100 µl of binding buffer added for each 100 mg of gel (equal volumes). Agarose was melted at 55 °C for 10 minutes, 100 µl of isopropanol were added followed by loading the mix onto a silica matrix column. Samples were centrifuged for 1 minute in a mini centrifuge at full speed. The DNA was washed with 700 µl of washing buffer and underwent centrifugation for 1

minute. DNA was eluted with 15µl of elution buffer and the concentration of the samples was measured by Nano drop.

3.4.8 Reverse transcription of miRNA:

The fact that miRNAs are very short and do not contain a poly A tail require a modified strategy to synthesise cDNA. The miScript II RT Kit ensures that mature miRNAs are polyadenylated by poly (A) polymerase and then reverse transcribed into cDNA using oligo-dT primers (Figure 3.1). Polyadenylation and reverse transcription are performed in parallel in the same tube. The oligo-dT primers have a 3' degenerate anchor and a universal tag sequence on the 5' end, allowing amplification of mature miRNAs in the real-time PCR step. The miScript II RT Kit, used in combination with SYBR Green PCR mix (Roche), enable quantification of mature miRNA. The combination of polyadenylation and the universal tag addition ensures that the assays do not detect genomic DNA.

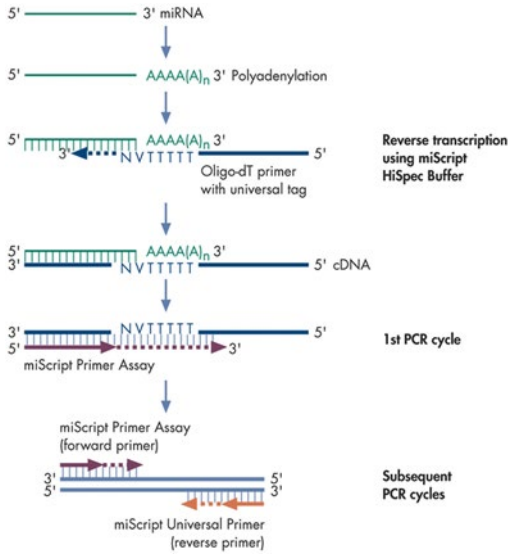

Figure 3-1 Selective conversion of mature miRNAs into cDNA using the miScript II RT Kit. In a reverse transcription reaction with miScript HiSpec Buffer, mature miRNAs are polyadenylated by poly (A) polymerase and converted into cDNA by reverse transcriptase with oligo-dT priming in order to increase length of miRNA. The cDNA is then used for real-time PCR quantification of mature miRNA expression. www.qiagen.com/ miScript-PCR-System-Handbook.

The reverse transcription reaction contained 2 µl of 5x miScript Hisep buffer, 1 µl of 10x miScript nucleotide mix, 1 µl of miScript transcriptase, 2 µl of RNA template (OKF6 cell line RNA) and RNAase free water (4 µl) to make a final volume of 10 µl (Table 3.2). This mixture was incubated at 37 ˚C for 60 minutes (Thermo Scientific Precision Water Bath). The reaction was stopped at 95˚C for 5 minutes in a heat block, then samples were diluted to 1/3 and 1/5 and stored at -20˚C.

Table 3-2 Pipetting protocol for RNA reverse transcription

Reagent	Quantity (µl)
5x miScript Hisep buffer	2µl
10x miScript Nucleotide mix	1µl
miScript reverse transcriptase	1µl
RNA template	2µl
RNase free water	4µl

3.4.9 *End point PCR*:

For end-point PCR reagents and polymerase GoTaq from Promega were used. Reactions contained GoTaq 5µl, universal primer 1µl, provided by Qiagen, miRNA-specific forward primer 1µl, cDNA (OKF6 cells) 1µl and RNAase free water 2µl to make a total volume of 10µl. The PCR reaction temperatures and cycling condition were: Initial denaturation (95 °C for 2 minutes), subsequent denaturation (96°C for 20 seconds) and different annealing temperature were applied for 35 cycles and extension (72 °C for 5 minutes). The finished reaction was held at 4˚C.

Table 3-3 Pipetting protocol for PCR reactions

Reagent	Quantity (µl)
GoTaq	5µl
Universal primer	1µl
Forward primer	1µl
cDNA	1µl
free RNase water	2µl

The forward primer sequences of specific miRNAs were obtained from http://www.mirbase.org/; Table 3.4 illustrates the sequence and the annealing temperature of each miRNA primer.

Subsequently, verification of PCR product size was performed by running the product on a 2% (w/v) agarose gel containing Gel Red (VWR, UK). The molecular weight marker hyper ladder IV (100 pb) was used (Bioline, UK).

Table 3-4 Primers for miRNAs detection

miRNA name	Accession number	Primer sequence 5'–3'	Annealing Temperature
miR-3195-5p	MIMAT0015079	CGCGCCGGGCCCGGGTT	71.1
miR-193a-5p	MIMAT0004614	TGGGTCTTTGCGGGCGAGATGA	63.3
miR-146a-5p	MIMAT0000449	TGAGAACTGAATTCCATGGGTT	54.2
miR-155-5p	MIMAT0000646	TTAATGCTAATCGTGATAGGGGT	53.9
mR-342-3p	MIMAT0004694	1AGGGGTGCTAUCTGUGATTGA	54.3
miR-21-5p	MIMAT0000076	TAGCTTATCAGACTGATGTTGA	50.9
miR-29a-3p	MIMAT0000086	TAGCACCATCTGAAATCGGTTA	53.7
miR-222-3p	MIMAT0000279	AGCTACATCTGGCTACTGGGT	57.6
miR-4516	MIMAT0019053	GGGAGAAGGGTCGGGGC	61.2
let-7c-5p	MIMAT0026472	CTGTACAACCTTCTAGCTTTCC	53
miR-23a-3p	MIMAT0000078	ATCACATTGCCAGGGATTTCC	61.6
miR-23b-3p	MIMAT0000418	ATCACATTGCCAGGGATTACCAC	59.6
miR-200b-3p	MIMAT0000318	TAATACTGCCTGGTAATGATGA	63.3
miR-149-5p	MIMAT0000450	TCTGGCTCCGTGTCTTCACTCCC	62.7
miR-27-3p	MIMAT0014534	AGAGCTTAGCTGATTGGTGAAC	54.9
miR-205-5p	MIMAT0000266	TCCTTCATTCCACCGGAGTCTG	58.6
miR-221-3p	MIMAT0000278	AGCTACATTGTCTGCTGGGTTTC	57.4
miR-95-3p	MIMAT0000094	TTCAACGGGTATTTATTGAGCA	52.4

3.4.10 Reverse transcription of RNA from OKF6 cells

For reverse transcription of total RNA from OKF6 cells, the OmniScript RT kit from Qiagen was used. The reaction volume was 20µl, the reagent volumes are shown in Table 3.5.

Table 3-5 Pipetting protocol for RNA reverse transcription

Reagent	Quantity µl
10X buffer	2µl
dNTP Mix	2µl
OligodT primer	2µl
OmniScript enzyme	1µl
RNA template +free RNase water *	13µl

* RNA amount depends on the concentration of the RNA template.

Afterward, the mixture was incubated for 60 minutes at 37˚C in a water bath (Sigma-Aldrich). The cDNA was then amplified and tested as previously described (paragraph 3.5).

3.4.11 Quantitative real time polymerase chain reaction

The level of RNA expression was analysed using Real Time PCR. Amplification during the exponential phase was monitored and thus, quantitative differences between miRNA expressions could be detected in the samples.

The SyBR Green Master Mix (Roche) and a QuntaStuido ™ 3 Real Time PCR machine (Thermo Fisher Scientific) were used to detect the amount of DNA template in the samples.

The total qPCR reaction consisted of cDNA from patients with OLP (diluted to 1:5 or 1:3 in nuclease free water), the miRNA-specific forward primer, SyBR Green Mix and nuclease free water (Table 3.6). Triplicate samples were loaded onto 96-well plates and run on a real time PCR thermocycling machine. β-actin was used as a reference gene to normalise expression levels.

Table 3-6 Pipetting protocol of the qPCR reactions

Reagent	Quantity
cDNA	1 µl
Universal primer	1 µl
Forward primer	1 µl
SyBR Green	5 µl
Free RNase water	2 µl

Relative differences of the miRNA and target genes levels in patient samples were calculated using the comparative Ct method (Schmittgen and Livak, 2008). Accordingly, Ct of the actin control was subtracted from the Ct value of the test sample (ΔCt). Data in the figures are presented as -ΔCt at a log2 scale. Similarly, in miRNA-mRNA, the calculation of ΔΔCt involves the subtraction of the Ct value of the target gene for the OLP and control group from the Ct for miRNA of similar groups.

3.4.12 Target gene selection

The analysis of miRNA expression by NanoString identified 9 significantly upregulated and 9 downregulated miRNAs. The next step was to select and validate target genes for each miRNA. Although computational prediction tools are useful and extensively used in miRNA target gene discovery, the percentage of false-positive and -negative findings is substantial.

To identify up- and down regulated miRNAs in OLP, the tools listed below were employed. Predicted targets were further narrowed down to focus on genes that influence signalling pathways in OLP.

1. Target Scan human (www.targetscan.org)
2. DIANA (www.diana.imis.athenainnovation.gr/DianaTools)
3. Exiqon (www.exiqon.com/miRSearch)
4. mirTarBase (www.mirtarbase.mbc.nctu.edu.tw)

For each miRNA, the most commonly predicted targets identified by the four predicting websites were compiled. The predictions were then assessed for a potential involvement in OLP pathogenesis with the aim of minimising the number of target genes.

3.4.13 Primer design for targeted genes

Primers for targeted human genes were designed by using software from NCBI (USA) or the Primer3Plus package. The parameters for primer selection were an amplicon size between 100 bp to 130 bp, an annealing temperature between 50˚C to 64˚C and GC content between 20 to 80% with the optimum being 50%. Alternatively, primer sequences from published work were used. Oligonucleotides were synthesised by IDT (UK). All primers are listed in Table 3.7.

Table 3-7 List of primers for target genes

Target gene	prime3plus	Published primers	Annealing temperature
MYC	F:GGCATTTAAATTTCGGCTCA	F:GCTGCTTAGACGCTGGATTT	59
	R:GATTCCAGAGAATCGGACA	R:CACCGAGTCGTAGTCGAGGT	60
ZEB	F: CACGCTTGCTGTCAGTGTTT	F:AGACATGTGACGCAGTCTG	50
	R:CACCAGCATGGATGAAATG	R:ATGTGTGAGCTATAGGAGC	55
CXCL12	F:AGGCTGCCTTAGGTCTCTCC	F:GAGCCAACGTCAAGCATCTCAA	64
	R:TGCAATCAATTGAGGGATGA	R:TTAGCTTCGGGTCAATGCACAC	64
IL6R	F:CCTCGACTTCCTGGTCTCAG	F:GAC AAT GCC ACT GTT CAC TG	63
	R:GCCTAGGTGTTCCAGAGCAG	R:GCT AAC TGG CAG GAG AAC TT	65
MMP1	F:GCGAGATCCTCTCCATTTTG	F:CTCTGGCCAGCCTGCAAGATA	65
	R:GGGTGGATGTGCAAAGAAGT	R:CCGGAACTCTCGATGGTGGTA	65
CCND1	F:CAGAGCTCCCTTCTGACACC	F: CAGAGGCGGAGGAGAACAAA	63
	R: GGATGTCGACCAGTCTGGAT	R:ATGGAGGGCGGATTGGAA	63
TAB2	F:CCACTGCTACAGCCAACTGA	F:TATTCAGCACCTCACGGACCCT	64
	R:CTTCTCCCCTCCTTCATTCC	R:CTTTGAAGTCGTTCCATTCTGGC	63
MCL1	F:CTTGGGTTTAATGGGAAGCA	F:GATGATCCATGTTTTCAGCGAC	63
	R:AGCCTTCGTAGCAACAGGAA	R:CTGGGATGGGTTTGTGGAG	63
CDK6	F:CTCAGTCACGAGCCATGAAA	F:TGGAGACCTTCGAGCACC	59
	R:AGTCTGGCCAAGCAAGTCAT	R:CACTCCAGGCTCTGGAACTT	59
CA12	F:GCCACAGAAGATGCACAAGA	F:GTC TTG GGA GCC TGT TTT GC	62
	R:TCTTTCTCTGGACGGTGCTT	R:TTG CTT CGT CAT GAG GGT TGT	62
BCL2	F:TGATGTGAGTCTGGGCTGAG	F:CTCGTCGCTACGTCGTGACTTCG	60
	R: GAACGCTTTGTCCAGAGGAG	R:CAGATGCGTTCAGTACTCAGTC	60
IL24	F:CTGGGGAGGAGAAAAAGACC	F:ATCCAGGTCAGAGAATGTC CAC	61
	R:CCTTCTCCATCGCAGTTCT	R:CACAGGCGGTTTCTGCTATTC	61

3.4.14 Statistical Analysis

Statistical analysis of q-PCR results was performed by non-parametric Mann-Whitney U test. The relationship between miRNA and target mRNA were determined using the Spearman correlation coefficient test. P-values ≤ 0.05 were considered statistical significant.

3.5 Results

3.5.1 Keratinocyte cell line

Although oral lichen planus pathogenesis is not yet fully clarified, there is agreement that in OLP chronic, cell-mediated immune damage occurs to basal keratinocytes in the oral mucosa. Therefore, the keratinocyte cell line OKF6, derived from oral mucosa, was considered to be a better model system for OLP than HEK293 kidney cells. Cytokines released by the affected keratinocytes and the associated inflammatory infiltrate play a significant role in the selective recruitment of the T-cell-dominated infiltrate characteristic of OLP. Through this process, adhesion molecule expression is induced and further cytokine and chemokine release is triggered.

Generally, the experiments using OKF6 cells follow the same strategy as HEK293 cells. For cell culture experiments, however, a keratinocyte serum-free medium with glutamine and bovine pituitary extract was used. The total RNA was extracted using TRIzol reagent and samples were stored at -20 °C for further procedures. To determine the integrity of the RNA, samples were tested on a 2% agarose gel (see Figure 3.2). The extracted RNA displayed two clear bands representing 28S and 18S ribosomal RNA. These distinct bands as well as the lack of degradation products reflect a good RNA quality. In addition, the quantity of RNA was tested by measuring the absorbance at $OD_{260/280}$ with 294.9 ng/µl and 283 ng/µl, respectively, obtained for the RNA samples.

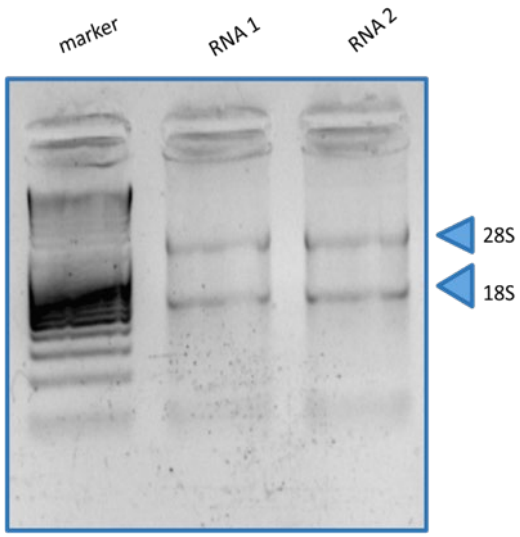

Figure 3-2 Extracted RNA from OKF6 cell lines. Lane 1 represents the DNA 1 kb ladder. Lanes 2 and 3 show the RNA samples. Arrows indicate 28S and 18S ribosomal RNA.

In the first instance, the list of genes to be investigated was established. The list was based on two criteria: First, genes were chosen with an established role in OLP and second they show confirmed expression in keratinocytes (Dickman 2015). This study describes the investigation of gene expression in normal cell lines such as OKF6 as well as a dysplastic cell line.

In the same study the gene expression level was investigated to define how these normal and dysplastic lines are similar to their parental lines. The list included the following thirteen genes *IL 6*, *INF-Y*, *ALOX 12*, *ANXA*, *IL1*B, *IL 27*, *IL 17*, *IL 29*, *SRGAP*, *ICAM*, *CX*CR, *CXCL* and *MMP*. RT-PCR was used to investigate the expression pattern for these genes. PCR primers were designed using the web based IDT primer design software (https://www.idtdna.com/site) similar to the procedure used for HEK293 cells. The parameters specified were an amplicon length <200 bp. Two different primers were designed for each gene. Moreover, a BLAST search analysis was performed for each primer to test its specificity. All primer parameters are shown in Table 3-8.

Table 3-8 The gene names, expression level, amplicon length, annealing temperatures and primer sequences are indicated

Gene	Expression Level	Amplicon Length	Annealing Temperature	Primer Sequence
IL 6	1.52	1- 162 bp	55C◦	F1:5'- ACAACCTG AACCTTCCAA AGA-3'
				R1:5-'GTAGTGAGGAACAAGCCAGAG-3'
		2- 186 bp	55C◦	F2:5'-GTAGTGAGGAACAAGCCAGAG-3'
				R2:5'-A ACTCATCTCATTCTGCGCA-3'
INF-Y	0.12	1- 171 bp	54C◦	F1:5'AAAGAGTGTGGAGACCATCAAG-3'
				R:5'-GGTCATTCAGATGTAGCGGATA-3'
		2- 141 bp	54C◦	F2:5' ATGTCCAACGCAAAGCAATAC3'
				R2:5'-TAGTCAGATGCTGTTTCAAGGT3'
ALOX12	5.61	1- 173 bp	55C◦	F1:5'GTTCCAGAAGCATCGAGAGAAG-3'
				R1:5'-TGAATGGACACTGAAGGCAG-3'
		2- 151 bp	54C◦	F2:5'GCAGACCGTAAGGATGATCTAC-3'
				R2:5'TGGAACTGCCTAGAAGACTTTG-3'
ANXA 1	101.6	1- 139 bp	54C◦	F1:5'GGCCTTGGAACTGATGAAGA-3'
				R1:5'CATAACTCAGACACATCTGGAG-3'
		2- 156 bp	54C◦	F2:5'-GGAACGCTTTGCTTTCTCTTG-3'
				R2:5'CAATACATCCTTACCACCAGAA-3'
IL1B	278.7	1- 120 bp	54C◦	F1:5' CATGGGATAACGAGGCTTATGT-3'
				R1: GGTGGAGAGCTTTCAGTTCAT-3'
		2- 199 bp	54C◦	F2: 5'GCACCTTCTTTCCCTTCATCT-3'
				R2: 5'ACCACTT GTTGCTCCATATCC-3'
IL 27	41.50	1- 169 bp	54C◦	F1:5-' CTCCTTGGAGCTCGTCTTATC-3'
				R1: 5'-GCCAAGACTCCAGTCCTAAA-3'
		2- 117 bp	55C◦	F2: 5'-TGCCAGGAGTGAACCTGTA-3'
				R2: 5'TGGTGGAGATGAAGCAGAGA-3'
IL 17	46.9	1- 139 bp	54C◦	F1: 5' GACAGCCTCATTTCGGACTAA-3'
				R1:5' GTACTCAGTCAACCTTCCTTCT-3'
		2- 100 bp	55C◦	F2: 5'-ACCGGAATACAATACCAATCC-3'
				R2: 5'-GGATATCTCTCAGGGTCCTCAT-3'
IL 29	5.799	1- 192 bp	54C◦	F1: 5-'GAGGCATC TGTCACCTTCAA-3'
				R1:5-' AGGGCTGCAGCTTCATAAATA-3'
		2- 142 bp	54C◦	F2: 5-'CC ACATTGGCAGGTTCAAATC-3'
				R2:5-' AAGCCTCAGGTCCCAATTC-3'
SRGAP	8.474	1- 185 bp	55C◦	F1: 5'-TGACGTCTCCAGCCAAATTC-3'
				R1: 5-'GTCCATCTCAATCTCTGCCTTC-3'
		2- 164 bp	54C◦	F2:5-' AAGCGGTCTTGGAGGTATTG-3'
				R2: 5'-CGGATCTCTTGACCTGAGTATC-3'
ICAM	27.15	1- 135 bp	55C◦	F1: 5'-CCCAAGTTGTTGGGCATAGA-3'

		2- 191 bp	55C◦	R1: 5’- CCCATCAGGGCAGTTTGAATA-3’ F2:5’CCGATTGCTTTAGCTTGGAAATT3’ R2: 5’-GGGCGCGTGATCCTTTAT-3’
CXCR	0.94	1- 193 bp 2- 164 bp	54C◦ 55C◦	F1:5’TTTGACCGCTACCTGAACATAG-3’ R1:5’-CCACCTGTGGGAAGTTGTATT-3’ F2:5’-CCCAGACTTCATCTTCCTGTC-3’ R2:5’-GGATGTGGGCATAGCAGTAG-3’
CXCL	113.1	1- 184 bp 2- 195 bp	54C◦ 55C◦	F1:5’GGAACAGAAGAGGAAAGAGAC-3’ R1:5-’TAGGACAGTGTGCAGGTAGA-3’ F2:5’-CGAAGTCATAGCCACACTCAA-3’ R2:5’-GCTGTGTCTCTCTTTCCTCTTC-3’
MMP	7.86	1- 178 bp 2- 111 bp	54 °C 55 °C	F1:5’-GAGCTTCCTAGCTGGGATATTG-3’ R1:5’-CCACATCTTGCTCTTGTGTTTC-3’ F2:5’-GCCTTCCAACTCTGGAGTAATG-3’ R2:5’-AGGAGAGTTGTCCCGATGAT-3’

Initially, the genes were divided into three groups. Each of the groups followed the same protocol. The cDNA synthesis was performed using the Omniscript kit (Qiagen) in 10 µl total reaction volume. DNA sequencing of the amplified PCR fragment by Source Bioscience confirmed gene specificity.

The first group of genes included *IL6*, *INF-Y*, *ALOX 12*, and *ANXA*. The initial PCR included two different primer pairs, 54 ˚C annealing temperature and 40 cycles. As shown in figure 3.3, certain genes appear to be expressed in OKF6 as the bands of the expected length were obtained. *ANXA* primer pairs amplified expected clear bands of 139 bp and 156 bp (lanes 2 and 3), however, there were unspecific bands underneath. *ALOX* 1 and 2 primers were expected to yield bands of 173 bp and 151 bp respectively, though both products were longer (lanes 4 and 5). Similarly, *IL6* primers and *IFN-Y* primers only resulted in unspecific bands (lanes 6-9).

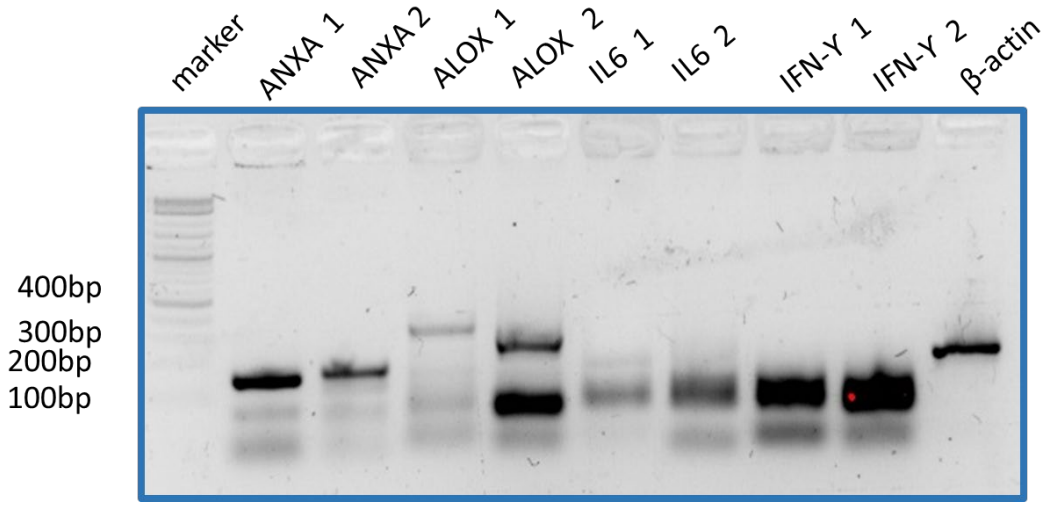

Figure 3-3 Gel photo of PCR reactions for the first group of genes. Lane 1 represents the DNA ladder, lanes 2-9 show *ANXA* specific fragments at 139, 156 bp, *ALOX* (expected 173 and 151 bp), *IL6* (162 and186 bp) and *IFN-Y* (171 and 141 bp, respectively). Lane 10 exhibits β-actin at 149bp.

To improve the outcome for unsuccessful reactions PCR conditions were modified. The annealing temperature was optimised with four different temperatures, 52 °C, 54 °C, 56 °C, 58 °C (see figures 3.4 A and B).

Figure 7A

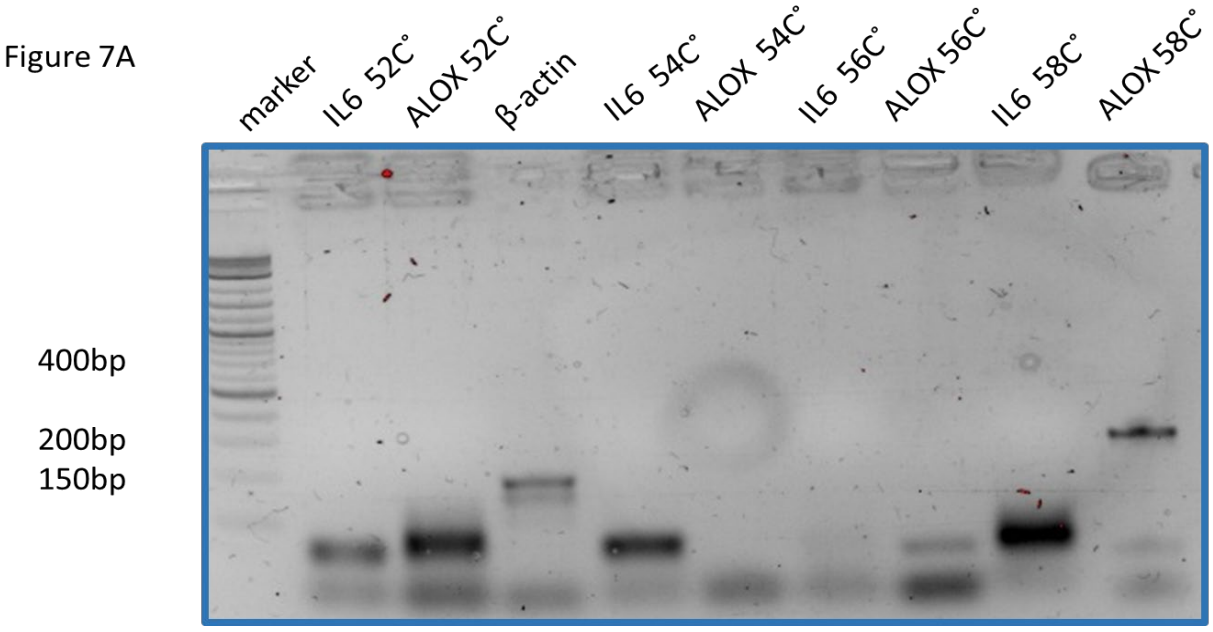

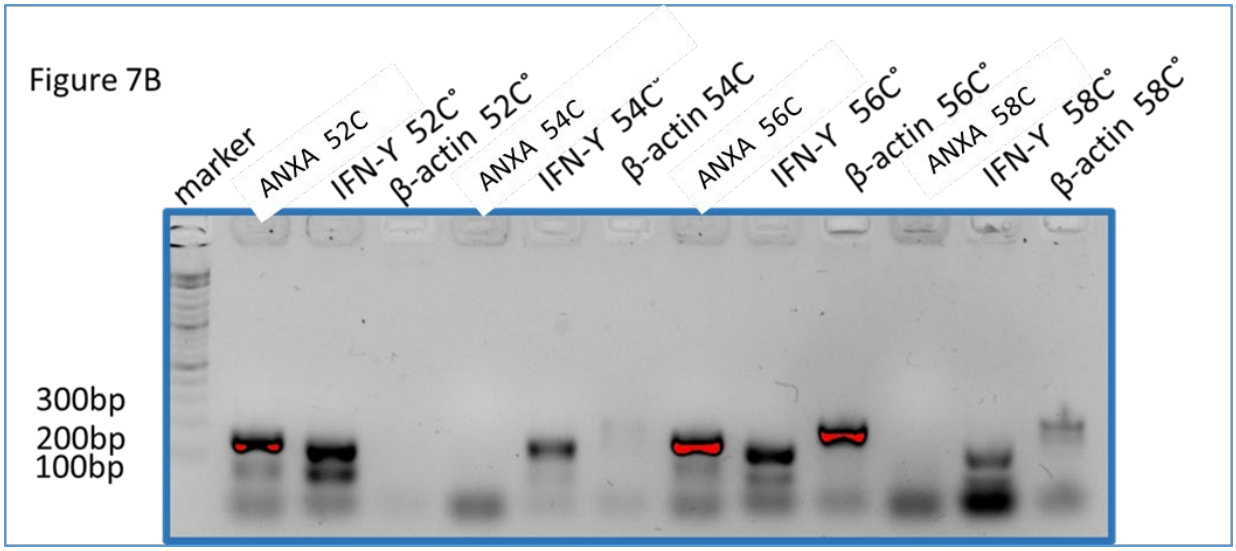

Figure 3-4 A and B Optimisation of annealing temperatures for PCR reactions for the first group of genes. (A) Annealing temperature optimisation for IL6 and ALOX. Expected amplicon sizes are 162 bp (*IL6*) and 173 bp (*ALOX*). β-actin was used as a reference gene. (B) Annealing temperatures optimisation for *ANXA* (139bp amplicon length) and *IFN-Y* (171bp amplicon length). β-actin as a reference gene.

The PCR optimisation revealed unspecific bands for *ALOX12* (173bp amplicon length) at 52 °C, 54 °C and 58 °C, although the band obtained with 56 °C was close to the expected band length. Regarding the *IL6* and *INF-Y* genes, the bands represented unspecific amplification because of the wrong band size or multiple bands, as with the *IFN-Y* primer pair 1 at 56 °C and 58 °C. Although there was no signal for *ANXA* with 54 °C and 58 °C annealing temperature at 56 °C, a single strong band was obtained (Figure 7B lane 8). *INF-Y*, *IL6* and *ALOX 12* primer pairs gave multiple amplicons. Based on these results, 56 °C degree was considered the optimal annealing temperature for this group of genes and reactions were repeated with these settings (Figure 3.5).

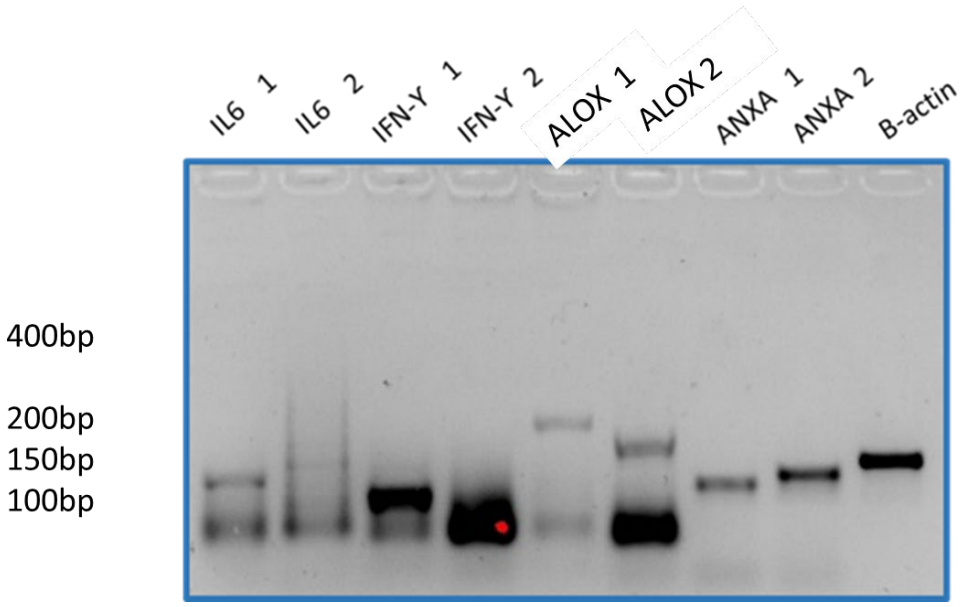

Figure 3-5 PCR samples for genes *IL6*, *IFN-Y*, *ALOX* and *ANXA* in OKF6 cells at 56 °C annealing temperature

To prove the validity of the amplified fragments the DNA was sequenced (Source Bioscience). As the additional bands in the reactions *ALOX12*, *INF-Y* and *IL6* may interfere with DNA sequencing, the bands were extracted from the gel (figures 3.6 A and B). Conversely, the band amplified with *ANXA* specific primers did not require size selection and was directly purified using the PCR purification protocol (see material and method section).

Figure 9A

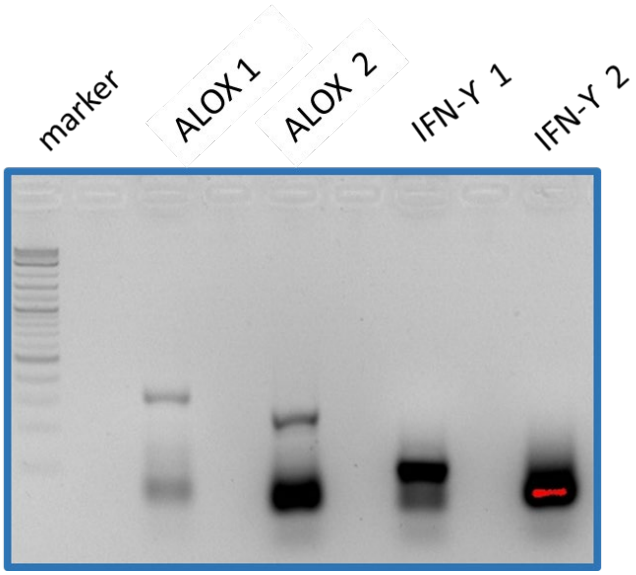

Figure 9B

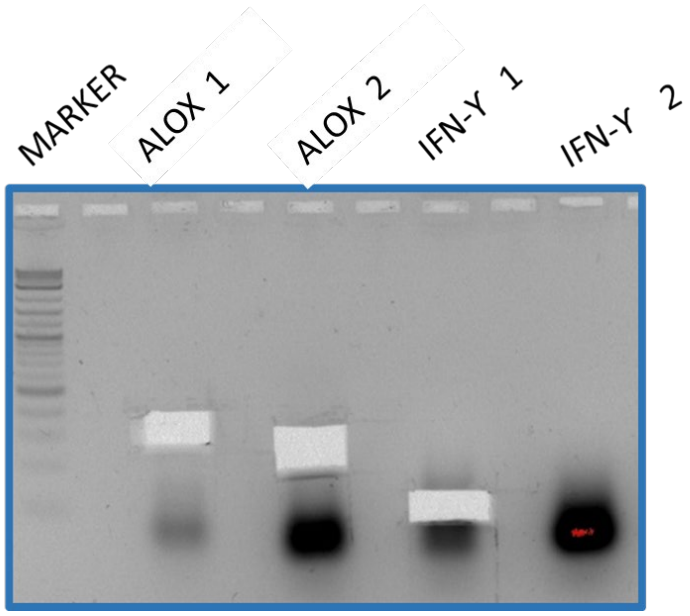

Figure 3-6 A and B gel photo of PCR fragment purification. (A) Bands for genes *ALXO* and *IFN-Y*. (B) Gel after cutting out the bands for purification**.** Note, *ALOX* 1 and 2 are representing *ALOX12* band in agarose gel also how extracted from the gel, same with *INF-γ* 1 and 2

The DNA sequencing of PCR samples was performed by Source Bioscience. *ALOX12* and *IL6* have a level of expression of 5.5 and 1.5 in OKF6 cells, respectively as reported by published data. The DNA sequence was tested by BLAST which confirmed the

identity of *ALOX 12* and *IL6* (Figure 3-7). The *ANXA* gene has high expression levels in OKF6 cells, the DNA sequence was readable and a BLAST search confirmed the identity.

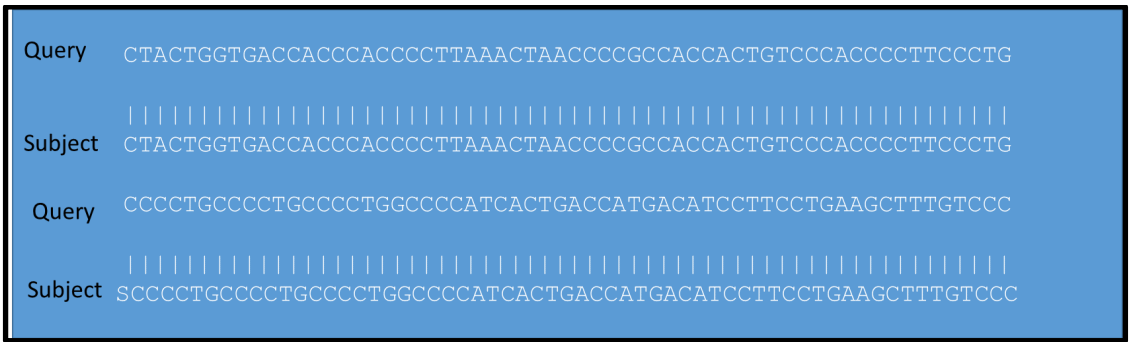

Figure 3-7 A fragment of the 173bp amplicon for ALOX12 shows identity between the query sequence and the gene.

The experiments focusing on the second group of genes, *IL1B*, *IL27*, *IL17* and *IL29* followed the same strategy of cDNA synthesis, PCR reaction and optimisation as the previous experiments. Figure 3.8 shows the agarose gel photo of the reactions with two different primer pairs per gene. The gel revealed the expected bands for *IL1B* using both primer pairs (120 and 190 amplicon length). The saturated signal indicated efficient amplification. *IL27* at 169 bp exhibits a clear expected band. Conversely, there was no band visible for the other *IL27* primer pair (117bp). The *IL17* and *IL29* bands revealed the same pattern of expression where both genes show a band with the first primer pair at 139 and 192 bp, respectively. Both the *IL17* and *IL29* band are faint although they represent the expected size.

As in the previous experiments, the amplicons were sequenced to confirm the correctness of the sequence from the OKF6 cells. All bands were cut out of the gel with the intention of being sequenced. The results confirmed the DNA sequence for *IL1B*, *IL27*, *IL17* and *IL29*, respectively.

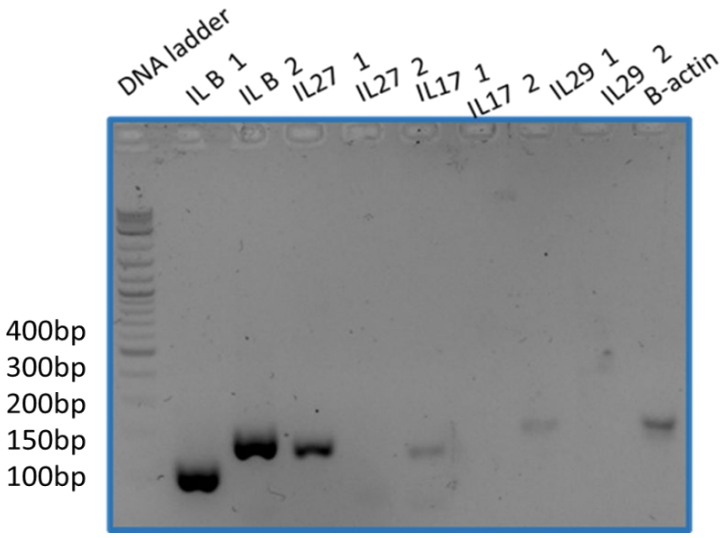

Figure 3-8 Amplicons from the second group of genes on agarose gel. Expression of genes *IL1B*, *IL 27*, *IL17*, *IL29* in OKF6 cells detected by two different primer pairs for each gene. Lane 1 represents the DNA ladder, lanes 2 and 3 *IL1B* (120 and 199bp amplicon length), lanes 4,5 illustrate *IL27* at 169 and 117bp amplicon length, lanes 6,7 represent *IL17* at 139 and 100bp amplicon length, lanes 8,9 show *IL29* at 192 and 142bp amplicon length. The last lane presents β-actin at 149bp as a positive control.

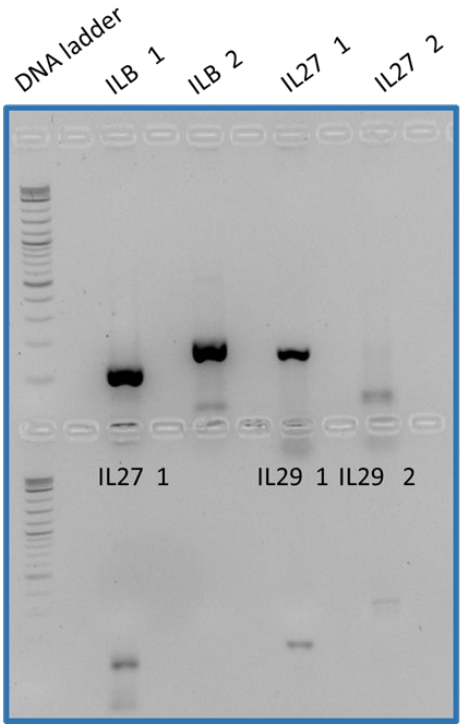

Figure 3-9 Agarose gel with PCR samples for the second group of genes prior to cutting out the DNA for sequencing.

For the last group of genes, *SRGAP*, *ICAM*, *CXCR*, *CXCL*, *MMP*, the first PCR reaction was performed with an annealing temperature of 54 °C. Two different primers pairs were utilised for each gene to investigate their expression in the OKF6 cells. The *SRGAP* bands were of the expected size with 185 bp. However, the second signal exhibited unspecific bands underneath the expected band. With regard to the *ICAM*, the bands at 135bp and 191bp were clear, strong and of the expected size (Figure 3.9). In contrast, the *CXCL* bands were not of the expected length and there were no *MMP* and *CXCR* bands. Different annealing temperatures were applied (52 ˚C and 56 ˚C) to amplify *CXCL*, *CXCR* and *MMP* (Figure 3.10).

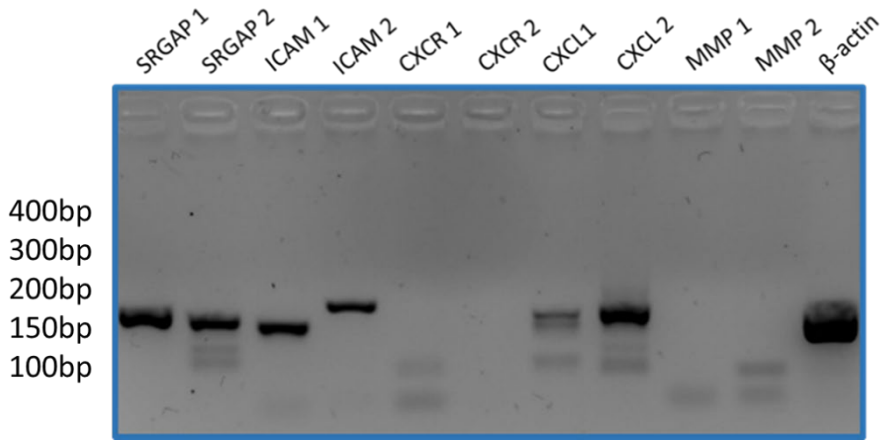

Figure 3-10 Amplicons from the last group of genes on agarose gel and their expression in OKF6. Lanes 1-2 show *SRGAP* at 185 bp and 164 bp, lanes 4-5 show *ICAM* at135 and 191 bp, lanes 5-6 show *CXCR* at 193 bp and 164 bp, lanes 7-8 show *CXCL* at 184 and 195 bp, lanes 9-10 show *MMP* at 178 and 111 bp. The last lane presents β-actin as a reference at 149 bp.

The gel photo (Figure 3.11) represents the outcome of optimised PCR reactions using different annealing temperatures. Interestingly, both temperatures gave similar bands for *CXCL*, *CXCR* and *MMP*. *CXCL* primer pair 1 (184 bp amplicon) revealed the expected faint band at 52 °C in addition to unspecific bands underneath. The annealing temperature of 56 °C gave a strong band of the expected size. The second *CXCL* primers exhibit a strong band of expected 195 bp at both annealing temperatures.

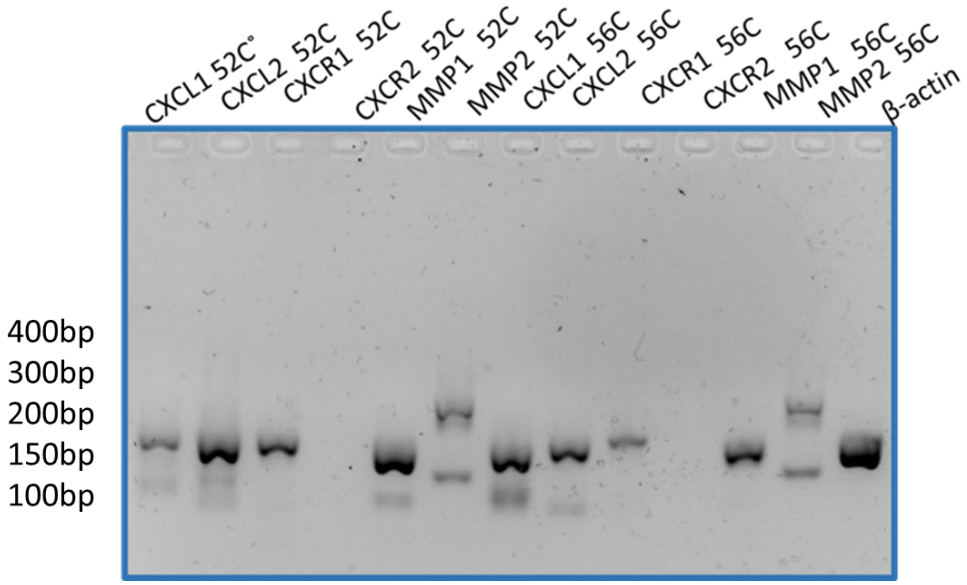

Figure 3-11 Agarose gel photo of PCR optimisation. Annealing temperatures of 52 °C and 56 °C were used for gene fragments of *CXCL*, *MMP* and *CXCR* with two different primers. β-actin was used as a control.

The *CXCR* primer pair 1 (193 bp amplicon) gave an expected strong band at 52 °C and a faint one at 56 °C. No band was amplified with *CXCR* primer pair 2 (164 bp amplicon) at the two different temperatures. In regard to the MMP primer pair, a clear strong single band of the expected 178 bp was obtained at 52 °C as well as at 56 °C. The second *MMP* reaction delivered a 111 bp band at 52 °C and 56 °C with faint unspecific bands. DNA sequencing confirmed the correctness of all the bands described above. Table 3.9 shows a summary of DNA sequencing results of all the tested genes.

Table 3-9 Summary of DNA sequencing results

Gene name	DNA sequence
ANXA	Confirmed with 156bp Primer
ALOX12	Confirmed with both Primers
IL6	Confirmed with both Primers
IFN-Y	Non-Readable
IL1B	Confirmed with both Primers
IL17	Confirmed with 139bp Primer
IL27	Confirmed with 169bp Primer
IL29	Confirmed with 192bp Primer
SRGAP	Confirmed with both Primers
ICAM	Confirmed with both primers
CXCR	Confirmed with 193bp primer
CXCL	Confirmed with both primers
MMP	Confirmed with 178bp primer

3.5.2 RT-PCR analysis of miRNA expression in OKF6 cells

In the previous chapter we have found nine upregulated and nine downregulated miRNAs. To confirm these findings with quantitative RT-PCR (q-PCR), we used OKF6 cell line that reflects well the oral mucosa and should have similarity in miRNA expression with native tissue, to setup the experiments. Thus, the target gene assays were also established with OKF6 RNA as it follows.

RNA was extracted from the OKF6 cell line and mature miRNAs were polyadenylated by poly (A) polymerase and reverse transcribed into cDNA. End-point RT-PCR analysis was performed to assess the endogenous expression of upregulated and down regulated miRNAs.

As shown in figure 3.12, the PCR experiments produced a clear band on the agarose gel for miR-205, miR-23b and let-7 (left panel). Comparable results were obtained for miRNAs miR-155, miR-222 and miR-29a, miR-23a, miR-146a and miR-342 did not produce distinct products. The actual length of these miRNAs is roughly 22 bp. However, the polyadenylation and the attached linker-primer extends the short miRNA so that it can be detected on the gel at a length of about 100-120 bp.

The results in figure 3.12 confirm the validity of the approach and the miRNA primers to measure expression levels of miR-205, miR-23b let-7, miR-146a, mir-155, mir-222 and miR-29a in RNA from OLP and control patient samples. However, primer dimers were detected on the agarose gel, observed as a 30-50 base-pair (bp) band or smear of moderate to high intensity. PCR primer dimers, as the name suggests, can form from primer molecules that hybridise as a result of the complimentary base strings in the primers. Due to competition for PCR reagents caused by the DNA polymerase amplifying the primer dimer, the PCR amplification of the target DNA sequence may be inhibited. Primer dimers may also obstruct precise quantification in quantitative PCR. However, primer dimers can be identified by their melting-curve features since they often consist of short sequences and denature at a lower temperature than the target sequence. Using alternative primers is the most effective way to reduce the likelihood for primer dimers.

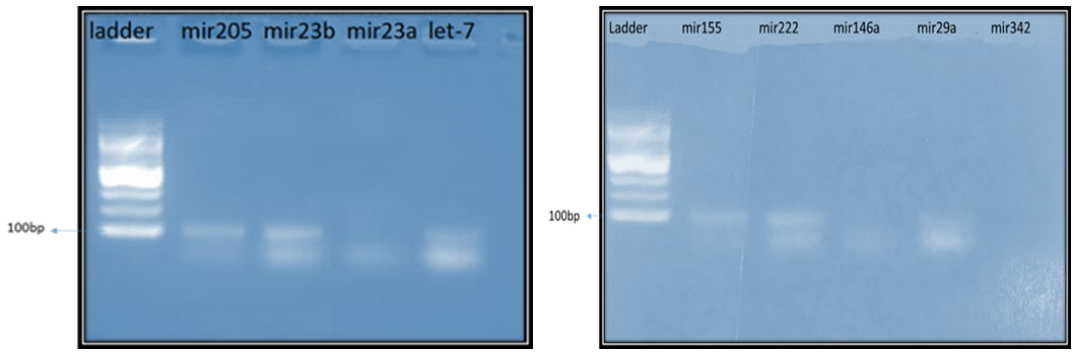

Figure 3-12 End-point PCR fragments of differentially expressed miRNAs (miR-205, miR-23a and b, let-7, miR-155, miR-222, miR-146a, miR-29a and miR-342). miRNA specific amplicons are approximately 100 bp. The lower signal represents primer dimers.

3.5.3 Quantitative RT-PCR analysis of miRNA expression in OLP patient samples

The RNA was extracted from the fresh frozen samples of 10 OLP patients who were diagnosed clinically and pathologically with disease and 8 controls. The RNA was extracted using the Qiagen RNAeasy mini kit. cDNA was prepared using a reverse transcription kit (miScript II RT Kit Qiagen). qPCR was performed using miRNA specific

primers and the adaptor primers from RT priming. The mean fold change was calculated using ΔCt values as described above.

The expression between OLP and control group was significantly reduced for miR-205 and miR-23b (P= 0.00044 and 0.0088 respectively). In contrast, let-7 expression was significantly increased in OLP patient samples compared to the control group (*p*= 0.01468) (Figure 3.13). Hence, let-7 qPCR result displays a different expression trend as compared to the NanoString data.

In addition, the miRNAs that were upregulated in OLP patients according to the NanoString analysis, i.e. miR-146a, miR-222, miR-342, miR-155 and miR-29a, were all confirmed by RT-qPCR. As shown in (Figure 3.14), miRNAs in OLP group represented a higher expression than the control group with significant *p* values of 0.0012, 0.00086, 0.00214, 0.00512 and 0.00062, respectively.

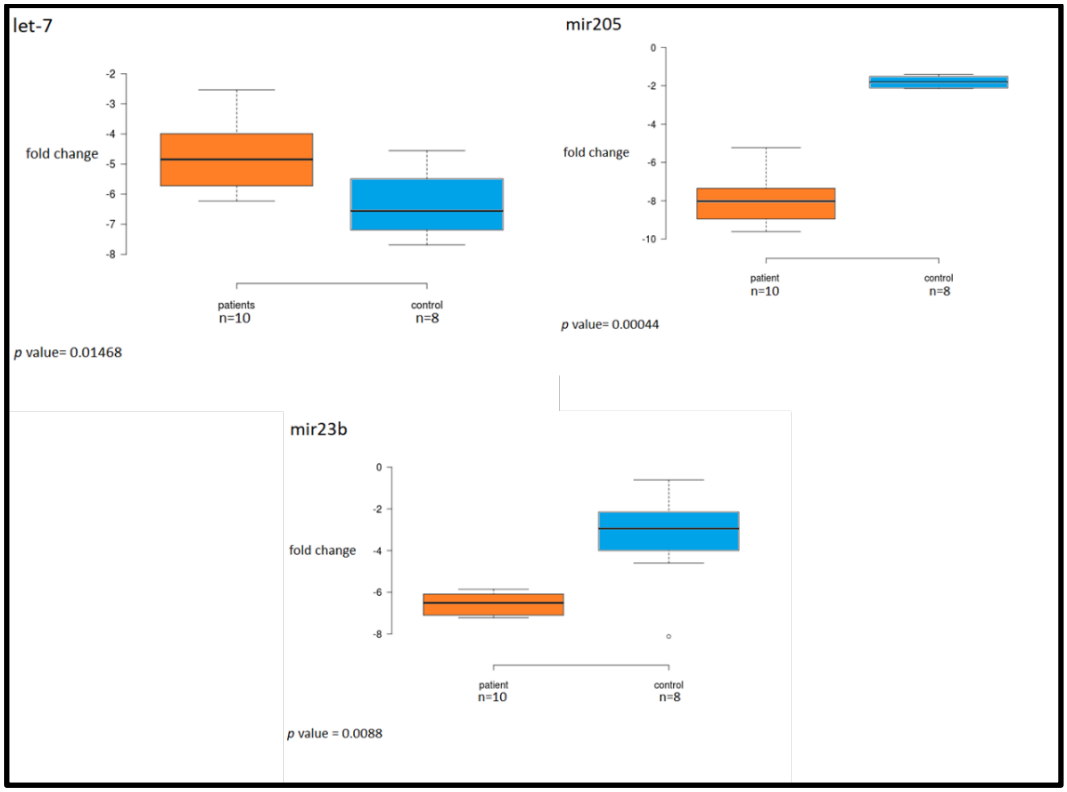

Figure 3-13 Expression of downregulated miRNA (as determined by Nano String) in OLP patients and the control group. The difference between OLP and control was determined by comparing the relative miRNA levels given as fold change compared to the NanoString controls (a combination of synthetic controls and housekeeping controls, see 2.4.6 Data analysis). Statistical significance was assessed by nonparametric Mann Whitney Test. The median value in patient samples for let-7, miR-205 and miR-23b were -4.844, -8.027 and -6.506 respectively. Whereas the median value in control samples were -6.555, -1.8101 and -2.951 in the same order.

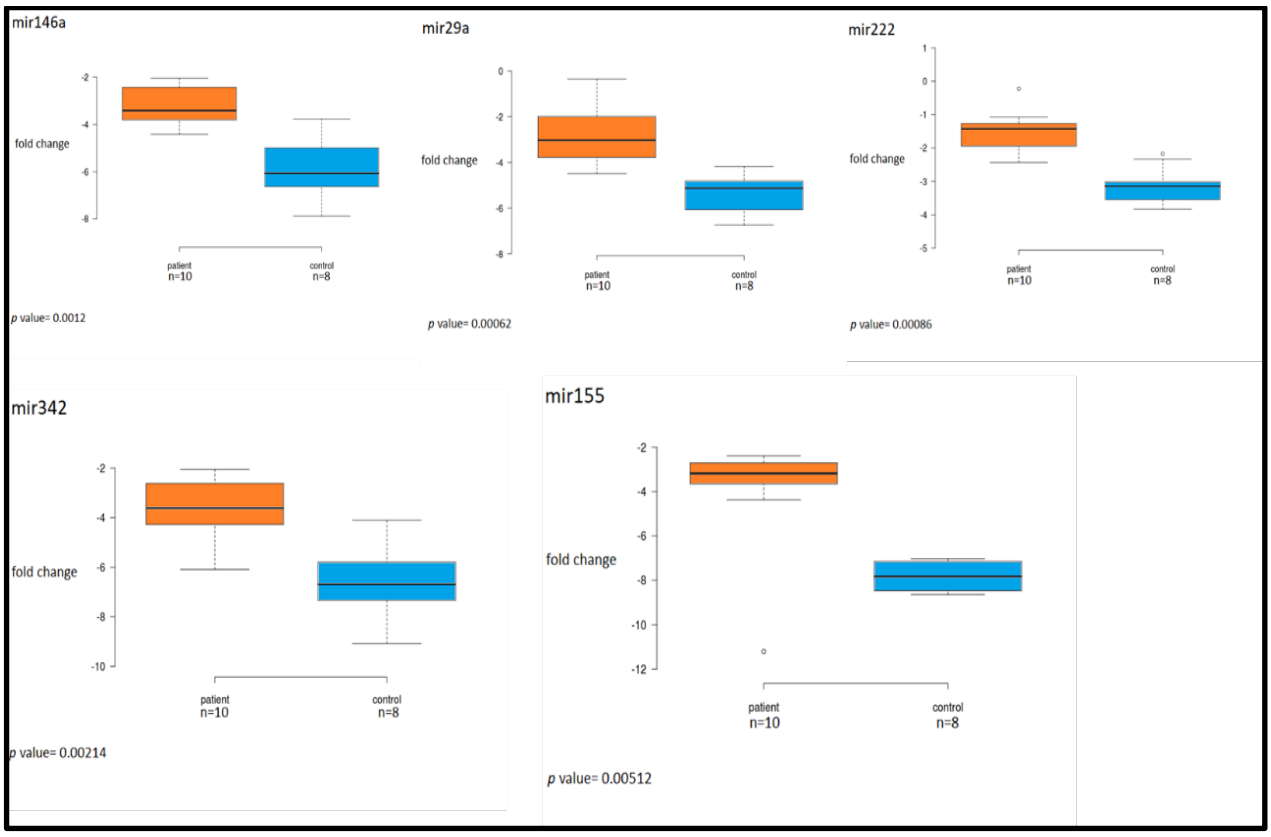

Figure 3-14 Expression of upregulated miRNA (as determined by NanoString) in OLP patients and the control group. The difference between OLP and control was determined by comparing the relative miRNA levels given as fold change compared to the Nanostring controls (a combination of synthetic controls and housekeeping controls, see 2.4.6 Data analysis. Statistical significance was assessed by nonparametric Mann Whitney Test. The median values of patient samples of miR-146a, miR-29a, miR-222, miR-342 and miR-155 were -3.4107, -3.033, -1.426, -3.618 and -3.189, respectively. Whereas the median value of control samples was -6.0716, 5.1301, 3.294, 6.69181 and 7.829 in the same order.

3.5.4 RT-PCR analysis of potential miRNA target genes

miRNAs are regulators of specific genes and each miRNA has multiple targets. The next series of experiments aimed to identify and validate candidate genes that are potentially regulated by the differentially expressed miRNAs identified in the previous chapters. Various online tools were employed to search for predicted miRNA target genes. These lists were compared and common calls were given preference. Moreover, genes that relate to OLP pathogenesis and are potentially targeted by miRNAs were the selected. Tables 3.10 and 3.11 show a selection of target genes from four prediction websites for upregulated and downregulated miRNAs. Moreover, these genes play an established role in OLP development and progress. For example, MYC enhances the expression of TNF-ϒ which is involved in OLP pathogenies. CCND1 regulates TNF-α which may be a useful diagnostic tool and a potential prognostic marker in OLP. Inhibition of MMP1 activation

inhibits T-cell accumulation in OLP. Accordingly, by inhibiting MMP9, the cleavage of collagen is prevented, preserving the integrity of the basement membrane. In OLP lesions CDK6 is expressed in the epithelial basement cell layer which may induce cytokines that activate p53 and cause the progression of OLP.

The four gene prediction websites (DINAN, target Scan, exiqon and miRTarbase) use and weigh prediction parameters differently, hence divergence in the list of target gene was expected, as illustrated in tables 3.10 and 3.11. In our project we considered the first 100 target genes of each website then chose the common ones in all four predicting websites. In order to minimise the number of target genes for upregulated and downregulated miRNAs we focused on target genes with an established role in oral lichen planus. Table 3-12 lists the relation taken into consideration.

Table 3-10 List of most common target genes for upregulated miRNAs

miR-146a	**miR-155**	**miR-21**	**miR-222**	**miR-29a**	**miR-4516**	**miR-3195**	**miR-342**	**miR-139a**
TRAF6	*TAB2*	*TP53*	*CDKN1B*	*BCL2*	*STAT3*	*AIP*	*CA12*	*TP73*
MYC	*CCND1*	*IL12A*	*MMP1*	*CDK6*		*APC2*	*BMP7*	*ERBB2*
CXCR4	*MYC*	*BCL2*	*CDK6*	*MCL1*			*IL24*	*PTK2*
TLR2	*MMP1*	*MMP9*	*IL24*	*IL24*			*MYC*	
NFKB1		*PTEN*	*MYC*	*MYC*				

Table 3-11 List of most common target genes for downregulated miRNAs

miR-205	**miR-23a**	**miR-23b**	**miR-27**	**miR-221**	**miR-200**	**Let-7**	**miR-149**	**miR-95**
ZEB1	*CXCL12*	*NOTCH1*	*NOTCH1*	*CDKN1B*	*ZEB1*	*MYC*	*ACLY*	*CXCR1*
BCL2	*PTPN11*	*CDK6*	*CYP1B1*	*TIMP3*	*BAP1*	*CCND1*	*CCR4*	
IL24	*IL6R*	*TAB2*	*ST14*			*BCL2*		
MMP1		*MYC*	*MMP13*			*MHMGA2*		
TAB2		*CCND1*				*TAB2*		

Table 3.12: Target genes and their relation to OLP disease

Target gene	How related to OLP
MYC	Up regulates IL8, IL10 that relate to OLP progression
NOTCH1	Inhibited by TNF
BCL2	Induces TNF and activates NFκB
IL24	Inhibited by TNF-α
CCND1	Induced by TNF-α
MMP1	Detected in OLP as P53 regulator
TAB2	Inhibits IL1 and TNF-α
IL6R	Involved in NFκB pathway in OLP
CXCL12	Increases IL10 amount that stimulated by P53
ZEB	Increases TNF-α production
BMP7	Suppressor TNF
CXCR4	Regulate IL10
PTEN	Induce TNF-α
PTK2	Upregulated by TNF-α
CXCR1	Enhance IL8

These genes listed in table 3.12 can potentially play a role in the development and progression of OLP. For example, IFN- γ, which is involved in OLP pathogenesis, inhibits *c-MYC* gene expression (Harel-Bellan, Ferris et al. 1988). TNF-α which is highly

expressed in OLP may regulates *CCND1* (Krenn, Hofbauer et al. 2016). Inhibition of MMP1 activation inhibits T-cell accumulation in OLP (Suvarna, Chaitanya et al. 2020).

With the aim to determine the expression levels of potential target genes, primers were designed and tested using end-point PCR with RNA from OKF-6 cells. Moreover, the housekeeping gene β-actin was used to normalise the expression of each selected target gene. In the first step, end-point PCR was performed to test the primers. The results of the PCR showed the expected band lengths at an annealing temperature of 55 ˚C (Figures 3.15 A and B). However, the amplification efficiency appears to differ for the various genes analysed. The sequence was confirmed by DNA sequencing for the fallowing 7 target genes, i.e., matrix metalloproteinase1 (*MMP1*), carbonic anhydrase12 *(CA12*), interleukin 24 (*IL24*), cyclin dependent kinase 6 (*CDK6*), *MYC* proto-oncogene (*MYC*), TGF β-activated kinase binding protein (*TAB2*) and cyclinD1 (*CCND*1). All sequencing data are available in the appendix.

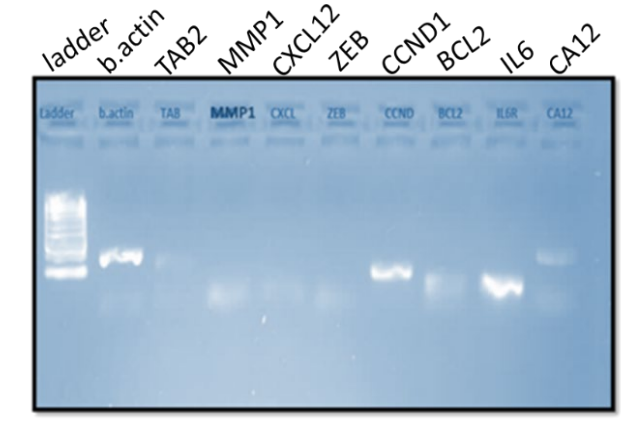

A

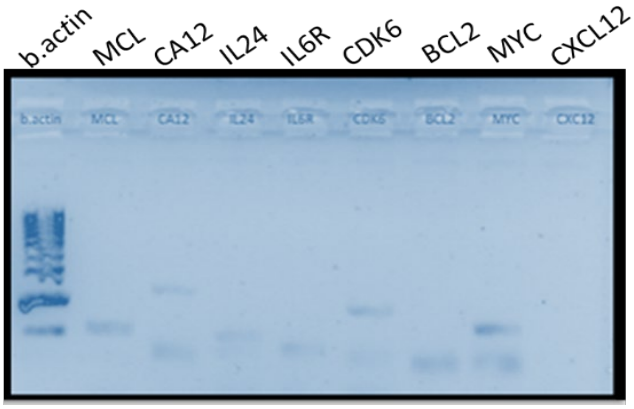

B

Figure 3-15 A and B: Agarose gel displaying amplified fragments of the target genes expressed in OKF-6 cell lines**.** The length of the amplified fragments is as follows: *MCL* 192 bp, *CA12* 182 bp, *IL24* 85 bp, *IL6R* 150 bp, *CDK6* 141 bp, *BCL2* 152 bp, *MYC* 103bp, CXCL12 108bp, *MMP1* 135 bp, *TAB2* 130 bp, *CCND1* 100 bp, *ZEB* 111 bp and *β-actin* 149 bp.

3.5.5 Quantitative RT-PCR analysis of target gene expression in OLP patient samples and controls

The cDNA samples of 10 patients with OLP as well as 8 controls were prepared using OmniScript RT kit from Qiagen and used for qPCR. The fold change was calculated according to the formula: Fold chance = $2^{-\Delta Ct\ (patients/control) - \Delta Ct\ (actin)}$

The mRNA expression levels of *MYC, IL24, CCND1, TAB, CA12, MMP1* and *CDK6* were assessed.

The mRNA expression of *MYC* was significantly decrease in OLP (p = 0.00086) compared to the white lesion control group. The fold change between patients and control was -1.53. Significance was tested using the nonparametric Wilcoxon Mann-Whitney test as shown in Figure 3.16

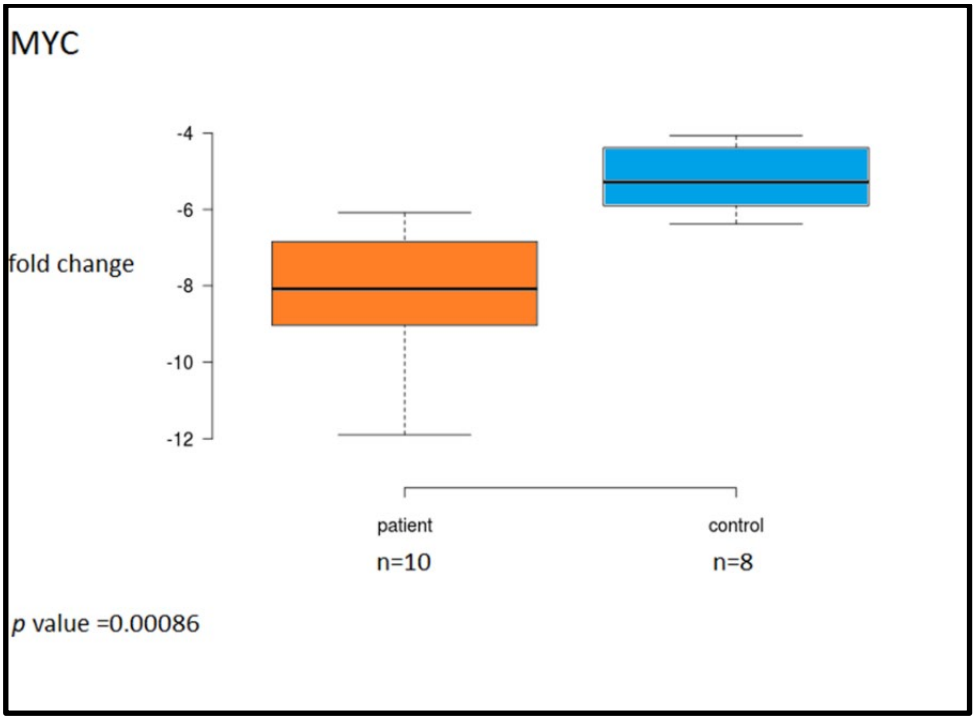

Figure 3-16 Expression of *MYC* mRNA in OLP patients and control samples. mRNA levels were determined by RT-qPCR and compared to β-actin. Fold change was calculated (ΔΔCt) and the median value of fold change was -1.53. Statistical significance was established using nonparametric Mann-Whitney Test.

The expression levels of target gene *IL24* in OLP patients and white lesion controls were next tested by RT-qPCR. The mRNA expression of IL24 in OLP samples was significantly reduced and the fold change between patients and control was -1.28 (Figure 3.17).

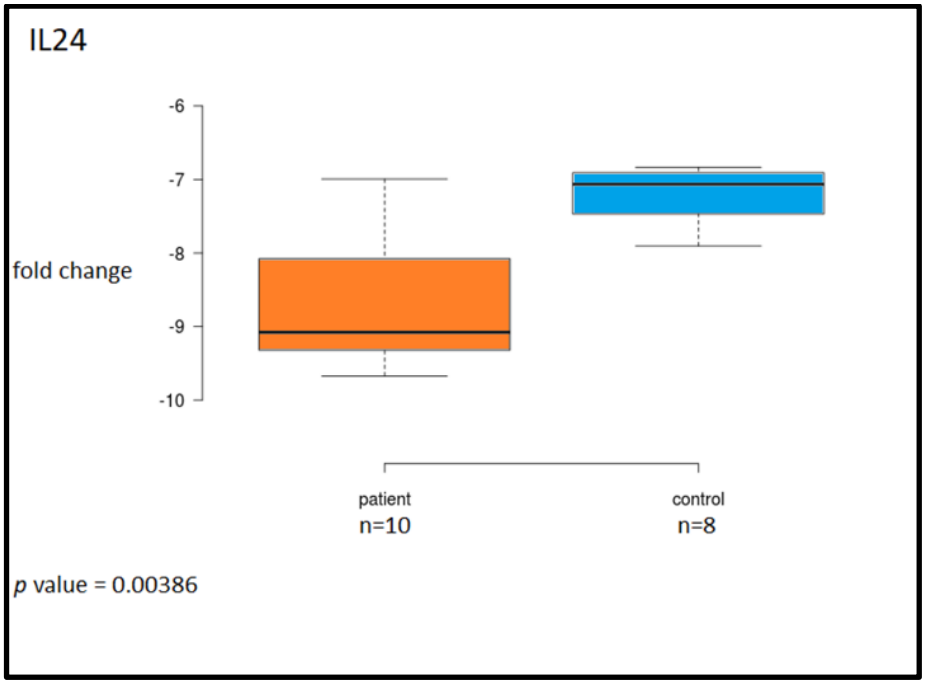

Figure 3-17 Expression of *IL24* mRNA in OLP patients and control samples. mRNA levels were determined by RT- qPCR and compared to β-actin. Fold change was calculated (ΔΔCt) and the median value of fold change was -1.28. Statistical significance was established using nonparametric Mann-Whitney Test.

For the target genes *MMP1*, *CDK6*, *CA12* and *TAB2*, the expression levels in OLP patients were significantly increased in comparison to the control group. The fold change was calculated between patients and control and the values were -0.55, -0.54, -0.52 and -0.58, respectively. The corresponding *p* values were 0.00214, 0.00044, 0.00062 and 0.00018 (Figure 3.18).

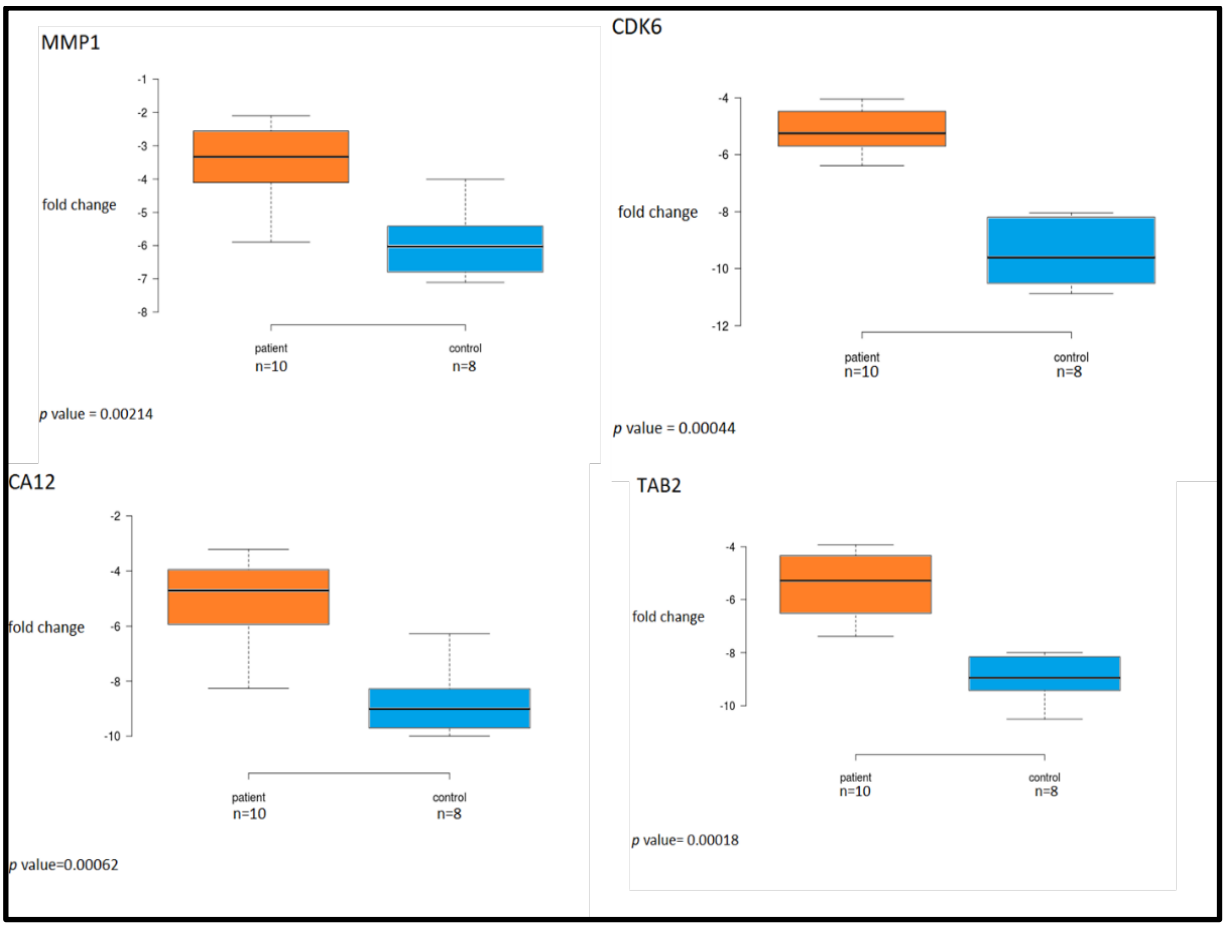

Figure 3-18 Expression of *MMP1, CDK6, CA12* and *TAB2* mRNA in OLP patients and control samples. mRNA levels were determined by RT- qPCR and compared to β-actin. Fold change was calculated (ΔΔCt) and the median values of fold change were (-0.55, -0.54, -0.52 and -0.58) respectively. Statistical significance was established using nonparametric Mann-Whitney Test.

The expression level of the target gene *CCND1* was also increased in OLP patients compared to white lesion controls but the difference was not significant ($p = 0.3$) and the fold change was -0.83 (Figure 3.19).

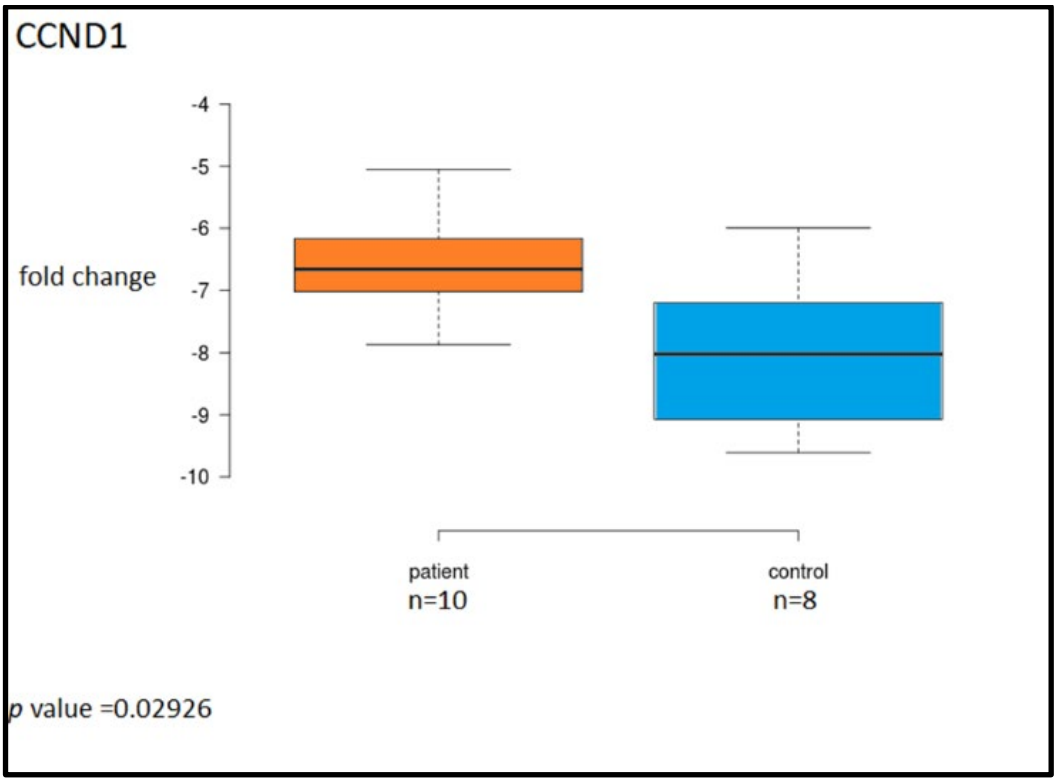

Figure 3-19 Expression of *CCND1* mRNA in OLP patients and control samples. mRNA levels were determined by RT- qPCR and compared to β-actin. Fold change was calculated (ΔΔCt) and the median value of fold change was -0.83. Statistical significance was established using nonparametric Mann-Whitney Test.

3.5.6 miRNA-mRNA relation

To identify potential miRNA-mRNA interaction networks, the quantitative miRNA and mRNA data from both OLP and control patients were compared in two different ways. First, the relationship between miRNA and target mRNA were determined using the Spearman correlation coefficient test (ρ). Correlations were calculated for the 3 downregulated miRNAs (miR-205, miR-23b and let-7) and the 5 upregulated miRNAs (miR-155, miR-146a, miR-222, miR-29a and miR-342) with their 7 potential target genes (*MYC*, *MMP1*, *CCND1*, *CDK6*, *TAB2*, *IL24* and *CA12*). Table 3.13 shows a summary of

the correlations between the target gene (mRNA) and miRNA in both the OLP patient group and the white lesion control group.

The Pearson Correlation Coefficient, which has a values between -1 and 1, is the most used method for measuring the linear relationship between two variables. The number one denotes a completely adverse linear association. Zero means there is no linear association. A perfect linear association is indicated with a value of 1.

The Pearson Correlation Coefficient, which is frequently represented by the symbol "r", enables us to determine how closely two variables are related. The link between the two variables is stronger the further r is from zero.

The following table shows a rule of thumb for interpreting the strength of the relationship between two variables based on the value of r:

Absolute value of r	**Strength of relationship**
$r < 0.25$	No relationship
$0.25 < r < 0.5$	Weak relationship
$0.5 < r < 0.75$	Moderate relationship
$r > 0.75$	Strong relationship

According to the assumption that high miRNA levels have a negative impact on the level of their target gene, a negative correlation would be expected between miRNA levels and the target gene. This effect should be observed in both OLP and control samples. This is indeed the case for miR-155-TAB2 and all the miR-23b targets (Table 3.13). All the other miRNA gene pairs demonstrate a positive correlation in at least one of the groups. A potential direct interaction between the two RNAs is therefore less likely and would not involve a canonical miRNA mechanism of action.

Table 3-8 Spearman correlation coefficients and its adjusted p values are listed in OLP patients and control group

	OLP group			**control group**		
miRNA-gene	r	details	p value	r	details	p value
miR-155-MYC	-0.381	negative weak	0.00222	0.16667	no relation	0.00094
miR-155-TAB2	-0.5091	negative moderate	0.00578	-0.2381	no relation	0 .12852
miR-155-CCND1	-0.579	negative moderate	0.00278	0.16667	no relation	0.00736
miR-155-MMP1	0.0303	no relation	0.01732	-0.45238	negative moderate	0.00194
miR-146a-MYC	0.7625	positive strong	0.00018	-0.07143	no relation	0.31732
miR-222-MYC	0.9697	positive very strong	0.00019	0.07143	no relation	0.00094
miR-222-CDK6	0.4047	positive moderate	0.00018	0.07143	no relation	0.00098
miR-222-IL24	0.3726	positive weak	0.00018	0.07143	no relation	0.00094
miR-222-MMP1	0.90736	positive very strong	0.00034	-0.28571	negative weak	0.00088
miR-342-MYC	0.27273	positive weak	0.00024	0.42857	positive moderate	0.04036
miR-342-IL24	0.409	positive moderate	0.00018	0.42857	positive moderate	0.01031
miR-342-CA12	-0.03	no relation	0.03752	0.42857	positive moderate	0.01352
miR-29a-MYC	-0.303	negative weak	0.00018	0.07143	no relation	0.79486
miR-29a-CDK6	-0.033	no relation	0.00044	0.7143	positive strong	0.00005
miR-29a-IL24	0.1272	no relation	0.00018	0.17144	no relation	0.00019
miR-23b-MYC	-0.1415	no relation	0.0114	-0.11905	no relation	0.02382
miR-23b-CDK6	-0.67607	negative weak	0.001	-0.11905	no relation	0.00138
miR-23b-CCND1	-0.67607	negative moderate	0.72786	-0.11905	no relation	0.00386
miR-23b-TAB2	-0.13939	no relation	0.14156	-0.619	negative moderate	0.00194
miR-205-MMP1	0.4384	positive moderate	0.00028	0.430952	positive moderate	0.00094
miR-205-IL24	0.09091	positive weak	0.030772	-0.53714	negative moderate	0.00004
miR-205-TAB2	-0.85481	negative strong	0.00906	0.51429	positive moderate	0.000044

let-7-CCND1	-0.3654	negative weak	0.00168	0.03	positive weak	0.01828
let-7-MYC	-0.42121	negative moderate	0.000023	0.2321	positive weak	0.05238
let-7-TAB2	-0.3333	negative weak	0.30772	0.40476	positive moderate	0.00544

Another way of testing a potential miRNA-RNA interaction involves the comparison of the differentially expressed miRNAs and establish whether upregulated miRNAs cause a decrease in the target genes and vice versa. The expression profiles of all differentially expressed miRNAs is presented in figures 3.20 – 3.27.

3.5.6..1 miR-155

The bioinformatics analysis predicted that miR-155 has four common target genes including *CCND1*, *MMP1*, *MYC* and *TAB2*. By quantitative real-time qPCR analysis, the expression of both miRNA and mRNAs were examined. miR-155 is significantly upregulated in OLP patients as compared to control patients in both NanoString and qPCR experiments. As outlined in figure 3.20, all the potential target genes of miR-155 are either expressed at a comparable level between the two groups or do show a slightly opposite trend to the miRNA levels, as one would expect with canonical miRNA action. Hence, the altered miRNA level may support an interaction between miR-155 and the proposed target genes.

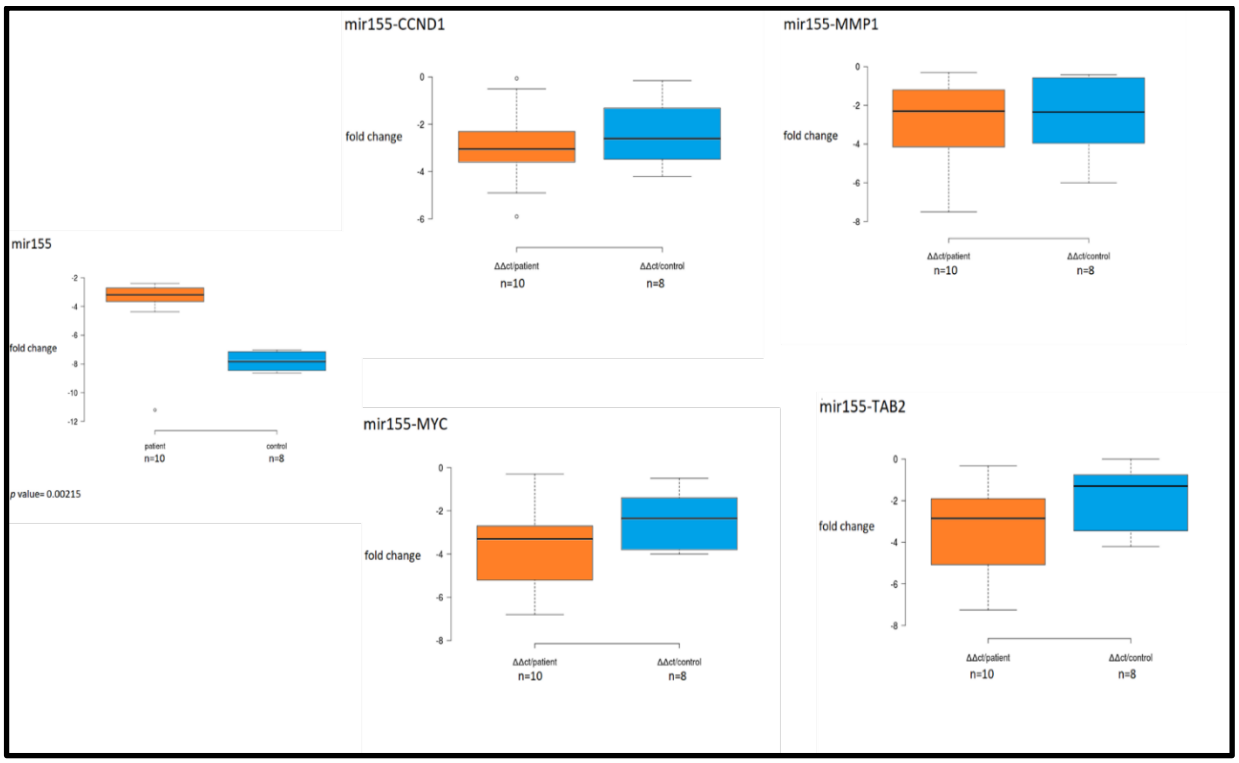

Figure 3-20 Comparison of expression between miR-155 and the proposed target genes (*CCND1*, *MMP1*, *MYC* and *TAB2*) in OLP patients and control group the miRNA levels given as fold change compared to the mRNA of target genes was determine by RT-qPCR and the median values of fold change in patients of miR-155 and their target genes were (-0.47, -0.95, -0.39 and -0.6) respectively. Statistical significance was established using nonparametric Mann-Whitney Test.

3.5.6..2 mirR-146a

According to the prediction websites, the *MYC* mRNA potentially binds to miR-146A. The expression of both the target gene and the related miRNA was significantly upregulated in the OLP group and the control group (Figure 3.21). The *p* value was 0.00018 and a very strong positive correlation was found according to the Spearman test (*r* value 0.7625). A canonical miRNA-mRNA interaction is therefore unlikely.

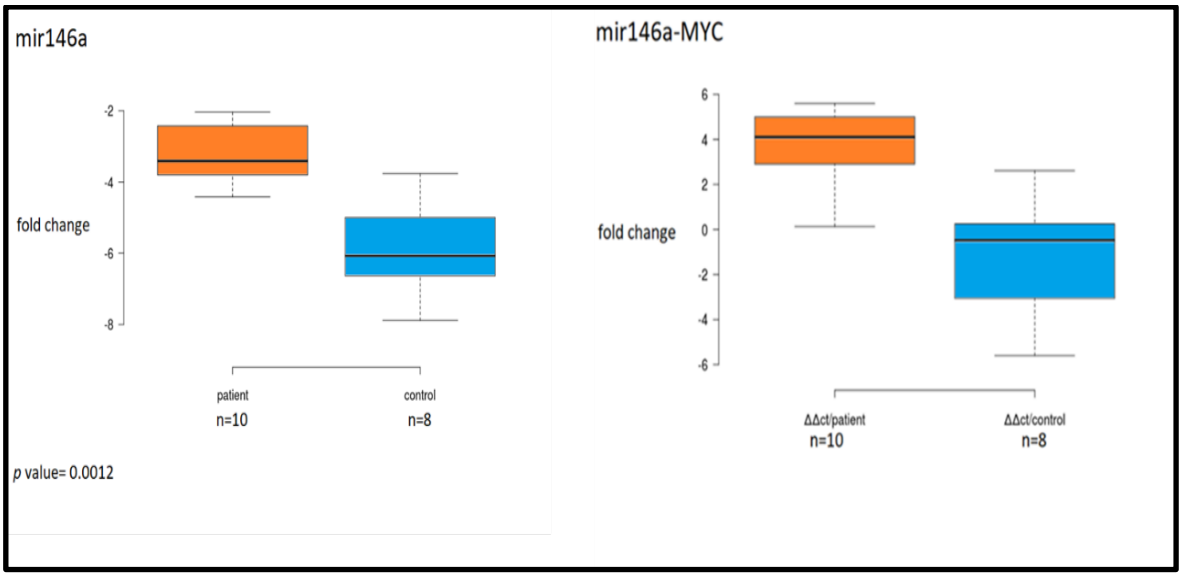

Figure 3-21 Expression correlation of miR-146a and *MYC* mRNA in OLP patients and control samples the miRNA levels given as fold change compared to the mRNA of target genes was determine by RT-qPCR the median value of fold change was -0.42. Statistical significance was established using nonparametric Mann-Whitney Test**.**

3.5.6..3 miR-222

The OLP patient group revealed significant upregulation of both miR-222 and the proposed target genes (*MYC, CDK6, IL24* and *MMP1*) with *p* values of 0.00019, 0.00018, 0.00018 and 0.00034, respectively. Figure 3.22 shows that all the potential target genes of miR-222 are either expressed at a comparable level between the patients and control groups or do reveal the same trend as the miRNA levels (and not an opposite trend as one would expect with canonical miRNA action). Therefore, the altered miRNA level does not appear to significantly affect the proposed target gene levels.

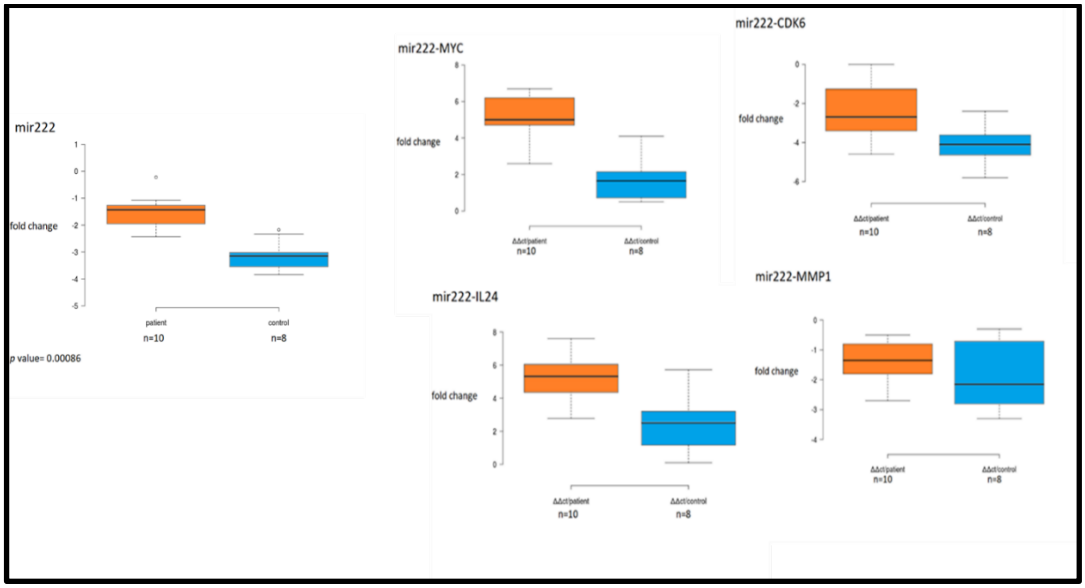

Figure 3-2 : Expression correlation of miR-222 and its potential target genes (*MYC, CDK6, IL24* and *MMP1*) mRNA in OLP patients and control samples the miRNA levels given as fold change compared to the mRNA of target genes was determine by RT-qPCR and the median values of fold change in patients were (-0.17, -0.27, -0.15 and -0.42) respectively. Statistical significance was established using nonparametric Mann-Whitney Test.

3.5.6..4 miR-342

The expression of miR-342 was significantly upregulated in the OLP group as compared to the control group. The same trend was observed for the target genes *MYC* and *IL24*. In contrast, comparable expression levels were determined for *CA12* in OLP as well as in the control group (Figure 3.23).

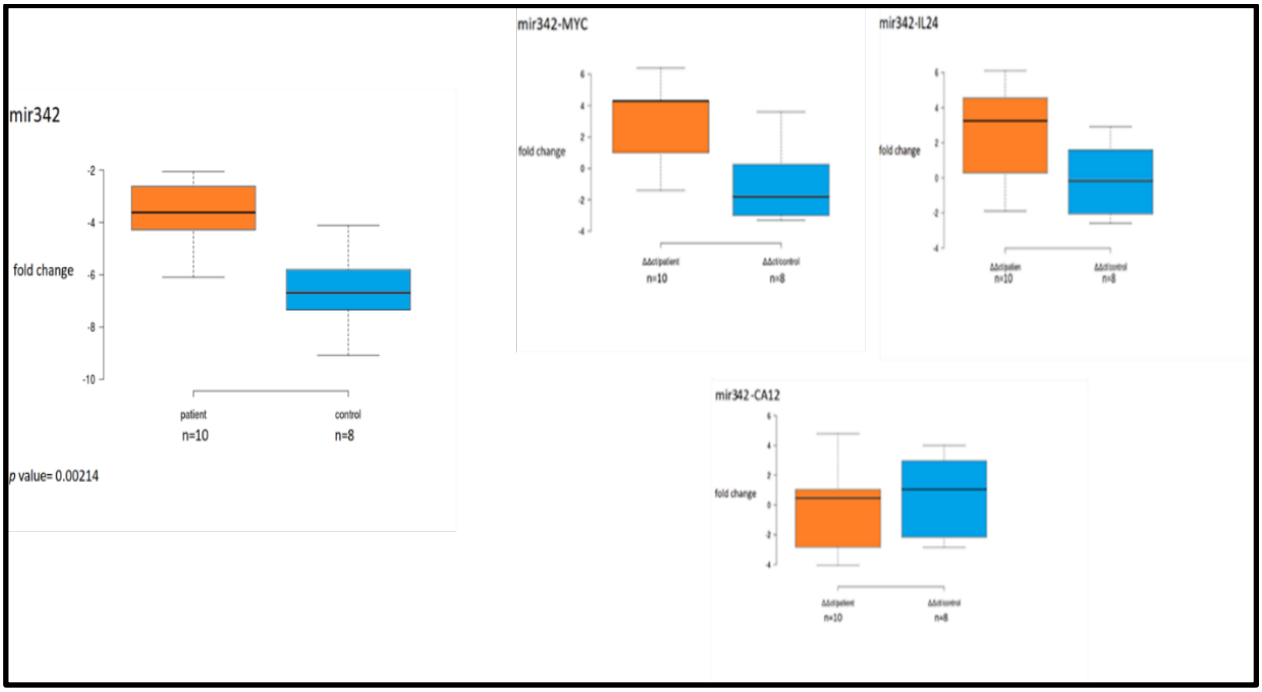

Figure 3-23 Expression correlation of miR-342 and its potential target genes (*MYC*, *IL24* and *CA12*) in OLP patients and control samples the miRNA levels given as fold change compared to the mRNA of target genes was determine by RT-qPCR and the median values of fold change in patients were (-0.44,-0.93 and -0.83) respectively.. Statistical significance was established using nonparametric Mann-Whitney Test.

3.5.6..5 miR-29a

miR-29a shows upregulated expression in the OLP patients, the predicted target genes for miR-29a are *MYC*, *CDK6* and *IL24*. The target gene *MYC* exhibits a significant downregulation in the OLP group, whereas the other two target genes (*CDK6* and *IL24*) were expressed at a similar level in the OLP and control groups. According to these results, miR-29a could be directly regulating *MYC*, while an inhibition of *CDK6* or *IL24* expression by the miR-29a is not warranted by these findings (Figure 3.24).

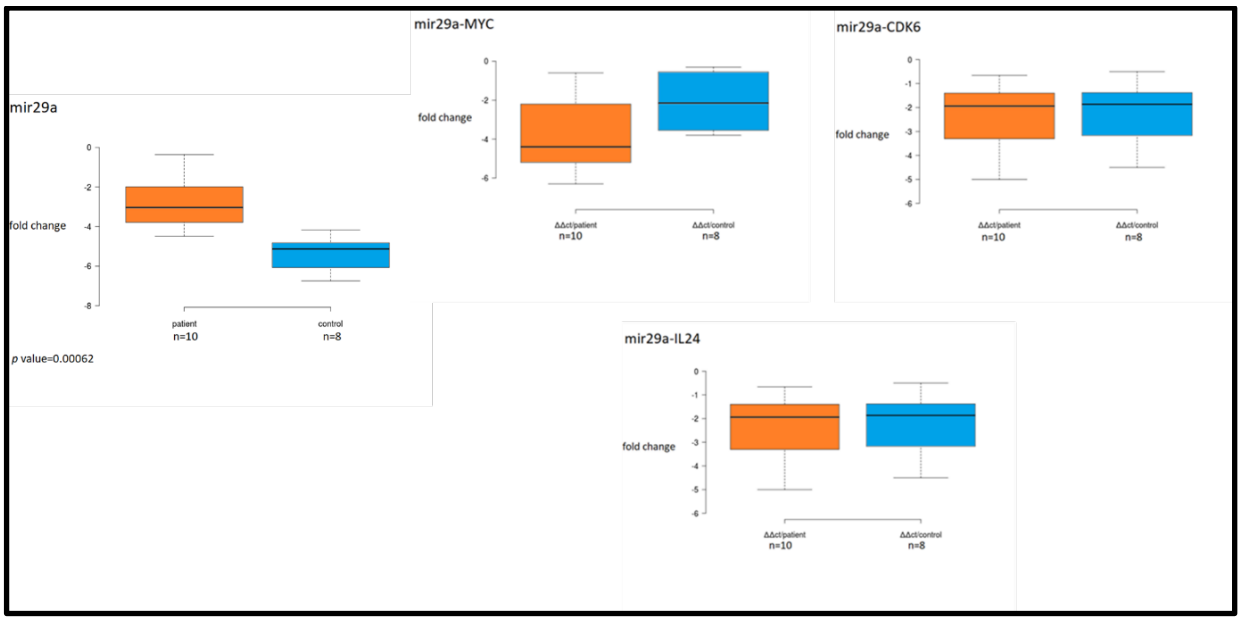

Figure 3-3 Expression correlation of miR-29a and its potential target genes (*MYC, CDK6* and *IL24*) mRNA in OLP patients and control samples the miRNA levels given as fold change compared to the mRNA of target genes was determine by RT-qPCR and the median values of fold change in patients were (-0.37,-0.57 and -0.33) respectively.. Statistical significance was established using nonparametric Mann-Whitney Test.

3.5.6..6 miR-23b

The qPCR results showed that miR-23b is significantly reduced in OLP as compared to the control group. The proposed target genes *MYC*, *CCND1*, *CDK6* and *TAB2* exhibited a similar trend, particularly *CDK6* and to a lesser extent *CCND1* and *TAB2*. The expression levels of *MYC* are comparable in OLP patients and the control group (Figure 3.25). Thus, the altered miRNA level does not appear to have a direct impact on the levels of the predicted target genes.

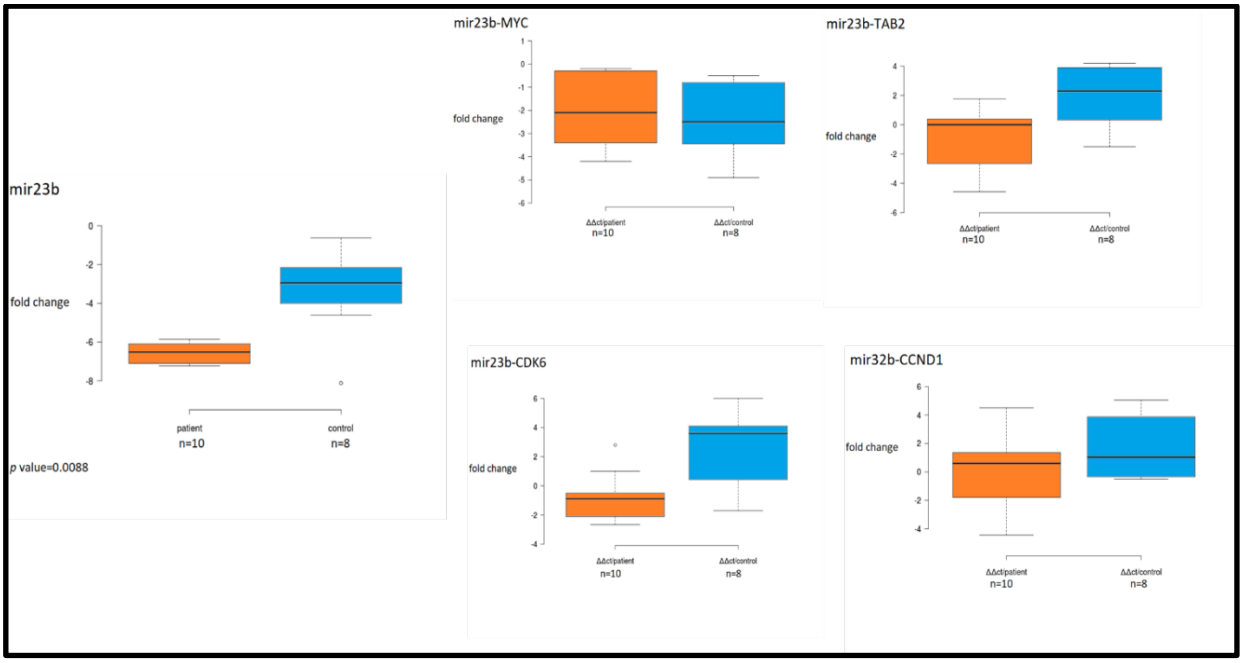

Figure 3-25 Expression correlation of miR-23b and its potential target genes (*MYC, CDK6, CCND1* and *TAB2*) mRNA in OLP patients and control samples the miRNA levels given as fold change compared to the mRNA of target genes was determine by RT-qPCR and the median values of fold change in patients were (-0.8, -1.23, -1.24 and -0.97) respectively. Statistical significance was established using nonparametric Mann-Whitney Test.

3.5.6..7 miR-205

The expression of miR-205 in OLP patients is downregulated confirming the NanoString results. Target gene prediction identified *IL24, MMP1* and *TAB2* mRNA as potential targets. RT-qPCR experiments revealed that in OLP patient samples *IL24* and *MMP1* were upregulated as compared with the control samples, although the relationship between miR-205 and *TAB2* was parallel (Figure 3.26). Thus, the altered miRNA levels may have an impact on the levels of the predicted target genes *MMP1* and *IL24*, while direct interaction with *TAB2* appears unlikely.

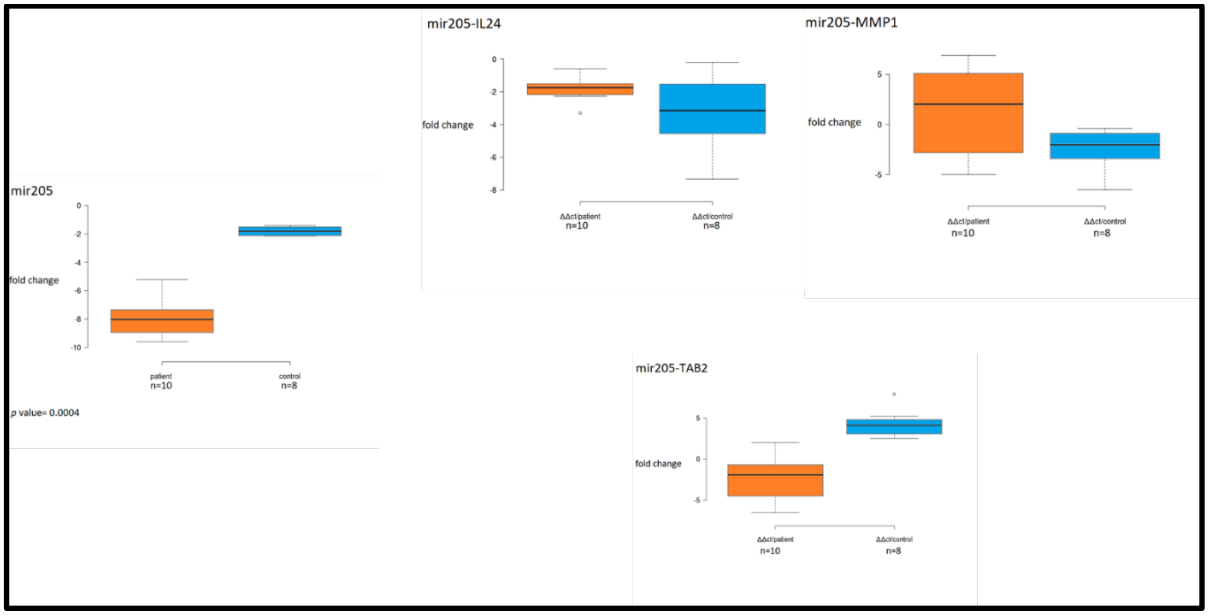

Figure 3-4: Expression correlation of miR-205 and its potential target genes (MMP1, IL24 and TAB2) mRNA in OLP patients and control samples the miRNA levels given as fold change compared to the mRNA of target genes was determine by RT-qPCR and the median values of fold change in patients were (-0.88, -2.40 and -1.51) respectively.. Statistical significance was established using nonparametric Mann-Whitney Test.

3.5.6..8 Let-7

The RT-qPCR results revealed a discrepancy with the NanoString data in the OLP patients for the let-7 when compared to control samples. Whereas NanoString reported a decreased expression, RT-qPCR showed a slightly increased expression in OPL. This may reflect the choice of patient samples (only 10 out of 24 were tested by RT-qPCR). The expression of the proposed target genes exhibited only minor, not significant differences in the expression between the OLP and control (Figure 3.27). Therefore, the changed miRNA level is unlikely to impact on the levels of the predicted target gene mRNAs *MYC, TAB2* and *CCND1*.

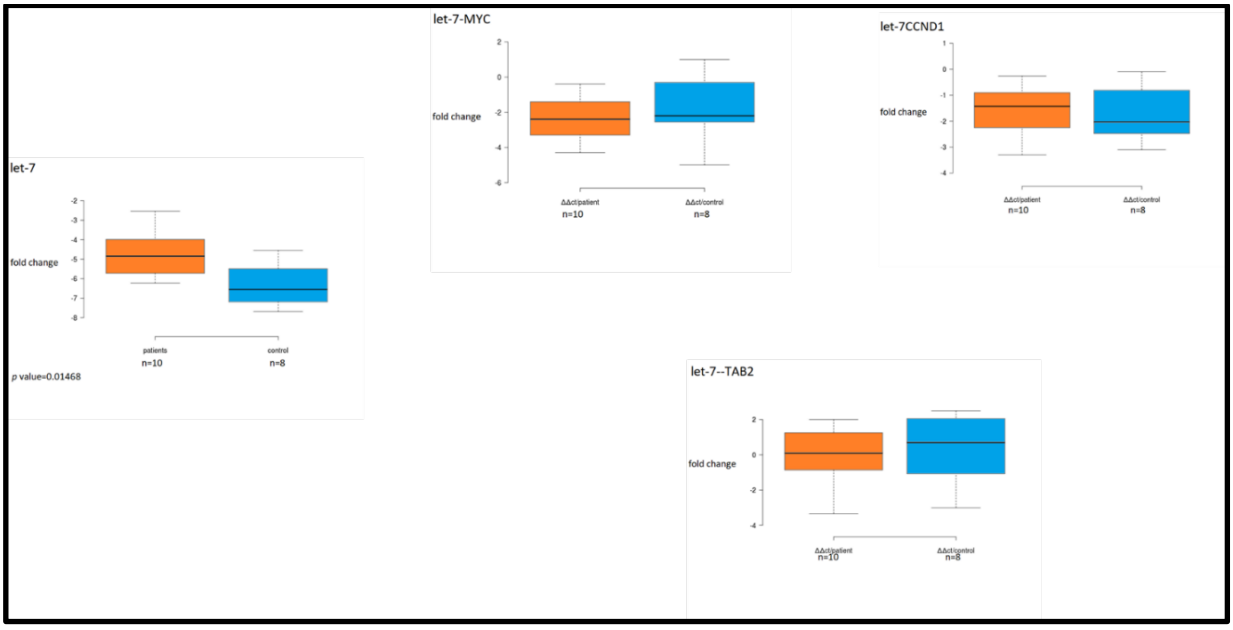

Figure 3-27 Expression correlation of let-7 and its potential target genes (CCND1, MYC and TAB2) mRNA in OLP patients and control samples the miRNA levels given as fold change compared to the mRNA of target genes was determine by RT-qPCR and the median values of fold change in patients were (-0.59, -0.72 and -0.91) respectively. Statistical significance was established using nonparametric Mann-Whitney Test

3.6 Discussion

In this chapter, the work concerned predicting potential target genes that are related to differentially expressed miRNAs established in the previous chapter. The downregulated miRNAs were let-7, miR-23b and miR-205 whereas the upregulated were miRNAs miR-29a, miR-155, miR-222, miR-342 and miR-146a. The expression levels of both miRNAs and potential target genes were examined by means of RT-qPCR. The following paragraphs will discuss the results for each of the differentially expressed miRNAs.

3.6.1 Downregulated miRNAs

3.6.1..1 Let-7

Let-7 is considered a tumour suppressor and has a positive effect on cellular proliferation (Mulholland, Green et al., 2019). The let-7 gene is frequently altered or deleted in human malignancies, demonstrating a potential role as tumour suppressors (Johnson, Esquela-Kerscher et al., 2007). For example, let-7 shows a down-regulated expression in breast cancer (Aceto, Sausgruber et al., 2012), lung cancer (Yin, Zhao et al., 2017) and in oral squamous cell carcinoma (Chien, Wang et al., 2015). The RT-qPCR experiments revealed that let-7 is highly expressed in OLP patients compared to the control group, although the NanoString results showed the opposite trend. The reason for this discrepancy is uncertain, though it may be down to the fact that not all OLP patient samples were tested by RT-qPCR and a potential bias may have been introduced even though the samples were randomly selected.

A computational search was conducted to identify let-7 target genes that were tested by RT-qPCR including *MYC, TAB2* and *CCND1*. However, the PCR based assay for *HMGA2* and *BCL2* failed to produce a specific product and these two genes were not further investigated.

Dysregulated expression or function of MYC is a common abnormality in human malignancy (O'Donnell, Wentzel et al., 2005). Of note, the expression of let-7 is controlled by *MYC* binding to the let-7 promoter. The let-7 levels have been reported to reduce in *MYC*-mediated tumorigenesis models and to increase when *MYC* is inhibited by chemicals. Moreover, overexpression of let-7c resulted in downregulation of the expression of *MYC* and proliferation in lymphoma cells (Sampson, Rong et al., 2007).

The findings in this study presenting a significantly downregulated expression of *MYC* in OLP patients suggests that let-7 may indeed regulate *MYC* in OLP patients.

Jakymiw et al determined that let-7b, but not let-7c, was significantly reduced in oral cancer cell lines compared with control cells (Jakymiw, Patel et al. 2010) Hence, let-7 down-regulation contributes to oral cancer progression and over-expressing let-7 could be a potential therapy target for inhibition of cancer cell proliferation. In contrast, there was a significant upregulation of let-7c in aggressive tumours (Hilly, Pillar et al., 2016).

The target gene *CCND1* is often overexpressed in human diseases through translocation, amplification or post-transcription regulation (Xu and Lin, 2018). Let-7 lowers *CCND1* expression and cell cycle progression (Wang and Cai, 2020). Moreover, Zhan et al. (Zhan, Qu et al., 2013), identified that let-7c inhibited cell proliferation and tumorigenesis by directly targeting the 3'UTR of HOXA1 mRNA, which consequently decreased the expression of *CCND1*. Furthermore, the ectopic expression of let-7c downregulated mRNA and the protein levels of *CCND*1 in hepatocellular carcinoma cells.

Interestingly, (Liu, Long et al., 2014), discovered that let-7c expression in nasopharyngeal carcinoma was significantly upregulated after the suppression of *CDK4* with a strong effect on let-7c, which in turn suppressed cell proliferation by controlling *CCND*1. On the other hand, we found a significantly upregulated expression of *CCND1* in the OLP patient group.

3.6.1..2 miR-23b

Fukumoto and colleagues found that overexpression of miR-23b in cancer cells significantly inhibited cancer cell migration and invasion (Fukumoto, Koshizuka et al. 2016). Similarly, miR-23b was downregulated in several cancers including OSCC indicating that miR-23b acts as a tumour suppressor miRNA by targeting oncogenic genes (Goto, Kojima et al., 2014). A different report explained that miR-23b blocks cancer cell proliferation and migration by regulating a cohort of pro-metastatic genes (Zhang, Hao et al., 2011).

miR-23b has various roles in cancer development; for example, miR-23b promotes tumorigenesis of breast cancer cells (Jin, Wessely et al. 2013). Conversely, miR-23b inhibits carcinogenesis in prostate cancer cells, colon cancer and hepatocellular carcinoma and suppresses lymph node metastasis in breast cancer (Jin, Wessely et al., 2013).

Moreover, miR-23b has recently been linked with an innate immune response (Hu, Zhai et al., 2017). Accordingly, mir23b was found to target IKKα in primary chondrocytes, resulting in inhibition of IL-17 and a reduction in IL-6.

In this study, miR-23b was significantly decreased in OLP patients compared to the control. In regard to the predicted target genes for miR-23b, all four web tools suggested four common target genes including *CDK6, MYC, TAB2* and *CCND1.*

This study revealed that both miR-23b and the proposed target gene *CDK6* were significantly downregulated in OLP patients and controls. This indicates that if the two molecules interacted it would not be through the canonical, Argonaute-2 mediated mechanism. Yadahalli and colleagues illustrated that miR-23b was differentially expressed in oral leucoplakia compared to control tissues (Yadahalli, Sarode et al., 2021). These observations suggested that miR-23b and possibly miR-29a expression may be implicated in the transformation of leucoplakia from the normal epithelium. Nevertheless, overexpression of miR-23b downregulated *CDK6* in leucoplakia cases compared with normal tissues. Moreover, miR-23b represses CDK-activating kinase and downstream functional targets to suppress cell cycle progression and basal transcription (Wang, Nguyen et al., 2014).

Lopez-Rincon and colleagues suggest that there is a strong relationship between P53 signalling and miR-23b and other miRNAs as some of miRNAs work as direct and indirect mediators of the P53 activity and components of its pathway (Lopez-Rincon, Mendoza-Maldonado et al., 2020). P53 is an important tumour suppressor that regulates the expression of many genes and is also considered to be a mutual modifier of gene expression in cancer. Moreover, the normal function of this tumour suppressor helps the maturation of some miRNAs with growth-suppressing function.

This study established that miR-23b is down-regulated in OLP although it proposed a non-significant effect on the proposed target gene *MYC*. In contrast, Chen et al. found that *MYC* may suppress the expression of miR-23b resulting in additional neuronal apoptosis during hypoxia (Chen, Zhang et al., 2015). Moreover, miR-23b is significantly decreased in human prostate cancer as compared with normal prostate tissue which appear to be directly caused by *MYC* (Gao, Tchernyshyov et al., 2009). Fulcinti and colleagues reported upregulated expression of MYC in the U266 cell line (human myeloma cell line) and reduced miR-23b levels. It should be mentioned that the relationship was direct between *MYC* and miR-23b in multiple myeloma, thus *MYC* was suppressed by miR-23b

in myeloma cells suggesting that miR-23b has tumour suppressor activity (Fulciniti, Amodio et al., 2016).

MYC appears to regulate the expression of miR-23b also in prostate cancer cells: The levels of miR-23b decreased with diminished *MYC* expression levels (Liu, Le et al., 2012). Moreover, (Chen, Li et al., 2012) proved that *MYC* has a crucial role in glutamine metabolism by transcriptionally inhibiting miR-23b, resulting in increased expression mitochondrial glutaminase.

This study found parallel down-regulation of miR-23b and target gene *TAB2* in the patient group and the control group. (Cui, Liu et al. 2017), demonstrated that miR-23b correlated temporally with decreased *TAB2* levels which in turn enhanced IL-12 production in monocyte and macrophages. In autoimmune diseases such as lupus or rheumatoid arthritis miR-23b suppresses *IL-17* and tumour necrosis factor α (TNF-α) that results in induced NF-κB activation and inflammatory cytokine expression by upregulated TAB2 (Zhu, Pan et al., 2012).

CCND1 was also investigated for a link with miR-23b. Wang et al. proved that the expression levels of miR-23b were downregulated in hepatocellular carcinoma tissues which lead to an increase in the expression of the direct target gene *CCND1* (Wang and Zhao, 2021). Likewise, the same study revealed that miR-23b and *CCND1* might construct an important signal network to modulate the progression of osteoporosis either in a direct or indirect way. However, our study failed to demonstrate a connection between miR-23b and *CCND1* in OLP.

3.6.1..3 miR-205

The third downregulated miRNA in our list is miR-205. Generally, this miRNA is involved in the genesis and progression of human malignancies. Dysregulation of miR-205 expression was detected in numerous tumours and was associated with the regulation of cell apoptosis, proliferation and metastasis. A number of studies have shown that miR-205 is downregulated in different tumours. For example, Zhang and colleagues found that mir205 is significantly downregulated in gastric cancer tissues, compared with adjacent normal tissues (Zhang, Zhang et al., 2021). Other studies reported that miR-205 was up-regulated in breast cancer (Xiao, Humphries et al., 2019), prostate cancer (El Bezawy, Tinelli et al., 2019), oesophageal cancer (Hezova, Kovarikova et al., 2016) and head and neck carcinomas Moreover, the expression of miR-205 has been found to be up-regulated in oesophageal squamous cell carcinoma (Hezova, Kovarikova et al., 2016).

This study predicted target genes for miR-205 including *IL24, MMP1* and *TAB2*. The expression correlation between miR-205 and IL24 as well as miR-205 and TAB2 showed the opposite correlation within the OLP and control groups. In contrast, the miR-205 and *MMP1* revealed a positive correlation in both sample groups. The RT-qPCR experiments established opposite expression between miR-205 and *IL24* and *MMP1,* whereas *TAB2* was also downregulated in OLP.

Interestingly, Wang, Li et al. (2013), identified that IL24 is a direct target gene of miR-205. They also suggested that in prostate cancer, miR-205 influence the expression of tumour suppressor genes via IL24 at both the messenger RNA and protein levels. Furthermore, Panneerselvam and colleagues suggested that miR-205 interacted directly with the promoter target sequence of IL24 as the IL24 gene in the KB cells line was up-regulated by the over-expression of mir205 (Panneerselvam, Munshi et al., 2013).

In regard to *MMP1*, Hezova et al. identified two potential indirect miR-205 targets, *MMP1* and *MMP10,* which were validated in the oesophagus squamous cell carcinoma cell line. In KYSE-150 cells inhibition of miR-205 expression and *MMP10* were both significantly downregulated, whereas *MMP1* was also downregulated, but without statistical significance (Hezova, Kovarikova et al., 2016). Hence, these genes were considered indirect targets of miR-205.

3.6.2 Upregulated miRNA

3.6.2..1 miR-155

miR-155 is one of the upregulated miRNAs that has been confirmed in this study. Many reports suggest that miR-155 is involved in carcinogenesis and tumour progression and that the relationship is positive between miR-155 levels and cytokine release. Furthermore, miR-155 is the first miRNA that was identified as an oncogene in numerous cancer types. For example, in breast, colon, cervical and lung cancer, the level of expression was increased (Tao, Ai et al., 2019).

This miRNA is important for tumour development, functioning predominantly as a tumour-promoting factor (Tili, Michaille et al., 2013). Moreover, there is evidence that miR-155 plays a role in immunity since it shows an increased expression in activated immune cells and has a significant impact on these cells. Therefore, the abnormal expression of miR-155 results in an impaired immune responses and is associated with a variety of diseases (Faraoni, Antonetti et al., 2009). Regarding OLP, miR-155 is

upregulated, but the principal underlying mechanisms remains unclear. As miR-155 has a direct impact on immune cells it is possible that miR-155 is involved in the pathogenesis of OLP by regulating the immune system (Ebrahimi, Boldrup et al., 2008).

Moreover, miR-155 exhibits upregulated levels in oral white lesion cancer and is related to cisplatin resistance. Interestingly, miR-155 mediated exosome signalling is involved in the process (Kirave, Gondaliya et al., 2020).

Our findings indicate that miR-155 is significantly upregulated in OLP patients compared with the control group. We also predicted and analysed four target genes including *MYC, MMP1, TAB2* and *CCND1*.

The correlation within the sample groups was negative in both for the miR-155-TAB2 interaction. The RT-qPCR results confirmed this trend and also established a slightly opposite regulation for miR-155 and the *CCND1* and *MYC* target genes. *MMP1* levels were expressed at similar levels in OLP and the control group.

A previous study revealed that overexpression of *MYC* significantly increased the levels of a number of miRNAs in U87 cells including miR-155 in glioma cells which enhancing malignant properties (Xiao, Li et al., 2020). This finding again points to *MYC* regulating miR-155 expression and not vice versa.

Conversely, Sun and colleagues noticed that high expression levels of miR-155 could significantly downregulate cancer cell proliferation and attachment. The level of miR-155 was found to influence endogenous MYC expression in SGC-7901 cells by binding to the 3'-UTR of *MYC*. This suggests that miR-155 contributes to cancer pathogenesis of gastric carcinoma and supports a function of miR-155 to regulate cancer-related genes via the inhibition of *MYC* (Sun, Sun et al., 2014).

TAB2 was identified as a potential target gene for miR-155. Our findings illustrate a significant downregulation of *TAB2* in the OLP patients group, whereas mir155 is upregulated as opposed to the control group. Other studies investigated *TAB2* as a potential target for miR-155. It was indeed demonstrated that *TAB2* is suppressed directly by miR-155 in monocyte-derived dendritic cells (Zhou, Huang et al., 2010). Similarly, a knockdown of *TAB2* reduced IFN-α production by plasmacytoid dendritic cells. mir155 is consistently up-regulated in tumour cells, that could cause an inhibition of IFN production, which in turn prevents the proliferation of the tumour cells (Alivernini, Gremese et al. 2018).

Dendritic cells are specialised antigen-presenting cells that recognise, capture and respond to antigens. Numerous studies have demonstrated that DCs are controlled by mir155 (Song, Dong et al., 2018). Accordingly, *TAB2* is a direct target gene and the levels of *TAB2* were increased during monocyte-derived DC maturation. Moreover, mir155 may have an essential role in reducing the inflammatory response in human dendritic cells by directly targeting *TAB2* (Xu, Ren et al., 2013). Interestingly, *TAB2* protein expression was elevated in dendritic cells derived from active Behcet's disease patients and expression of TNF-α, *IL-6*, and *IL-1β* was decreased once *TAB2* was downregulated (Liang, Zhou et al., 2021).

A different study by Xu et al. demonstrated that miR-155 inhibits the immunosuppressive capacity of mesenchymal cells by reducing the expression of TAB2 (Xu, Ren et al., 2013). Hence, miR-155 negatively regulates *TAB2* expression in MSCs. miR-155 can also be induced by IFNγ in combination with TNFα and *IL-1β*. Hence, stimulating human mesangial cells with IFN-γ and TNF-α results in miR-155 being promoted and TAB2 and *NF-κB* being negatively regulated. Therefore, the relationship between miR-155 and target gene *TAB2* may play a role in the regulation of inflammatory and immune reactions in many cancers, including kidney cancer (Bayraktar and Van Roosbroeck, 2018). Additionally, in lung cancer the cytokine IL-13 inhibits TAB2 expression via the upregulation of miR-155 in human bronchial smooth muscle cells, thus regulating asthma-associated inflammation (Mahesh and Biswas, 2019).

The third proposed target gene for miR-155 is *CCND1*. The findings in this project suggested that whereas miR-155 was upregulated in OLP, the expression levels of *CCND1* did not change significantly between the OLP patient groups as compared to the control.

A previous study mentions the association between miR-155 and *CCND1* in different diseases, as Wan et al. identified *CCND1* as a target for miR-155 in in the pathogenesis of pancreatitis (Wan, Yang et al., 2019).

Mineta and colleagues suggest that amplification of *CCND1* plays a role in colorectal cancer via a link between increased *CCND1* and the activation of the p53 pathway (Mineta, Borg et al., 1997). *CCND1* and other genes (*CDK6* and *CCNB1*) are all enriched in the p53 signalling pathway, providing an indication that these genes may have vital roles in the progression of colorectal cancer by the regulation of the p53 signalling

pathway. An extensive number of miRNAs downregulated the expression of *CCND1*, including miR-155, miR-200b and let-7b.

Moreover, miR-155 plays an important effect on the pathogenesis of gastric cancer as Kuo et al. identified a relationship between miR-155 and *CCND1* (Kuo, Huang et al., 2014). Notwithstanding, any expression change in *CCND1* could partially simulate the effects of miR-155 in gastric cancer cells though miR-155 could exert an antitumor effect through targeting *CCND1*. These findings are supported by Chen and colleagues who established that decreased expression of miR-155 leads to increased endogenous *CNND1* expression at both the mRNA and protein levels in gastric cancer cells (Chen, Wang et al., 2015).

Another study revealed that miR-155 causes significant downregulation of *CCND1* and other genes that could regulate the invasive properties of melanoma cells as they might represent a novel approach in treating melanoma cells and hence present novel targets to treat melanoma patients (Peng, Liu et al., 2017)

Wu et al. demonstrated that WNT/β-catenin signalling mediated the malignant behaviour of cells by suppressing β-catenin and *CCND1*. However, increased levels of *CCND1* appeared to be related to its capacity to sponge miR-155 leading to an unfavourable prognostic in OSCC (Wu, Talbot et al., 2016).

A few studies mention the correlation between mir155 and *MMP1* as a direct target gene, (Wang, Feng et al., 2020; Nygaard and Firestein, 2020). These reports suggest that in rheumatoid arthritis, the over expression of mir155 induced by IL-1β and TNF-α synovial fibroblasts down-regulates the production of matrix metalloproteinase *MMP1* and *MMP3*. Hence, an important mechanistic clue into the destructive and inflammatory effects of rheumatoid arthritis is provided. Interestingly, the expression of mir155 in CD14+ monocytes/macrophages present in the synovial fluid of rheumatoid arthritis patients was determined to be higher than the levels detected in peripheral blood CD14+ cells. These findings indicate that miR-155 could act as a protective miRNA that locally down-regulates the expression of *MMP1*.

3.6.2..2 miR-222

miR-222 represents the second upregulated miRNAs in this project. According to the prediction of the websites, there are four common target genes for miR-222, *MYC*, CDK6, *IL24* and *MMP1*. However, our RT-qPCR findings suggest that miR-222 does not act as

canonical miRNAs on these targets. *MYC* shows a significant upregulation in OLP patients as compared to the control group in line with the study conducted by Kim et al. who reported stimulation of miR-222 by *MYC* (Kim, Mori et al., 2010). Hence, *MYC* may ensure repression of target genes at a posttranscriptional level via an increased expression of miR-222 via p27 which plays a role in cell cycle progression.

Although miR-222 is upregulated in oral squamous cell carcinoma (Jiang, Zhao et al. 2014), the way of action of miR-222 in oral squamous cell carcinoma and carcinogenesis has not been characterised. However, miR-222 inhibits oral tongue squamous cell carcinoma (OTSCC) cell invasion and therefore, it might serve as a novel therapeutic target for high risk metastatic oral tongue carcinoma (Liu, Yu et al., 2009). In pancreatic cancer, miR-222 was significantly upregulated and acted as an oncogene to enhance glycolysis and proliferation by directly targeting HIPK2 (Homeodomain-Interacting Protein Kinase 2).

The second target gene for miR-222 is *CDK6* which has the role of promoting cancer initiation in addition to progression and is therefore an attractive target for pharmacological inhibition. *CDK6* has regulatory functions as a cell cycle-dependent kinase and transcriptional regulator under homeostatic conditions as well as in malignant transformed settings (Scheicher, Hoelbl-Kovacic et al., 2015).

Interestingly, here, the relationship between *CDK6* and miR-222 was a positive correlation with a significant upregulation in both OLP patients and controls. In contrast, miR-222 was down-regulated in OSCC cells and stimulated apoptosis in non-malignant cases but may also participate in metastasis. In a further study, miR-222 was ascertained to be involved in pathways associated with cancer, affecting *CDK6* and MAPK (Mitogen-Activated Protein Kinase) (Bar, Gorn-Hondermann et al., 2015).

IL-24 was regulated in parallel with miR-222 and may act as an indirect target. *IL-24* is a unique cytokine/tumour suppressor gene that belongs to the *IL-10* cytokine family and is expressed in most human cancer cells. Accordingly, *IL-24* is highly expressed in oral squamous cell carcinoma, laryngeal squamous cell carcinoma and nasopharynx carcinoma (Qiu, Zhang et al., 2020). Additional studies have revealed that *IL24* mRNA can boost the immunogenicity of tumour cells via the upregulation of costimulatory molecules, such as CD80 and CD86 (Fonseca-Camarillo, Furuzawa-Carballeda et al., 2014). However, *IL24* expression did not show a significant correlation with tumour

prognosis, although *IL-24* can protect the body through the induction of tumour cell apoptosis and inhibition of angiogenesis (Hajikhan Mirzaei and Esmaeilzadeh, 2014).

There are reports that *IL-24* regulates the expression of the miRNA, miR-222. Accordingly, *IL-24* markedly reduced *HMGA1* (High Mobility Group Protein A1) mRNA and protein expression by downregulating miR-222 expression (Panneerselvam, Srivastava et al., 2014).

Pereira et al. suggested that MMP expression in oral cancer tissue was an essential tool in cancer prognosis since MMP expression became significant only after cancer started (Pereira, Dias do Carmo et al., 2012). Further studies also mention the relationship between miR-222 and MMP1. For example, Zhang and colleagues identified that miR-222 played a regulatory role in hypertrophic scarring by negatively regulating *MMP1* by binding with its 3'-untranslated region (Zhang, Lin et al., 2018). Moreover, miR-222 enhanced cell proliferation and inhibited apoptosis of hypertrophic scar fibroblasts through negative regulation of *MMP1*. These findings suggest that miR-222 and MMP1 might be applied as novel biomarkers and targets in diagnostic and therapeutic approaches for hypertrophic scars. Moreover, in tongue squamous cell carcinoma cell line, the ectopic transfection of miR-222 reduced the expression of *MMP* and was suggested to play a role in cell invasion and metastasis (Mg, 2019).

3.6.2..3 miR-342

The target predictions for miR-342 identified *MYC, IL24* and *CA12*. The correlation within the sample groups as well as the expression studies indicate that an indirect action of miR-342 on these target genes is more likely than the canonical negative effect of the miRNA on its target genes. However, Zhao et al. suggested that miR-342 regulated *MYC* in hepatocellular carcinoma (Zhao and Zhang, 2015).

miR-342 displays other critical roles in several physiological and pathological processes, such as in the osteogenic differentiation of umbilical cord mesenchymal stem cells (Song, Jin et al. 2019). miR-342 demonstrated decreased expression in hepatocellular carcinoma and may serve as a useful predictor of a poor prognosis (Gao, Zhang et al., 2017). Moreover, miR-342 demonstrated a decreased expression in non-small cell lung cancer (NSCLC), which may lead to increased cell proliferation. miR-342 expression was significantly reduced in OSCC tumour tissues compared to the adjacent non-cancerous specimens (Song, Jin et al., 2018), which suggested that miR-342 may have a tumour-suppressing role.

Tai et al. proposed that miR-342 indirectly regulated *MYC* and also affected the expression of transcription factor E2F1 in lung cancer (Tai, Kajino et al., 2015).

Wu and colleagues (Wu, Lai et al., 2021), established that miR-342 indirectly regulated *CA12* in chronic myeloid leukaemia (CML), which affected proliferation and DNA repair gene-sets.

3.6.2..4 miR-29a

Our findings revealed that miR-29a was significantly upregulated in OLP patients as compared with the control group. miR-29a plays an important role in OSCC where overexpression of miR-29a inhibits cell invasion and enhances apoptosis. Lu et al. suggested that miR-29a might be used as a biomarker and therapeutic target in oral squamous carcinoma (Lu, Xue et al., 2014).Cai et al. identified that OSCC responded to exosome-enclosed miR-29a. This finding indicates that miR-29a could be a messenger to adjust tumour surroundings and enable tumour proliferation and invasion. Interestingly, such exosome mediated messaging could form the basis for novel treatments of OSCC (Cai, Qiao et al., 2019).

Several reports linked miR-29a to lung adenocarcinoma tissue invasion and metastasis as well as hematologic neoplasms (Ma, Li et al., 2011; Plaisir, Pan et al., 2012; Zhao, Lin et al., 2010). miR-29a expression levels are inversely correlated with the prognosis of mantle cell lymphoma. Furthermore, it decreases cell growth and encourages apoptosis in primary acute myeloid leukaemia (AML) cells and other related cell lines.

The predicted target gene of miR-29a were *CDK6, MYC* and *IL-24*. *CDK6* and *IL-24* show similar expression levels in OLP and the control groups. In contrast, MYC was inversely expressed (miR-29a up, MYC down) in OLP in comparison to the controls.

CDK6 was discussed as a potential target of miR-29a in Swannoma. Accordingly, Ma et al. demonstrated that miR-29a negatively regulated the expression of CDK6 as mRNA and that protein expression of *CDK6* was downregulated by a miR-29a mimic and significantly upregulated when miR-29a was knocked down (Ma, Li et al., 2011).

In another study, Zhao found that activation of *CDK6* in primary Malton cell lymphoma (MCL) results in the down-regulation of miR-29a, which may cooperate with cyclin D1 in MCL pathogenesis (Zhao, Lin et al., 2010). Moreover, Schmitt and colleagues (Schmitt, Philippidou et al., 2012) provided evidence of inhibiting cell proliferation in melanoma, suggesting tumour-suppressing features of miR-29a family members.

Subsequently, the anti-proliferative effects of miR-29a was confirmed and *CDK6* was established as a direct miR-29a target in melanoma cells. Remarkably, *CDK6* was also established as a direct target gene for miR-29a in polycystic ovarian syndrome where overexpression of miR-29a significantly decreased the levels of CDK6 along with CDK4 and *CDK2* (Li, Liu et al., 2014).

This study revealed a significant upregulation of miR-29a in OLP patients in contrast to the control group and a down-regulation of *MYC*. Dey et al. confirmed a negative association between *MYC* and miR-29a expression (Dey, Kwon et al. 2020), although they speculated that a high amount of *MYC* in the nucleus may be responsible for miR-29a repression. Likewise, they suggested a potential interaction between *MYC* and miR-29a in pancreatic cancer. A further study by Mazzoccoli and colleagues (Mazzoccoli, Robaina et al., 2019) reported that miR-29a was regulated by *MYC* contributing to tumorigenesis in Burkett lymphoma cells.

3.6.2..5 miR-146a

Here, miR-146a was linked to *MYC* as a target gene. However, both the correlation within the sample groups and the expression comparison pointed to an indirect mechanism as the expression changes were in parallel. In previous reports, miR-146a was suggested to act as a tuning mechanism to prevent an overstimulated inflammatory state in human Langerhans cells where it is expressed at high levels. Min et al. proved that mir146a was upregulated in OSCC, suggesting that it provides a proliferative advantage to normal oral keratinocytes (Min, Jung et al., 2017). Moreover, miR-146a selectively neutralised the TRAF6-mediated (TNF Receptor Associated Factor 6) branch of TGF-β signalling in OSCC cell lines by sparing Smad4 (SMAD Family Member 4) involvement. miR-146a influences immune regulation, including the signalling pathways mediated by kinases and transcription (Visone, Rassenti et al., 2009). Monticelli and colleagues reported miRNA expression arrangements in various hematopoietic cell types exposed to conditions of Th1 and Th2 differentiation. miR-146a was remarkably upregulated in Th1 but not in Th2 cells and it could have a function in the differentiation of naive T cells into Th1 effector cells (Monticelli, Ansel et al., 2005). Lu et al. (2010), suggested that miR-146a decreased an IFN-γ-mediated Th1 response in regulatory T cells.

A potential target gene of miR-146a- *MYC* oncogenic transcription factor, caused the downregulation of miR-146a expression in human B-cell lymphomas (Chang, Yu et al., 2008). Recent studies also have evaluated the expression levels of miR-146a in acute

lymphocytic leukaemia and chronic lymphocytic leukaemia (Visone, Rassenti et al., 2009).

3.6.3 Conclusion

To conclude, expression levels of a substantial number of miRNAs and proposed target genes were investigated. Where all of the miRNAs have established functions in various cancers the relationship between miRNAs and predicted target genes is less clear in OLP. The majority of the interactions between miRNA and target genes do not follow the canonical inhibition pattern. However, promising targets were found for miR-29a (*MYC*) and miR-205 (*IL-24* and *MMP1*) that may be further investigated in future work.

Chapter 4. IMMUNOHISTOCHEMISTRY

4.1 Introduction

The principle of immunohistochemistry techniques is to identify antigens in tissue sections by means of immunological and chemical reactions. This technique is highly sensitive and specific and can detect a wide variation of antigens in multiple animal species (Ramos-Vara, 2011). IHC testing is also quick and inexpensive when compared to other methods and can be done on FFPE (fixed formalin paraffin embedded) specimens and provides morphologic assessment.

4.2 IHC protocol

The consecutive steps in IHC can be summarised as follows: antigen retrieval (AR), the addition of a primary antibody, application of a secondary antibody that binds the primary antibody and addition of a detection reagent to localise the primary antibody (Figure 4.1).

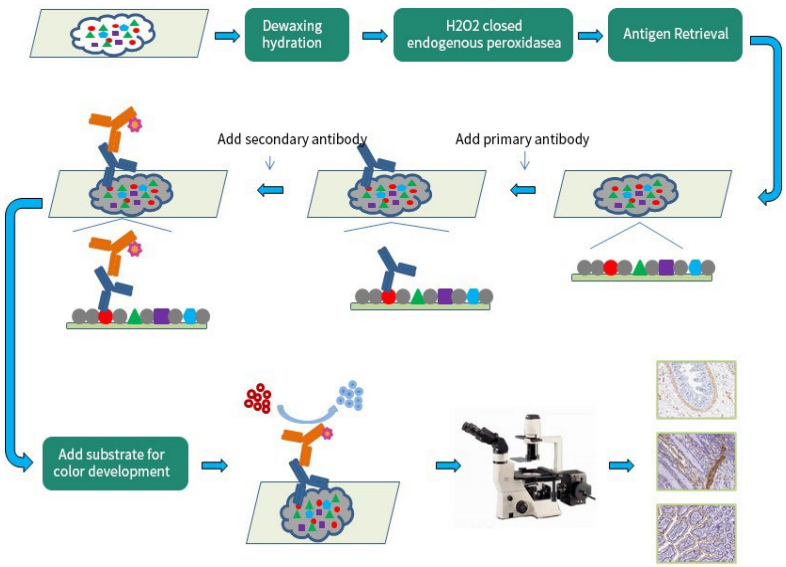

Figure 4-1 Immunohistochemistry flow chart available at www.debuglies.com

Consequently, the primary antibody is labelled with a secondary antibody, which is targeted against the immunoglobulin of the species in which the primary antibody was produced (Dabbs, 2017). There are two ways of labelling: the direct and the indirect method.

The positive and negative control should be performed with each run. Positive controls are tissues that contain an antigen known to stain with a certain antibody. Ideally it should be run on the same slide as the tissue of interest so that the control tissue undergoes the same reaction conditions as the sample tissue. However, the negative controls involve the sample tissue that undergoes the identical staining conditions minus the primary antibody or with a non-immune immunoglobulin from the same species (Cregger, Berger et al., 2006). False positives and negatives can be due to the immunohistochemical staining method itself but also to a number of other factors including preparation and fixation.
The last step of IHC is the assessment and principally, the use of scoring systems. Semi quantitative scoring systems are commonly used to convert subjective perception of IHC-marker expression by histopathologists into quantitative data, which is then used for statistical analyses and establishing the conclusion. Without the scoring system, the description of received data can be provided only in a subjective way, and expressed, for example, as “strong”, “weak”, “absent” with modifiers as “more” or “less” (Fedchenko and Reifenrath, 2014). To reduce subjectivity, it is recommended to have at least more than one observer in the study.

4.3 Aims

To investigate with IHC the expression of relevant cytokines and potential target genes of miRNAs in OLP and controls tissue

4.4 Material and methods

4.4.1 Sample collection

Oral biopsy specimens were collected from 24 patients who had been clinically and pathologically diagnosed with OLP and 8 controls patients affected by other diseases causing oral white patches. Details of the demographic and clinical characteristics of patients and controls have been described already in chapter 3. All experimental procedures were approved by the NRES Committee North East - Newcastle & North Tyneside (13/NE/0368) and the enrolled patients gave their informed written consent.

4.4.2 Antibody selection

The list of antibodies was compiled to detect the confirmed target genes related to OLP pathogenesis.

4.4.2..1 Signal transducer and activator of transcription 3 (STAT3)

STATs (Signal Transducers and Activators of Transcription) are a family of cytoplasmic proteins acting as signal messengers and transcription factors and participate in normal cellular responses to cytokines and growth factors. The STAT family consists of seven proteins in humans (STAT1–STAT4, STAT5A, STAT5B and STAT6). Activation of STATs, particularly STAT3 and STAT5 results in regulation of functions, such as cell proliferation, cell cycle progression, apoptosis, angiogenesis and immune evasion. Aberrant activation of STAT3 plays a pivotal role in the initiation, progression and metastasis of different cancers including head and neck cancers. Conversely, inhibition of STAT3 may lead to chemoprevention (Mali, 2015). However, STAT3 also works as either a pro- or anti-inflammatory factor. For example, when dendritic cells are stimulated by IL-6, STAT3 is pro-inflammatory, but when stimulated by IL-10, STAT3 is anti-inflammatory. The IL-10/STAT3-mediated anti-inflammatory response: recent developments and future challenges (Hutchins, Diez et al., 2013). Moreover, genetic deletion of STAT3 in T cells has been shown to abrogate Th17 differentiation, suggesting that STAT3 is a potential therapeutic target for inflammatory disease, such as OLP (Oh, Yu et al., 2011). Therefore, STAT-3 may be involved in OLP development and progression and account for different clinical manifestations (Du, Chen et al., 2018). There are also reports by Kuuliala, Kuuliala et al. (2015), asserting that STAT-3 is expressed in the local immune response of patients with OLP and correlated with clinical manifestations of OLP.

4.4.2..2 Interferon-gamma (IFN-γ)

Interferon gamma (INF-γ) is one of the most critical mediators of immunity and inflammation and plays an essential role in both innate and adaptive immune responses by activating macrophages and also by disrupting several anti-inflammatory feedback loops (Halma, Wheelhouse et al., 2004). INF-γ could help to up-regulate various inflammatory mediators to enhance Th1 responses by activating NK cells and macrophages. It also promotes the specific cytotoxic immunity via T cell activation (Hu and Ivashkiv, 2009).

In OLP inflammatory infiltrate there is an enrichment of CD45RO memory T cells that predominantly express Th1 cytokine such as IFN-γ and TNF-α (Walton, Macey et al., 1998).

Some studies show a higher expression of IFN-γ in isolated T-cell lines from the OLP biopsies (Piccinni, Lombardelli et al., 2014). The increased expressions of IFN-γ in OLP influence the clinical outcome and has been also associated with the clinical manifestations of OLP lesions (Carrozzo, Dametto et al., 2004).

4.4.2..3 Tumour Necrosis Factor-alpha (TNF-α)

Tumour Necrosis Factor-alpha (TNF-α) is expressed by T-cells in the sub epithelial lymphocytic infiltrate in OLP. Many studies have reported that TNF-α plays a key role in the immune regulation of OLP (Ma, Wu et al., 2016). A key and probably early event in OLP is the genetically induced increased production of TH1 cytokines, primarily TNF-α and IFN-γ (Carrozzo, 2014). A recent meta-analysis has confirmed that TNF-α-308 G/A polymorphism may be a risk factor for HCV-negative OLP patients and those with mixed ethnicity (Jin, Wang et al., 2012). Moreover, TNF-α may enhance the apoptosis of basal epithelial cells and activation of Langerhans cells, typically seen in OLP biopsies (Sugerman, Savage et al., 2002)

4.4.2..4 NOTCH

NOTCH signalling pathway is a highly protected mechanism that is found in almost all multicellular organisms. It plays an important role in cell fate through regulation of the programmes responsible for cell growth, apoptosis and differentiation (Artavanis-Tsakonas, Rand et al., 1999). Mammalians have four Notch genes (Bianchi, Dotti et al., 2006).

The NOTCH1 gene generally encode proteins which are expressed in prismatic mesoderm. NOTCH2 complements NOTCH1. Both are required to regulate the interaction of somite condensation cells. NOTCH3 and NOTCH4 have been only identified in mammals (Bianchi et al., 2006)

Increased Notch activity is associated with epidermal keratinocyte maturation, proliferation and innate immune activation via the maturation of dendritic cells, T cells and macrophages (Shang, Smith et al., 2016). Dysregulation of Notch signalling expression in oral epithelium has previously been reported in several oral epithelial diseases including oral dysplasia, oral squamous cell carcinoma (Nowwarote and

Osathanon, 2017) and OLP (Gokulan and Halagowder, 2014). However, Notch signalling regulation in OLP has not yet been investigated in detail.

4.4.2..5 Interferon λ3 (Interleukin 28B)

There are 3 Interferon Lambda (IFN-λ) genes that encode 3 distinct but highly related proteins: IFN-λ1, -λ2 and -λ3. These proteins are also known as interleukin-29 (IL-29), IL-28A and IL-28B, respectively (Donnelly and Kotenko, 2010).

IFN-λ3 (IL28B) plays pleiotropic roles in the regulation of immune responses in autoimmune diseases. IFN-λ3 (IL28B) exerts pro-inflammatory roles by means of promoting Th1, CD8, NK and B cell proliferation/function and through inhibiting Th2 cell generation. In contrast, IFN-λ3 (IL28B) also plays an anti-inflammatory role by enhancing IL-10 production and inhibiting DC function. IFN-λ3 (IL28B) has been detected in autoimmune diseases with a high expression level that positively correlated with IFN-γ levels, whereas it negatively correlated with IL-17 (O'Connor, Ahlenstiel et al., 2014).

4.4.2..6 Interleukin 27 (IL27)

Many studies have also discovered that IL-27 signalling has immunosuppressive effects, such as suppressing Th17 development and inducing co-inhibitory receptors on T cells. As a result, the precise role of IL-27 in infectious diseases remains a source of debate and ongoing research (Morita, Masters et al., 2021). IL-27's role during the early and late phases of immune responses is to resolve its recognised pro and anti-inflammatory actions, which could be therapeutically modulated to enhance the outcomes of infected patients.

In human peripheral blood mononuclear cells (PBMC), primary human monocytes, THP-1 cells and PMA developed THP-1 cells, IL-27 works as a costimulatory molecule with LPS, producing increased production of inflammatory cytokines (IL-12, TNF-α, and IL-6) (Petes, Odoardi et al., 2018). Wong, Lindsell et al., 2013, demonstrated that IL-27 could potentially be a diagnostic biomarker of sepsis (Wong, Lindsell et al. 2013). Based on micro array analysis, they found that among 221 differentially regulated gene probes, IL-27 had the highest prediction strength for patients with sepsis.

The development of OLP, leucoplakia and oral squamous cell carcinoma has been linked to and correlated with IL-27 (Wang, Huang et al., 2022). Yet again, IL-27 is a defence

molecule that expressed in the epithelium to prevent pathological changes in the epithelium while also helping to promote initial inflammation. These events build the suppressive inflammatory situation that impedes the development of disease (Fabbi, Carbotti et al., 2017).

4.4.2..7 B-cell lymphoma 2 (BCL-2)

The presence of inflammatory infiltrate is an important requirement in OLP lesions. The Bcl-2 protein is an essential component in the mechanism promoting the persistence of inflammatory cells (Valente, Pagano et al., 2001). Generally, the expression of Bcl-2 in normal buccal mucosa at the basal or suprabasal layers was low or absent. Therefore, Bcl-2 expression may be related to tumour development mediated by its inhibition of the apoptosis of dysplastic cells in the basal layer. Alternatively, it may contribute to the malignant transformation of lesions, possibly by supporting the persistence of the inflammatory infiltrate (González-Moles, Bascones-Ilundain et al., 2006).

4.4.2..8 Immunohistochemical reagents and conditions

Immunohistochemistry was performed by NovoPath in the Department of Cellular Pathology, The Newcastle Hospitals NHS Foundation Trust. 4µm sections were cut from formalin-fixed paraffin embedded tissue and immunohistochemically performed on either a Ventana Benchmark Ultra or a Ventana Discovery Ultra (Ventana Medical Systems Inc., USA) autostainer. The primary antibodies and optimised conditions are listed in (Table 4.1).

Table 4-1 Immunohistochemical reagents and conditions

Antibody	Clone	Species	Manufacturer	Dilution	Method	Retrieval[2]	Detection
STAT-3	Y705 D3A7	RABBIT	CELL SIGNALLING	1:400	BENCHMARK	SCC1	OM RB HRP
INF-ϒ	AB9657	RABBIT	ABCAM	1:100	DISOVERY	MCC1	OM RB HRP
TNF-α	2124	MOUSE	PROTEIN TECH	1:1000	BENCHMARK	SCC1	OM MS HRP
Notch1	EP1238Y	RABBIT	ABCAM	1:400	BENCHMARK	SCC1	OPTIVIEW
IL28B(IFN-λ3)	C767412	RABBIT	LS BIO	1:500	DISOVERY	SCC1	OM RB HRP
IL27	AB229139	RABBIT	ABCAM	1:500	DISOVERY	SCC1	OM RB HRP
Bcl-2[1]	NCL2/100/D5	MOUSE	LEICA	1:10	BENCHMARK	SCC1+AMP	OPTIVIEW

[1]Verified diagnostic test performed in an ISO accredited pathology laboratory. The remaining antibodies were optimised for the research study.[2]SCC1 and MCC1 are Ventana Benchmark Ultra automated retrieval protocols.

4.5 Results

4.5.1 STAT-3

Control samples of small bowel tissue were used to ensure the quality of the IHC staining, which demonstrated the expected staining of squamous epithelium for *STAT-3* (Figure 4.2 A). However, there was no significant difference in staining strength between white keratosis (B and C) or OLP (D-F). Most slides, whether white keratotic lesions or OLP tissue samples, have the same weak staining pattern, although the staining appears in the nuclei of lymphocyte cells in the inflammatory infiltrate band for OLP.

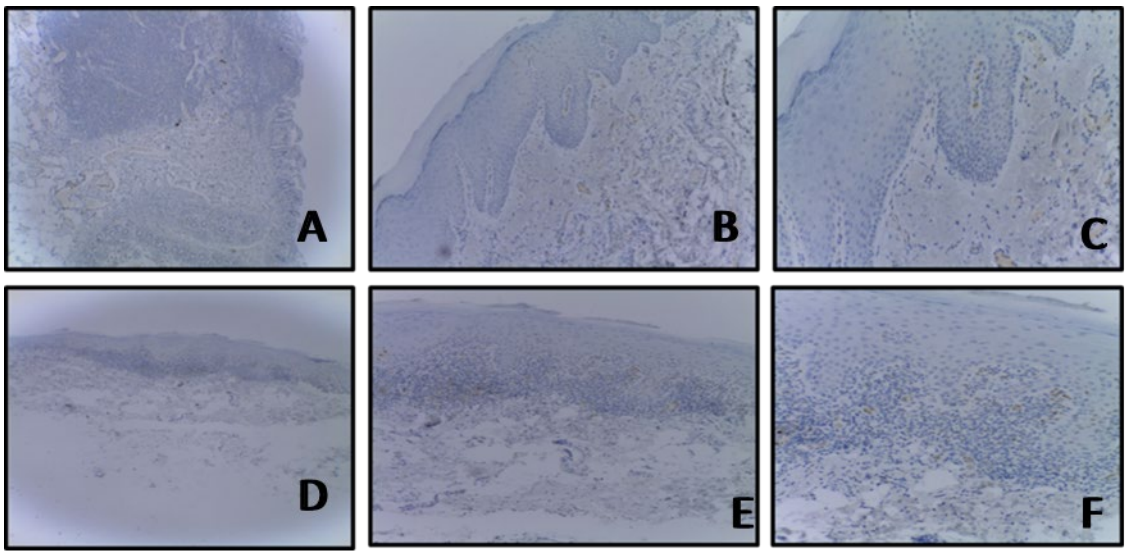

Figure 4-2 Expression profile of *STAT-3* Positive control in small bowel tissue (A); White keratosis (B-C) and oral lichen planus (D-E) showed weak staining of STAT-3 and also illustrate weak nuclear staining in the inflammatory infiltrate band for OLP. Magnification at x4 (A and D), x10 (B and E) and at x20 (C and F).

4.5.2 INF-Ɣ

Normal skin tissue was used as a positive control for *INF-γ* (Figure 5.3A) and IHC shows very strong staining in epidermal tissue elements. In oral white keratosis and OLP *IFN-γ* staining appears to be a combination of nuclear and cytoplasmic with a diffuse and strong staining of T-lymphocytes in the OLP tissue samples. The staining pattern in the controls was weaker than the OLP and predominantly epidermal (Figure 5.3B and D).

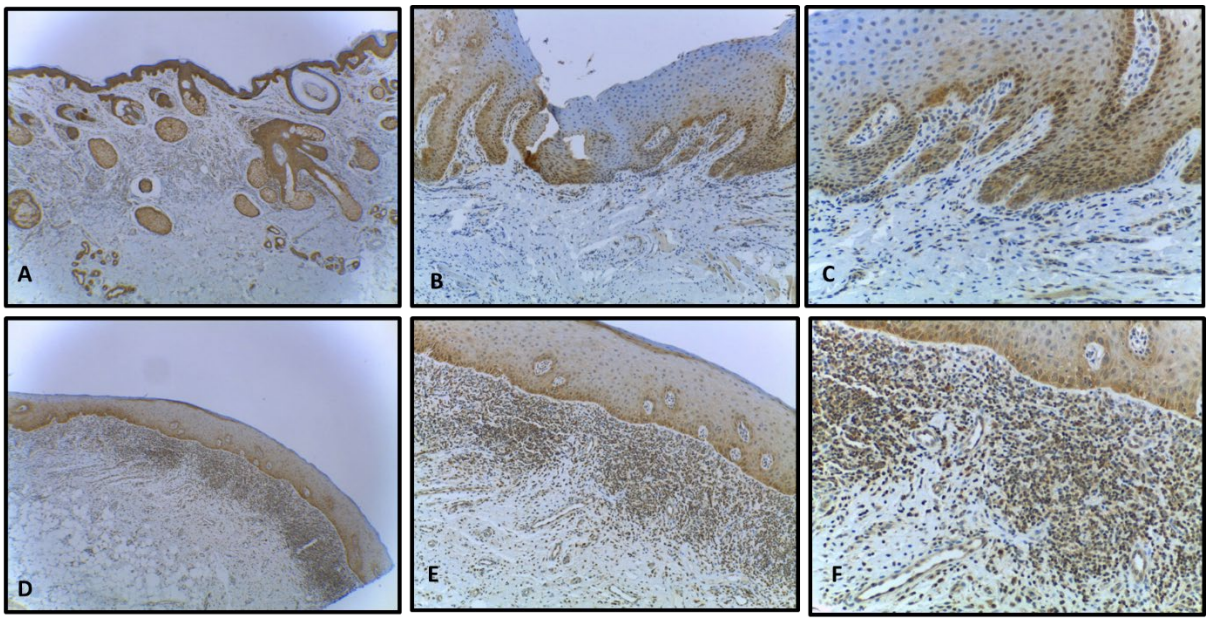

Figure 4-3 Expression profile of *INF-Ɣ* Positive control of normal skin tissue sample (A). Controls samples showed mainly epidermal staining (B and C), whereas the OLP tissues (D, E and F) shows that both epidermal and within the nuclear of inflammatory infiltrate. Magnification at X4 (A,D), x20 and (B,E) and x40 (C,F), respectively.

4.5.3 TNF-α

Figure (5.4 A) demonstrates the expression pattern of *TNF-α* in positive control of a small bowel tissue sample with an intense staining of lining cells. In the control group (B, C and D) and in the OLP patients (E, F and G), IHC displayed a fairly heterogeneous pattern of *TNF-α* expression in the epithelium elements not in the inflammatory infiltrate band. Therefore, the *TNF-α* is more likely to be expressed in keratinocyte cells than lymphocytes. The intensity of staining was stronger in patients' samples compared to the control group.

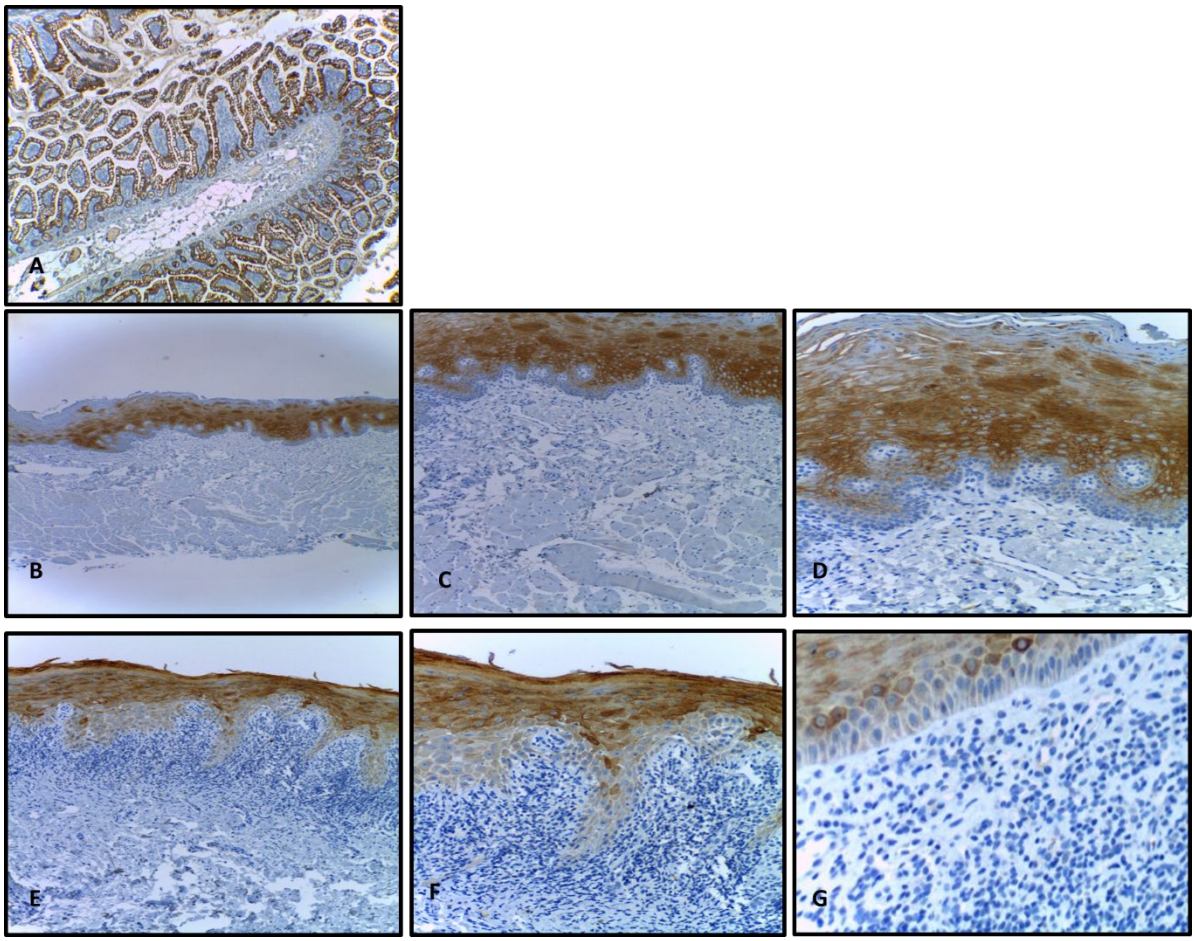

Figure 4-4 Expression profile of *TNF-α* Positive control of small bowel tissue (A). Intense epidermal staining in both controls (B, C and D) and oral lichen planus (E, F and G). Notably, the inflammatory infiltrate in the OLP is spread. Magnification x4 in A,B and E, x10 in C and F and X20 in D and G.

4.5.4 NOTCH1

NOTCH1 expression showed weak to moderate cytoplasmic staining for *NOTCH1* in the basal keratinocytes, whereas in the oral keratosis and OLP, the staining was stronger and mainly epithelial but in the OLP, *NOTCH1* exhibited some expression in the inflammatory infiltrate.

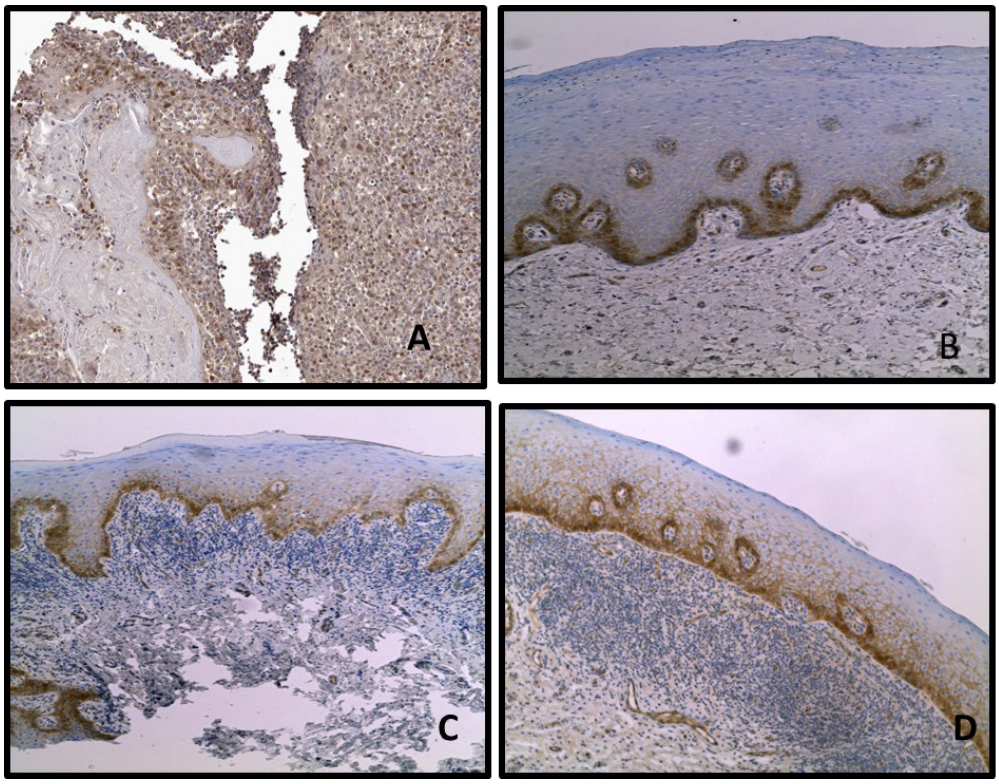

Figure 4-5. Expression of *NOTCH1*Weakly positive tonsil tissue (A), oral keratosis (B) and OLP (C and D) and oral lichen planus. Immunohistochemistry shows cytoplasmic expression staining of NOTCH but no stain in the inflammatory infiltrate; Magnification at x10 (A and C) and at x20 (B and D). slide (A) available at www.proteinatlas.org.

4.5.5 IL28B (INF-λ3)

Figure 5.6 illustrates the expression of *INF- λ3* in the positive control skin tissue with cytoplasmic expression in the epithelium elements (A). Likewise, in controls (B and C), there is a weak positive expression in the epithelium area. In the OLP, IHC of *INF-λ3* exhibits a patchy cytoplasmic weak expression in the inflammatory band but it is not nuclear (D, E and F). Interestingly, both the OLP and controls show a similar weak staining pattern.

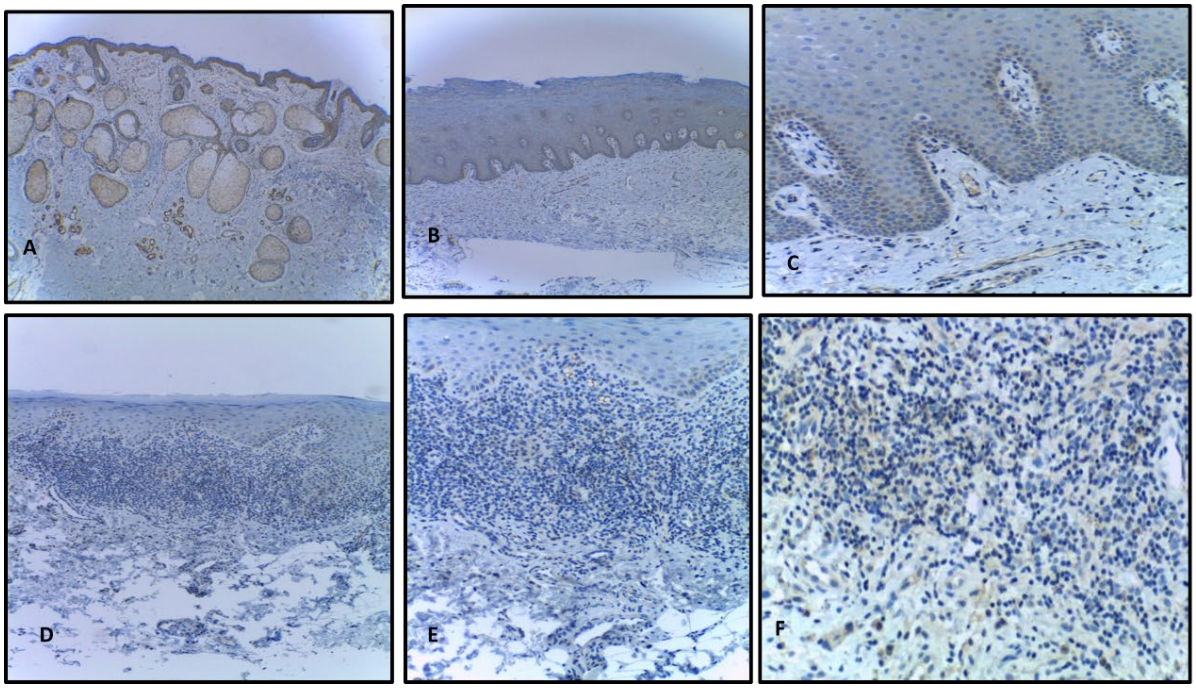

Figure 4-6 Expression of *IL28B (INF-λ3)* Positive control, normal skin tissue sample showing staining in the epidermal elements (A). Oral keratosis (B and C) and oral lichen planus. (D, E and F) revealed a similar weak epidermal staining also with some weak cytoplasmatic expression in the inflammatory infiltrate in the OLP. Magnification at x4 in (A, B and D) and at x10 in (C and E).

4.5.6 Bcl-2

For *Bcl-2* tonsillar, tissue samples were used as a positive control. Figure 5.7A shows that the expression of *BCL2* is very strong nuclear and cytoplasmatic and primarily observed in the lymphoid tissue, whereas there is no expression staining in the lymphoid follicles. In the OLP, the staining was predominant in the inflammatory band of OLP tissue samples (D-F), almost mirroring the expression seen for *INF-γ*, whereas in the controls, *Bcl-2* shows moderate staining (B and C).

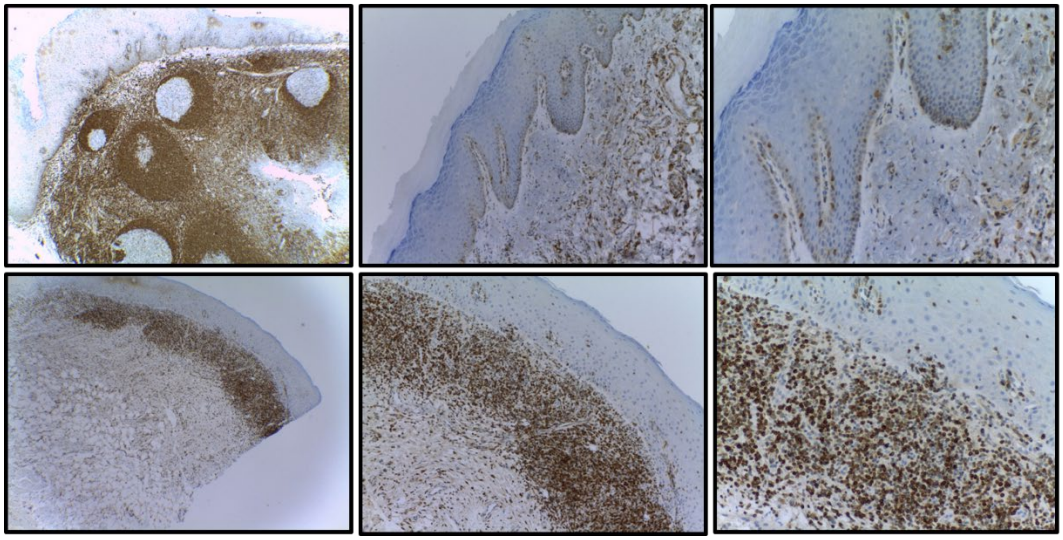

Figure 4-7 Expression of *Bcl-2* Positive control, tonsillar tissue, showing a strong expression in the lymphatic tissue but negative staining of the lymphoid follicles (A). Strong expression, mainly in the inflammatory infiltrate in the OLP (D, E and F), whereas the staining is positive but weaker in the oral keratosis (B and C); Magnification at 10 (A, B and E) and at x20 (C and F).

4.5.7 IL27

Figure 5.7 shows the positive skin sample control (A) that highlights the weak staining predominantly evident in the sebaceous glands. However, there was a higher expression of *IL27* especially around the blood vessels and also some weak staining of lymphocytes in the inflammatory infiltrate band of the OLP samples (D, E and F). Oral keratosis (B and C) showed weak staining. Nevertheless, the staining of the positive control skin tissue, oral keratosis and OLP was equally weak.

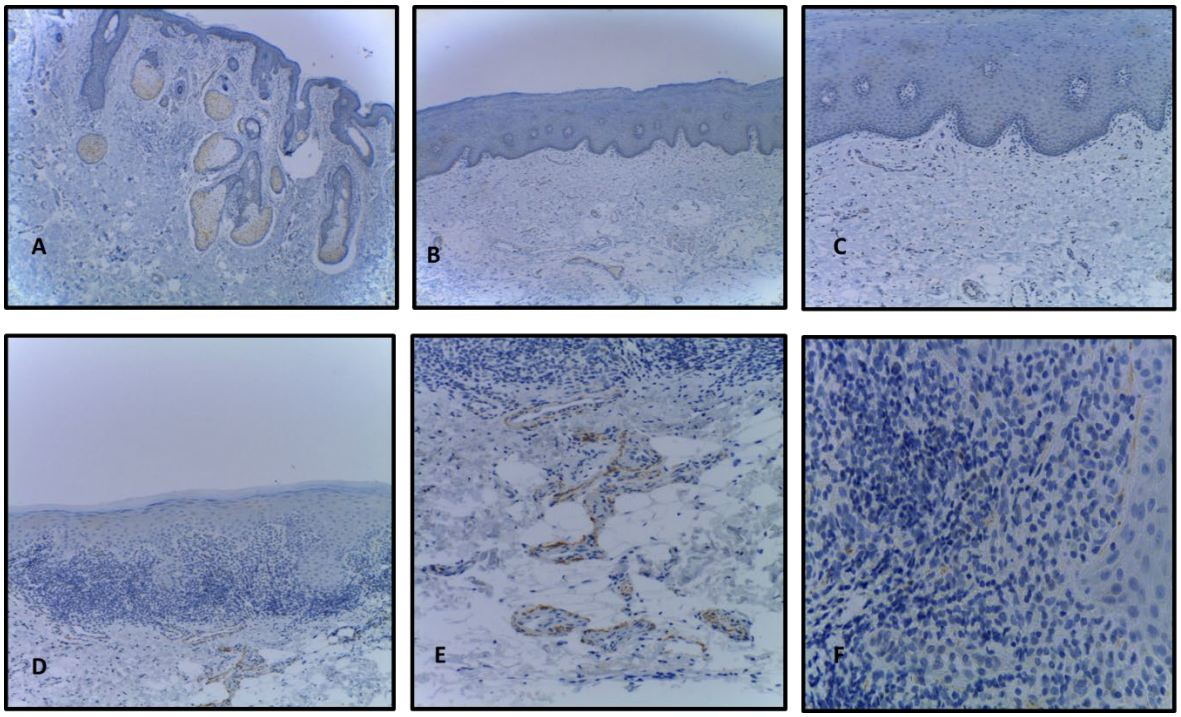

Figure 4-8 Expression of *IL27* Positive control, normal skin tissue sample exhibiting weak staining of sebaceous glands (A). The expression was also weak in oral keratosis (B and C) and oral lichen planus (D and E). In the latter, some nuclear expression of *IL27* in the inflammatory infiltrate could be noticed (F). Magnification at x4 in (A, B and D) and at x10 in (C and E).

4.6 Summary

Table 4.2 presents a summary of the IHC results in OLP and control samples as well as positive controls in different tissues. *STAT-3* showed a weak staining in all samples including the positive control. However, *NOTCH, IL27* and *BCL2* only revealed a weak staining in the positive control and control samples. Similarly, staining was weak for *IL28B* in OLP samples. *INF-γ* and TNF-α show a strong staining in the in epidermal region of control samples whereas *TNF-α* and *BCL2* reveal strong staining in OLP patient samples localized in the inflammatory infiltrate band area. On the other hand, OLP samples shows moderate intensity staining with *INF-γ, NOTCH* and *IL27* antibodies.

Table 4-2: Summary finding of IHC in OLP patients and control samples

Antibody	Positive control	OLP sample	Control sample
STAT-3	Weak	Weak	weak
INF-γ	Strong in skin tissue	Moderate in epidermal and inflammatory infiltrate band	Strong epidermal staining
TNF-α	Strong in small bowel	Strong in inflammatory infiltrate	Strong epidermal staining
NOTCH	Weak in tonsil tissue	Moderate staining in cytoplasmic area	Weak
IL-28B	Moderate in skin tissue	Weak in cytoplasmic and inflammatory infiltrate area	Weak in epidermal regions
BCL2	Weak in tonsils	Strong in inflammatory infiltrate region	Weak
IL27	Weak in skin tissue	Moderate in inflammatory infiltrate band	Weak

4.7 Discussion

OLP is a T cell–mediated autoimmune disease with keratinocyte apoptosis and subsequent overproduction of inflammatory cytokines that involves a complex deregulated signalling system (Khan, Farah et al. 2003).

Our results confirmed that OLP is a T cell-mediated disease characterised by a strong expression of *INF-ϒ* and *TNF-α*. However, these two cytokines are expressed in a very different topographic way, suggesting that their involvement in OLP pathogenesis has a different timeframe.

In the present study, *IFN-γ* was highly expressed around the inflammatory infiltrate. *IFN-ϒ* transcriptions were found within the infiltrating cells and keratinocytes in the OLP lesions by in situ hybridisation techniques (Mattsson, Jontell et al. 1998) and with enzyme-linked immunospot assay (Yamamoto and Osaki, 1995). This cytokine was

consistently detected by immunohistochemistry in the OLP tissues as observed in the present work (Khan, Farah et al., 2003). Of note, topical corticosteroids, that are the first line medications for OLP, can improve OLP significantly reducing *INF-Ɣ* expression

TNF-α potentially contributes to the accumulation of inflammatory cells seen in the epithelium layer and basal layer by inducing the expression of other cytokines. TNF-α therefore might play a significant role in the pathogenesis of OLP (Thongprasom, Dhanuthai et al., 2006). However, in this study, *TNF-α* expression was very different from *INF-Ɣ* and consistent with previous observations (Sklavounou, Chrysomali et al., 2000). In fact, *TNF-α* was strongly expressed within the epithelium, although there was no expression in inflammatory infiltrate band. This may possibly suggest that the main source of this cytokine in OLP are keratinocytes rather than immune cells.

Bcl-2 was also strongly expressed in the OLP tissues and almost exclusively noticed in the sub-epithelial inflammatory infiltrate mirroring *IFN-γ* staining. Overexpression of Bcl-2 has been suggested to possibly cause the absence or low rate of apoptosis observed in inflammatory cells in OLP, contributing to the persistence of the inflammatory infiltrate (Bascones-Ilundain et al., 2006). Notably, the *Bcl-2* staining pattern in OLP have been also described in other lichenoid disorders, such as acute graft-versus-host disease and erythema multiform (Sklavounou, Chrysomali et al., 2000).
NOTCH1 in the present study was seen in the OLP and control tissues mainly expressed in the lower third of the epithelium but also within the inflammatory infiltrate in OLP. Notably, recent in vivo studies indicate that *NOTCH* signalling is a major proinflammatory pathway in T cell alloimmunity and that *NOTCH* inhibition can dampen both allograft rejection and GVHD (Chung et al., 2016).

IL-28B (INF-λ3) has been shown to possess immunoregulatory purposes on T helper 2 responses by inhibiting a number of cytokine related to OLP pathogenesis such as *IL-3,* IL-4 and IL-15 (Dai, Megjugorac et al., 2009). However, regarding *IL-28B* (*INF-λ3*), the staining pattern between the OLP and controls was noticed to be similar.

Few studies have reported *STAT-3* expressions in the local immune response of patients with OLP and determined expression correlation with clinical manifestations of OLP.

Our findings confirmed that *STAT-3* staining was weak and the expression level was scarcely seen in the lymphocyte cells in OLP (Figure 5.2, D-F). It has been suggested that the role of this specific location is to preserve the highest number of epithelial stem cells

to protect the cell proliferation during the apoptotic process and to regulate the differentiation of keratinocytes. Du, Chen et al. (2018), reported that the expression of *STAT-3* was increased in OLP tissue compared with normal controls. Nonetheless, our results have not confirmed these findings. Huang, Zhou et al. (2016), demonstrate a greater expression of *IL-27* in the serum of OLP patients than those in the control normal healthy group. Moreover, correlation analysis revealed that *IL-12* and *IL-27* expression were positively associated. As OLP is mostly a chronic inflammatory condition, it is thought that *IL-12* may be involved in the pathogenesis of OLP together with *IL-27*. In this study, the intensity and extent of *IL-27* expression in both the epithelium and the lamina propria were slightly more elevated in OLP tissues, as compared to the control group, although the relevance of this finding is uncertain.

Chapter 5. General Discussion

Oral lichen planus (OLP), is likely a localised mucosal autoimmune disease that is more frequent in the fourth decade of life and principally occurs in female patients (Sugerman, Savage et al., 2002). .

Strong evidence suggests that OLPis a T-cell-mediated disease. The lymphocytic infiltrate in OLP is composed almost exclusively of T-cells and typical T-cell mediated diseases, for example, chronic graft-versus-host-disease (cGVHD) can be clinically and histopathologically indistinguishable from OLP (Carrozzo, 2014). Whilst the specific aetiological factors driving OLP remain elusive, evidence points to the development of a chronic, dysregulated immune response to OLP-mediating antigens presented by innate immune cells and oral keratinocytes leading to increased cytokine, chemokine and adhesion molecule expression (El-Howati, Thornhill et al., 2022).

miRNAs are small, highly preserved non-coding RNA molecules. That responsible for regulating innate and acquired immunity by contributing to the generation of immune cells, including T cells, B cells and dendritic cells.

As miRNAs are known to regulate the expression of inflammation-related cytokines, we assumed that miRNA–cytokines regulation pathway may be associated with the pathologic features of OLP.

5.1 Key findings

5.1.1 Immunohistochemistry

Traditionally, OLP is considered a Th1 mediated disease mainly because of the prevalent expression of TNF-α and IFN-γ (Khan et al., 2003). Our immunohistochemically findings confirmed the strong expression of both these cytokines in the OLP tissues, though we also confirmed a significant difference in the staining pattern between them. IFN-γ was indeed highly expressed around the inflammatory infiltrate, whereas TNF-α primarily showed epidermal staining particularly in the stratum spinosum and stratum granulosum, consistent with previous observation on both OLP and skin LP (Sklavounou, Chrysomali et al. 2000; Xu et al. 2007).

These observations suggest that the main sources of TNF-α and IFN-γ production in OLP may be different, being the keratinocytes for the former and T lymphocytes for the latter.

Several proteins of the Bcl gene family are involved in the regulation of programmed cell death either by preventing (Bcl-2, Bcl-xL, Bcl-w, Mcl-I) or by promoting (Bax, Bik, Bak, Bad, Bcl-xs) apoptosis (Abdel-Latif, Abuel-Ela et al., 2009). Bcl-2 has been consistently found to be overexpressed in OLP tissues (Abdel-Latif, Abuel-Ela et al., 2009) and (Bascones-Ilundain, Gonzalez-Moles et al. 2006), as confirmed by our immunohistochemical findings. In our study, Bcl-2 expression was almost exclusively seen in the sub-epithelial inflammatory infiltrate and was mirroring IFN-γ staining. Overexpression of Bcl-2 has been suggested to possibly cause the absence or low rate of apoptosis observed in inflammatory cells in OLP, contributing to the persistence of the inflammatory infiltrate and potentially increasing the likelihood of the onset of molecular disorders in epithelial cells and possibly favouring the development of cancer in OLP (Bascones-Ilundain, Gonzalez-Moles et al., 2006).

The Notch pathway is altered in head and neck squamous cell carcinoma. Several studies reported that Notch can have either an oncogenic or tumour suppressor effect. Moreover, Notch signalling is also important in T cell development and differentiation (Hosokawa and Rothenberg, 2021; Di Ianni, Del Papa et al., 2018). Notch staining in the present study was seen in the OLP and control tissues mainly expressed in the lower third of the epithelium but also within the inflammatory infiltrate in OLP. Notably, contemporary in vivo studies indicate that Notch signalling is a major pro-inflammatory pathway in T cell alloimmunity and that Notch inhibition can dampen both allograft rejection and GVHD (Chung, Deacon et al., 2016).

STAT-3, IL27 and IFN-λ3 (IL28b) were all weakly expressed at comparable levels in the OLP and control tissues, which seems to suggest that these molecules do not have a relevant role in OLP pathogenesis.

5.1.2 NanoString and qPCR analysis

Our NanoString findings suggest that 9 miRNAs were upregulated in OLP, namely miR-155, miR-146a, miR-3195, miR-342, miR-4516, miR-21, miR-29a, miR-193a and miR-222, while the other 9 miRNAs, let-7, miR-23a, miR-23b, miR-200b, miR-149, miR-205, miR-27b, miR-221 and miR-95 were downregulated. Two upregulated, specifically miR-4516 and miR-222 and 2 downregulated miRNAs, miR-149, miR-95, were novel discoveries, whilst the remaining miRNAs were confirmation of previous findings. Two others, miR-3195, miR-193, were determined to be upregulated but previous studies found them mainly downregulated in OLP (see Tables 3.1 and 3.2, Chapter 3).

This is also the first study on miRNAs expression in British patients. Different from many previous microarray studies, our NanoString findings have been confirmed by qPCR results for the following 5 upregulated miRNAs, specifically miR-155, miR-146a, miR-29a, miR-222 and miR-342 and two downregulated miRNAs, namely miR-205 and miR23b.

Other studies not only used different methods to investigate miRNAs expression but they also employed different sources of miRNAs, either peripheral blood or saliva (see Table 3.1 and 3.2, Chapter 3). Whereas in typical autoimmune disorders such as lupus erythematosus or rheumatoid arthritis, peripheral blood mononuclear cells (PBMC) may represent a reliable source of information to investigate immune-pathogenesis, this is less straightforward in OLP that is a more localised autoimmune disease (Carrozzo, 2014). Similarly, saliva can be a potentially helpful source of biomarkers for oral disorders but managing confounding factors such as, for example, periodontal disease, may be challenging.

As in our study, miR-155 has been consistently found upregulated in OLP in populations of different geographic background (Arão, Guimarães et al., 2012; Gassling, Hampe et al., 2013; Chen, Du et al., 2017). It is well-known that miR-155 is essential for immune system regulation but the underlying mechanisms in OLP have not yet been fully elucidated. Hu, Ye et al. (2015), ascertained that whilst miR-155 negatively regulates suppressor of cytokine signalling 1 (SOCS1) in $CD4^+$ T lymphocytes, it has a positive interaction with IFN-γ, which may facilitate a T helper type 1 cell (Th1) polarisation in OLP.

Similarly, to miR-155, miR-146a has been found to be mostly overexpressed in OLP (Arão, Guimarães et al., 2012; Wang et al., 2016; Chen, Du et al., 2017). Forkhead box P3 (Foxp3) and miR-146a elevated T regulatory cells and regulated tumour necrosis factor receptor-associated factor 6 (TRAF6) expression in $CD4^+$ T cells that were isolated from PBMC of patients with OLP (Wang, Zhang et al., 2018).

The other 3 upregulated, that is miR-222, miR-29a, miR-342 and the two downregulated, miR-205 and miR-23b whose expression have been confirmed by qPCR in our study, could be involved in malignant transformation of OLP more than its immunopathogenesis. Actually, abnormal expression of miR-222 has been mainly reported in several cancer tissues including breast, liver, skin, gastric, pancreatic and myeloma (Song et al., 2017). In a similar manner, miR-29a plays a pivotal role in cancer

metastasis (Roy, Singh et al., 2016), whereas miR-342 has been linked to melanoma prognosis (Kunz, 2013). However, recently it has been disclosed that anti-inflammatory roles of glucocorticoids may be mediated by Foxp3^{+}Regulatory T Cells via a miR-342-dependent mechanism (Kim, Nguyen et al., 2020). miR-205 plays important roles in the physiology of epithelia. Aberrant expression of miR-205 is frequently found in human cancers, where it was reported to act either as tumour-suppressor or oncogene depending on the specific tumour context and target gene (Ferrari and Gandellini, 2020). miR-29b has been involved in various cancers but also autoimmune diseases (Guo, Wu et al., 2021). In particular, bone marrow mesenchymal stem cells (BMSCs) loading overexpression miR-23b inhibits Th-17cell differentiation (Hu et al., 2021). Thus, under expression of miR-23b in OLP could in theory facilitate Th-17 differentiation.

5.1.3 Target gene selected microRNA interaction

After computational analysis a number of target genes for the up- and downregulated miRNA were identified. The predictions were then assessed for a potential involvement in OLP pathogenesis in order to minimise the number of target genes.

According to the assumption that high miRNA levels have a negative impact on the level of their target gene, a negative correlation would be expected between miRNA levels and the target gene.

The bioinformatics analysis predicted that miR-155 has four common target genes including cyclin D1 gene (CCND1), matrix metalloproteinase-1 (MMP1), MYC and TGF-Beta Activated Kinase 1 Binding Protein 2 (TAB2). All the potential target genes of miRNA 155 were either expressed at a comparable level between the two groups or exhibited a slightly opposite trend to the miR-155 levels, suggesting a possible interaction between miR-155 and the proposed target genes. The lack of statistical significance was possibly because of the relatively small sample size. Alternatively, it maybe that other target genes should be considered to fully understand the role of miR-155 in OLP pathogenesis. Interestingly, increased CCND1 relative gene expression already has been shown in OLP and related to the downregulation of another miRNA, miR-138 (Ghallab, Kasem et al., 2017).

In contrast, MYC, that was one of the predicted target genes for the upregulated miR-29a, was significantly downregulated in OLP. According to these results, miR-29a could be directly regulating MYC in OLP. Of note, it has been reported that MYC status on some

OLP lesions may predict a subgroup of patients with a higher risk of progression to oral squamous cell carcinoma (OSCC) (Segura et al., 2013).

Target gene prediction identified interleukin 24 (IL-24) and MMP1 as potential targets for a down regulated miRNA, namely miR-205. Real time-qPCR experiments revealed that in OLP patient samples IL-24 and MMP1 were upregulated as compared with the control. IL-24 was isolated in 1996 (Mitamura et al., 2020) and then characterised as a member of the IL-10 family of cytokines, which also contains IL-10, IL-19, IL-20, IL-22, IL-26, along with three members from the type III interferons, i.e., IL-28A,IL28B, and IL-29 (Zhong et al., 2022).

IL-24 was found upregulated in psoriasis, atopic dermatitis and systemic lupus erythematosus (Kumari et al., 2013; Mitamura et al., 2020) and may have a suppressive function on mucosal inflammation in ulcerative colitis and Crohn's disease (Andoh et al., 2009). IL-24 is thought to be produced by Th2 lymphocytes and keratinocytes stimulated by type 2 cytokines (Mitamura et al., 2020). Current data suggest that IL-24 may display both pro- and anti-inflammatory properties depending on the type of autoimmunity and the site of inflammation (Zhong et al., 2022). Moreover, IL-24 also is a well-known tumour suppressor gene in a variety of cancers (Kim et al., 2013), Notably, Kim et al. (2013), confirmed that transfection of miR-205 into KB oral cancer cells strongly induced IL-24.

This study is apparently the first showing abnormal expression of IL-24 in OLP. This cytokine could be involved in both immunopathogenesis and malignant transformation of the disease. Therefore, the suggestion that IL-24 expression could be regulated by miR-205.

Several studies have already shown that matrix metalloproteinase, particularly MMP-1, are overexpressed in OLP (Sutinen et al., 1998; Mazzarella et al., 2006; Tao et al., 2009) and our findings confirm these observations. Moreover, we showed for the first time, that MMP-1 expression could be, at least partially, regulated by miR-205.

5.2 Concluding and future work

In conclusion, the work presented in this thesis has made novel contributions to the understanding of the OLP pathogenesis pathway and in particular to the role of miRNAs in this disease. We confirmed that OLP is primarily a T-cell mediated disease characterised by the overexpression of IFN-γ and TNF-α and apoptosis markers. By using NanoString technology we were able to screen up to 800 genes without any amplification and find 9 upregulated and 9 downregulated miRNAs in OLP tissues. We confirmed the results using real time q-PCR in 5 upregulated (miR-155, miR146a, miR-29a, miR-222 and miR342) and 2 downregulated (miR-205, miR-23b) miRNAs. Our results suggest that miRNAs could be involved in both the immunopathogenesis and malignant transformation of OLP as shown by a variety of possible interactions with target genes, specifically MYC, IL-24 and MMP1.

Based on the present findings, areas of future research would include:

1. It would be interesting to investigate further the role of those miRNAs, for instance miR-155, miR-146a, miR-205 and miR23b that are likely involved in the immunopathogenesis of OLP and clarify by means of using either in vitro and in vivo models their effects on cytokines production and T-cell differentiation
2. It would be also interesting to specifically continue to study IL-24 role in OLP and clarify if it works principally as pro- or anti-inflammatory cytokine in this disease and explore its potential as a therapeutic target.
3. On account of our findings on miR-222, miR-342, miR-29a and miR-205 and the possible role of miRNAs in oral carcinogenesis, this should be further analysed to understand if these or other miRNAs could be used as biomarkers, maybe in combination with some key target genes, to better predict the malignant transformation of OLP.

Chapter 6. References

Abdel-Latif AM, Abuel-Ela HA, El-Shourbagy SH. (2009). "Increased caspase-3 and altered expression of apoptosis-associated proteins, Bcl-2 and Bax in lichen planus." Clinical and Experimental Dermatology: **34**(3): 390-395.

Aceto, N., et al. (2012). "Tyrosine phosphatase SHP2 promotes breast cancer progression and maintains tumor-initiating cells via activation of key transcription factors and a positive feedback signaling loop." Nature Medicine **18**(4): 529-537.

Aghbari SMH, Abushouk AI, Attia A, Elmaraezy A, Menshawy A, Ahmed MS, Elsaadany BA, Ahmed EM. (2017). "Malignant transformation of oral lichen planus and oral lichenoid lesions: A meta-analysis of 20095 patient data." Oral Oncology **68**: 92-102.

Akbari Moqadam F, Pieters R, den Boer ML. (2012). "The hunting of targets: Challenge in miRNA research." Leukemia: official journal of the Leukemia Society of America, Leukemia Research Fund, U.K **27**.

Al-Hashimi I, Schifter M, Lockhart PB, Wray D, Brennan M, Migliorati CA, Axéll T, Bruce AJ, Carpenter W, Eisenberg E, Epstein JB., et al. (2007). "Oral lichen planus and oral lichenoid lesions: diagnostic and therapeutic considerations." Oral Surgery, Oral Medicine, Oral Pathology, Oral Radiology, and Endodontology **103**: S25. e21-S25. e12.

Alaizari NA, Al-Maweri SA, Al-Shamiri HM, Tarakji B, Shugaa-Addin B.. (2016). "Hepatitis C virus infections in oral lichen planus: a systematic review and meta-analysis." Australian Dental Journal **61**(3): 282-287.

Alivernini S, Gremese E, McSharry C, Tolusso B, Ferraccioli G, McInnes IB, Kurowska-Stolarska M.. (2018). "MicroRNA-155—at the Critical Interface of Innate and Adaptive Immunity in Arthritis." Frontiers in Immunology **8**: 1932.

Alrashdan MS, Cirillo N, McCullough M. (2016). "Oral lichen planus: a literature review and update." Archives of Dermatological Research **308**(8): 539-551.

Andoh A, Tsujikawa T, Sasaki M, Mitsuyama K, Suzuki Y, Matsui T, Matsumoto T, Benno Y, Fujiyama Y. (2009). "Faecal microbiota profile of Crohn's disease determined by terminal restriction fragment length polymorphism analysis." Alimentary Pharmacology & Therapeutics **29**(1): 75-82.

Aradhya, S. and A. M. Cherry (2007). "Array-based comparative genomic hybridization: clinical contexts for targeted and whole-genome designs." Genet Med 9(9): 553-559.

Arão, T.C., Guimarães, A.L., de Paula, A.M., Gomes, C.C., Gomez, R.S. (2012). Increased miRNA-146a and miRNA-155 expressions in oral lichen planus. Archives of Dermatological Research. 2012 304(5):371-5.

Arrieta JJ, Rodriguez-Inigo E, Casqueiro M, Bartolomé J, Manzarbeitia F, Herrero M, Pardo M, Carreno V. (2000). "Detection of hepatitis C virus replication by in situ hybridization in epithelial

cells of anti–hepatitis C virus–positive patients with and without oral lichen planus." Hematology **32**(1): 97-103.

Artavanis-Tsakonas S, Rand MD, Lake RJ. (1999). "Notch signaling: cell fate control and signal integration in development." Science **284**(5415): 770-776.

Bai J, Lin M, Zeng X, Zhang Y, Wang Z, Shen J, Jiang L, Gao F, Chen Q. (2008). "Association of polymorphisms in the human IFN-γ and IL-4 gene with oral lichen planus: a study in an ethnic Chinese cohort." Journal of Interferon & Cytokine Research **28**(6): 351-358.

Balkwill, F. (2009). "Tumour necrosis factor and cancer." Nature Reviews Cancer 9(5): 361-371.

Bar J, Gorn-Hondermann I, Moretto P, Perkins TJ, Niknejad N, Stewart DJ, Goss GD, Dimitroulakos J. (2015). "miR Profiling Identifies Cyclin-Dependent Kinase 6 Downregulation as a Potential Mechanism of Acquired Cisplatin Resistance in Non–Small-Cell Lung Carcinoma." Clinical Lung Cancer **16**(6): e121-e129.

Bartel, D. P. (2009). "MicroRNAs: target recognition and regulatory functions." Cell 136(2): 215-233.

Bascones-Ilundain C, Gonzalez-Moles MA, Esparza-Gómez G, Gil-Montoya JA, Bascones-Martínez A. (2006). "Importance of apoptotic mechanisms in inflammatory infiltrate of oral lichen planus lesions." Anticancer Research **26**(1A): 357-362.

Bayraktar, R. and Van Roosbroeck, K. (2018). "miR-155 in cancer drug resistance and as target for miRNA-based therapeutics." Cancer and Metastasis Reviews 37(1): 33-44.

Byun JS, Hong SH, Choi JK, Jung JK, Lee HJ. (2015). "Diagnostic profiling of salivary exosomal micro RNA s in oral lichen planus patients." Oral Dis 21(8): 987-993.

Bianchi S, Dotti MT, Federico A. (2006). "Physiology and pathology of notch signalling system." Journal of Cellular Physiology **207**(2): 300-308.

Bloor BK, Malik FK, Odell EW, Morgan PR. (1999). "Quantitative assessment of apoptosis in oral lichen planus." Oral Surgery, Oral Medicine, Oral Pathology, Oral Radiology, and Endodontology **88**(2): 187-195.

Boyd, A. S. and K. H. Neldner (1991). "Lichen planus." Journal of the American Academy of Dermatology **25**(4): 593-619.

Brennecke J, Stark A, Russell RB, Cohen SM. (2005). "Principles of microRNA–target recognition." PLoS Biology **3**(3): e85.

Calautti E, Avalle L, Poli V. (2018). "Psoriasis: a STAT3-centric view." International Journal of Molecular Sciences **19**(1): 171.

Carrozzo M, Porter S, Mercadante V, Fedele S. (2019). "Oral lichen planus: A disease or a spectrum of tissue reactions? Types, causes, diagnostic algorhythms, prognosis, management strategies." Periodontology 2000 **80**(1): 105-125.

Carrozzo, M. (2014). "Understanding the pathobiology of oral lichen planus." Current Oral Health Reports 1(3): 173-179.

Carrozzo M, Uboldi de Capei M, Dametto E, Fasano ME, Arduino P, Broccoletti R, Vezza D, Rendine S, Curtoni ES, Gandolfo S. (2004). "Tumor necrosis factor-α and interferon-γ polymorphisms contribute to susceptibility to oral lichen planus." Journal of Investigative Dermatology **122**(1): 87-94.

Carrozzo, M. and R. J. Thorpe (2009). "Update on oral lichen planus." Expert Review of Dermatology **4**(5): 483-494.

Chang TC, Yu D, Lee YS, Wentzel EA, Arking DE, West KM, Dang CV, Thomas-Tikhonenko A, Mendell JT. (2008). "Widespread microRNA repression by Myc contributes to tumorigenesis." Nature Genetics **40**(1): 43-50.

Chattopadhyay E, Singh R, Ray A, Roy R, De Sarkar N, Paul RR, Pal M, Aich R, Roy B (2016). Expression deregulation of mir31 and CXCL12 in two types of oral precancers and cancer: importance in progression of precancer and cancer. Sci Rep. 2016 Sep 6; 6:32735

Chen B, Li H, Zeng X, Yang P, Liu X, Zhao X, Liang S. (2012). "Roles of microRNA on cancer cell metabolism." Journal of Translational Medicine **10**(1): 228.

Chen J, Feng J, Chen X, Xu H, Zhou Z, Shen X, Bao Z, Liu W, Shen Z. (2013). "Immunoexpression of interleukin-22 and interleukin-23 in oral and cutaneous lichen planus lesions: a preliminary study." Mediators of Inflammation 2013:801974

Chen J, Du G, Wang Y, Shi L, Mi J, Tang G. (2017). "Integrative analysis of mRNA and miRNA expression profiles in oral lichen planus: preliminary results." Oral Surgery, Oral Medicine, Oral Pathology and Oral Radiology **124**(4): 390-402. e317.

Chen Q, Zhang F, Wang Y, Liu Z, Sun A, Zen K, Zhang CY, Zhang Q. (2015). "The transcription factor c-Myc suppresses MiR-23b and MiR-27b transcription during fetal distress and increases the sensitivity of neurons to hypoxia-induced apoptosis." PLoS ONE **10**(3): e0120217.

Chen, S., et al. (2015). "Host miR155 promotes tumor growth through a myeloid-derived suppressor cell-dependent mechanism." Cancer Research **75**(3): 519-531.

Chien CS, Wang ML, Chu PY, Chang YL, Liu WH, Yu CC, Lan YT, Huang PI, Lee YY, Chen YW, Lo WL, Chiou SH. (2015). "Lin28B/Let-7 Regulates Expression of Oct4 and Sox2 and Reprograms Oral Squamous Cell Carcinoma Cells to a Stem-like State." Cancer Research **75**(12): 2553-2565.

Chitturi RT, Sindhuja P, Parameswar RA, Nirmal RM, Reddy BV, Dineshshankar J, Yoithapprabhunath TR. (2015). "A clinical study on oral lichen planus with special emphasis on hyperpigmentation." Journal of Pharmacy & Bioallied Sciences **7**(Suppl 2):S495-8

Chung E, Deacon P, Marable S, Shin J, Park JS. (2016). "Notch signaling promotes nephrogenesis by downregulating Six2." Development **143**(21): 3907-3913.

Cregger M, Berger AJ, Rimm DL. (2006). "Immunohistochemistry and quantitative analysis of protein expression." Archives of pathology & laboratory medicine**130**(7): 1026-1030.

Cribier B, Frances C, Chosidow O. (1998). "Treatment of lichen planus: an evidence-based medicine analysis of efficacy." Archives of Dermatology **134**(12): 1521-1530.

Cui B, Liu W, Wang X, Chen Y, Du Q, Zhao X, Zhang H, Liu SL, Tong D, Huang Y. (2017). "Brucella Omp25 upregulates miR-155, miR-21-5p, and miR-23b to inhibit interleukin-12 production via modulation of programmed death-1 signaling in human monocyte/macrophages." Frontiers in Immunology **8**: 708.

Dabbs, D. J. (2019). Diagnostic Immunohistochemistry E-Book: Theranostic and Genomic Applications, Elsevier, Philadelphia, USA

Dai J, Megjugorac NJ, Gallagher GE, Yu RY, Gallagher G. (2009). "IFN-λ1 (IL-29) inhibits GATA3 expression and suppresses Th2 responses in human naive and memory T cells." Blood, The Journal of the American Society of Hematology **113**(23): 5829-5838.

Dang Y, Zhao S, Qin Y, Han T, Li W, Chen ZJ. (2015). "MicroRNA-22-3p is down-regulated in the plasma of Han Chinese patients with premature ovarian failure." Fertil Steril 103(3): 802-807.e801.

Dey S, Kwon JJ, Liu S, Hodge GA, Taleb S, Zimmers TA, Wan J, Kota J. (2020). "miR-29a Is Repressed by MYC in Pancreatic Cancer and Its Restoration Drives Tumor-Suppressive Effects via Downregulation of LOXL2." Molecular Cancer Research: MCR **18**(2): 311-323.

Dickman, C. T. (2017). Secreted microRNAs and their role in cancer promotion and detection, University of British Columbia.

Di Ianni M, Del Papa B, Baldoni S, Di Tommaso A, Fabi B, Rosati E, Natale A, Santarone S, et al. (2018). "NOTCH and graft-versus-host disease." Frontiers in Immunology: 1825.

Didiano, D. and O. Hobert (2006). Perfect seed pairing is not a generally reliable predictor for miRNA-target interactions. Nature Structural & Molecular Biology **13** (9): 849-851.Donnelly, R. P. and Kotenko S. V (2010). "Interferon-lambda: a new addition to an old family." Journal of Interferon & Cytokine Research **30**(8): 555-564.

Danielsson K, Ebrahimi M, Wahlin YB, Nylander K, Boldrup L. (2012). "Increased levels of COX-2 in oral lichen planus supports an autoimmune cause of the disease." Journal of the European Academy of Dermatology and Venereology 26(11): 1415-1419.

Du G, Chen J, Wang Y, Cao T, Zhou L, Wang Y, Han X, Tang G. (2018). "Differential expression of STAT-3 in subtypes of oral lichen planus: a preliminary study." Oral Surgery, Oral Medicine, Oral Pathology and Oral Radiology **125**(3): 236-243. e231.

Dwivedi S, Purohit P, Sharma P. (2019). "MicroRNAs and Diseases: Promising Biomarkers for Diagnosis and Therapeutics." Indian Journal of Clinical Biochemistry 34(3): 243-245.

Ebrahimi M, Boldrup L, Coates PJ, Wahlin YB, Bourdon JC, Nylander K. (2008). "Expression of novel p53 isoforms in oral lichen planus." Oral Oncology **44**(2): 156-161.

Eisen D, Carrozzo M, Bagan Sebastian JV, Thongprasom K. (2005). "Number V Oral lichen planus: clinical features and management." Oral Diseases **11**(6): 338-349.

El-Howati A, Thornhill MH, Colley HE, Murdoch C. (2022). "Immune mechanisms in oral lichen planus." Oral Diseases. doi: 10.1111/odi.14142. Online ahead of print

Fabbi M, Carbotti G, Ferrini S. (2017). "Dual roles of IL-27 in cancer biology and immunotherapy." Mediators of Inflammation **2017**:3958069.

Faraoni I, Antonetti FR, Cardone J, Bonmassar E. (2009). "miR-155 gene: a typical multifunctional microRNA." Biochemical and Biophysical Acta **1792**(6): 497-505.

Farhi, D. and N. Dupin (2010). "Pathophysiology, etiologic factors, and clinical management of oral lichen planus, part I: facts and controversies." Clinics in Dermatology 28(1): 100-108.

Farmer, H. S. (1985). "Model of career and achievement motivation for women and men." Journal of Counseling Psychology **32**(3): 363.

Farthing, P. and A. Cruchley (1989). "Expression of MHC class II antigens (HLA DR, DP and DQ) by keratinocytes in oral lichen planus." Journal of Oral Pathology & Medicine **18**(5): 305-309.

Feitelson, M. A., et al. (2015). "Sustained proliferation in cancer: Mechanisms and novel therapeutic targets." Seminars in Cancer Biology 35: S25-S54.

Ferrari, E. and P. Gandellini (2020). "Unveiling the ups and downs of miR-205 in physiology and cancer: transcriptional and post-transcriptional mechanisms." Cell Death Diseases **11**(11): 1-10. 980.

Fonseca-Camarillo G, Furuzawa-Carballeda J, Granados J, Yamamoto-Furusho JK. (2014). "Expression of interleukin (IL)-19 and IL-24 in inflammatory bowel disease patients: a cross-sectional study." Clinical and Experimental Immunology **177**(1): 64-75.

Fortuna G, Aria M, Schiavo JH. (2017). "Drug-induced oral lichenoid reactions: a real clinical entity? A systematic review." European Journal of Clinical Pharmacology **73**(12): 1523-1537.

Fukumoto I, Koshizuka K, Hanazawa T, Kikkawa N, Matsushita R, Kurozumi A, Kato M, Okato A, Okamoto Y, Seki N. (2016). "The tumor-suppressive microRNA-23b/27b cluster regulates the MET oncogene in oral squamous cell carcinoma." International Journal of Oncology **49**(3): 1119-1129.

Fulciniti, M., et al. (2016). "miR-23b/SP1/c-myc forms a feed-forward loop supporting multiple myeloma cell growth." Blood Cancer Journal 6(1): e380.

Gandolfo S, Richiardi L, Carrozzo M, Broccoletti R, Carbone M, Pagano M, Vestita C, Rosso S, Merletti F. (2004). "Risk of oral squamous cell carcinoma in 402 patients with oral lichen planus: a follow-up study in an Italian population." Oral Oncology **40**(1): 77-83.

Gao P, Tchernyshyov I, Chang TC, Lee YS, Kita K, Ochi T, Zeller KI, De Marzo AM, Van Eyk JE, Mendell JT, Dang CV. (2009). "c-Myc suppression of miR-23a/b enhances mitochondrial glutaminase expression and glutamine metabolism." Nature **458**(7239): 762-765.

Gao Y, Zhang SG, Wang ZH, Liao JC. (2017). "Down-regulation of miR-342-3p in hepatocellular carcinoma tissues and its prognostic significance." European Review for Medical and Pharmacological Sciences **21**(9): 2098-2102.

Gassling V, Hampe J, Açil Y, Braesen JH, Wiltfang J, Häsler R. (2013). "Disease-associated miRNA-mRNA networks in oral lichen planus." PLoS ONE **8**(5): e63015

Geiss, G. K., et al. (2008). "Direct multiplexed measurement of gene expression with color-coded probe pairs." Nature biotechnology 26(3): 317-325

Ghallab NA, Kasem RF, El-Ghani SFA, Shaker OG. (2017). Gene expression of miRNA-138 and cyclin D1 in oral lichen planus. Clinical Oral Investigation. **21**(8):2481-2491.

Ghalwash, D. M. (2020). "Diagnostic and prognostic value of salivary biomarkers in oral cancer and precancer: Review article." Journal of Oral and Maxillofacial Surgery, Medicine, and Pathology 32(6): 538-543.

Giuliani M, Troiano G, Cordaro M, Corsalini M, Gioco G, Lo Muzio L, Pignatelli P, Lajolo C. (2019). "Rate of malignant transformation of oral lichen planus: A systematic review." Oral Diseases **25**(3): 693-709.

Gokulan, R. and D. Halagowder (2014). "Expression pattern of Notch intracellular domain (NICD) and Hes-1 in preneoplastic and neoplastic human oral squamous epithelium: their correlation with c-Myc, clinicopathological factors and prognosis in Oral cancer." Medical Oncology **31**(8): 126.

González-Moles MA, Bascones-Ilundain C, Gil Montoya JA, Ruiz-Avila I, Delgado-Rodríguez M, Bascones-Martínez A.. (2006). "Cell cycle regulating mechanisms in oral lichen planus: molecular bases in epithelium predisposed to malignant transformation." Archives of Oral Biology **51**(12): 1093-1103.

Goto Y, Kojima S, Nishikawa R, Enokida H, Chiyomaru T, Kinoshita T, Nakagawa M, Naya Y, Ichikawa T, Seki N. (2014). "The microRNA-23b/27b/24-1 cluster is a disease progression marker and tumor suppressor in prostate cancer." Oncotarget **5**(17): 7748-7759.

Guan H, Fan D, Mrelashvili D, Hao H, Singh NP, Singh UP, Nagarkatti PS, Nagarkatti M. (2013). "Micro RNA let-7e is associated with the pathogenesis of experimental autoimmune encephalomyelitis." European journal of immunology **43**(1): 104-114.

Guo Y, Wu Y, Shi J, Zhuang H, Ci L, Huang Q, Wan Z, Yang H, Zhang M, Tan Y, Sun R, Xu L, Wang Z, Shen R, Fei J.. (2021). "miR-29a/b1 Regulates the Luteinizing Hormone Secretion and Affects Mouse Ovulation." Frontiers in endocrinology **12**: 610.

Hadzi-Mihailovic M, Raybaud H, Monteil R, Cakic S, Djuric M, Jankovic L.. (2010). "Bcl-2 expression and its possible influence on malignant transformation of oral lichen planus." Journal of BUON **15**(2): 362-368.

Hajikhan Mirzaei, M. and A. Esmaeilzadeh (2014). "Overexpression of MDA-7/IL-24 as an anticancer cytokine in gene therapy of thyroid carcinoma." Journal of Medical Hypotheses and Ideas **8**(1): 7-13.

Halma MA, Wheelhouse NM, Barber MD, Powell JJ, Fearon KC, Ross JA. (2004). "Interferon-γ polymorphisms correlate with duration of survival in pancreatic cancer." Human immunology **65**(11): 1405-1408.

Harel-Bellan A, Ferris DK, Vinocour M, Holt JT, Farrar WL. (1988). "Specific inhibition of c-myc protein biosynthesis using an antisense synthetic deoxy-oligonucleotide in human T lymphocytes." The Journal of Immunology **140**(7): 2431-2435.

Hart PH, Ahern MJ, Jones CA, Jones KL, Smith MD, Finlay-Jones JJ. (1993). "Synovial fluid macrophages and blood monocytes differ in their response to IL-4." J Immunol 151(6): 3370-3380.

Hartl, M. and K. Bister (2013). Oncogenes. Brenner's Encyclopedia of Genetics (Second Edition). S. Maloy and K. Hughes. San Diego, Academic Press: 164-166.

Hezova R, Kovarikova A, Srovnal J, Zemanova M, Harustiak T, Ehrmann J, Hajduch M, Sachlova M, Svoboda M, Slaby O. (2016). "MiR-205 functions as a tumor suppressor in adenocarcinoma and an oncogene in squamous cell carcinoma of esophagus." Tumour Biology **37**(6): 8007-8018.

Hilly O, Pillar N, Stern S, Strenov Y, Bachar G, Shomron N, Shpitzer T. (2016). "Distinctive pattern of let-7 family microRNAs in aggressive carcinoma of the oral tongue in young patients." Oncology Letters **12**(3): 1729-1736.

Hosokawa, H. and E. V. Rothenberg (2021). "How transcription factors drive choice of the T cell fate." Nature Reviews Immunology **21**(3): 162-176.

Hu J, Zhai C, Hu J, Li Z, Fei H, Wang Z, Fan W. (2017). "MiR-23a inhibited IL-17-mediated proinflammatory mediators' expression via targeting IKKα in articular chondrocytes." International Immunopharmacology **43**: 1-6.

Hu JY, Zhang J, Ma JZ, Liang XY, Chen GY, Lu R, Du GF, Zhou G. (2015). "MicroRNA-155-IFN-γ Feedback Loop in CD4+ T Cells of Erosive Type Oral Lichen Planus." Scientific Reports **5**(1): 1-10.

Hu R, Lv W, Zhang S, Liu Y, Sun B, Meng Y, Kong Q, Mu L, Wang G, Zhang Y, Li H, Liu X. (2021). "Combining miR-23b exposure with mesenchymal stem cell transplantation enhances therapeutic effects on EAE." Immunology Letters **229**: 18-26.

Hu, X. and Ivashkiv, L. B. (2009). "Cross-regulation of signalling pathways by interferon-γ: implications for immune responses and autoimmune diseases." Immunity **31**(4): 539-550.

Huang Y, Zhou S, Cai Y. (2016). "Expression of interleukin-12 and interleukin-27 proteins and immune status in serum of patients with oral lichen planus." Hua xi kou Qiang yi xue za zhi= Huaxi Kouqiang Yixue Zazhi= West China Journal of Stomatology **34**(2): 140-144.

Hutchins, A. P., et al. (2013). "The IL-10/STAT3-mediated anti-inflammatory response: recent developments and future challenges." Briefings in Functional Genomics **12**(6): 489-498.

Hwang, H. and J. Mendell (2006). "MicroRNAs in cell proliferation, cell death, and tumorigenesis." British Journal of Cancer **94**(6): 776-780.

Ichimura K, Casais C, Peck SC, Shinozaki K, Shirasu K. (2006). "MEKK1 is required for MPK4 activation and regulates tissue-specific and temperature-dependent cell death in Arabidopsis." Journal of Biological Chemistry **281**(48): 36969-36976.

Ismail SB, Kumar SK, Zain RB. (2007). "Oral lichen planus and lichenoid reactions: etiopathogenesis, diagnosis, management and malignant transformation." Journal of Oral Science **49**(2): 89-106.

Jakymiw A, Patel RS, Deming N, Bhattacharyya I, Shah P, Lamont RJ, Stewart CM, Cohen DM, Chan EK. (2010). "Overexpression of dicer as a result of reduced let-7 MicroRNA levels contributes to increased cell proliferation of oral cancer cells." Genes Chromosomes Cancer 49(6): 549-559.

Jang DI, Lee AH, Shin HY, Song HR, Park JH, Kang TB, Lee SR, Yang SH. (2021). "The Role of Tumor Necrosis Factor Alpha (TNF-α) in Autoimmune Disease and Current TNF-α Inhibitors in Therapeutics." Int J Mol Sci 22(5).

Jemal A, Bray F, Center MM, Ferlay J, Ward E, Forman D. (2011)." Global Cancer Statistics. A Cancer Journal for Clinicians **61**: 69-90.

Ji, Y., et al. (2015). "miR-155 augments CD8+ T-cell antitumor activity in lymphoreplete hosts by enhancing responsiveness to homeostatic γc cytokines." Proceedings of the National Academy of Sciences USA **112**(2): 476-481.

Jiang F, Zhao W, Zhou L, Zhang L, Liu Z, Yu D. (2014). "miR-222 regulates the cell biological behavior of oral squamous cell carcinoma by targeting PUMA." Oncology reports **31**(3):1255-62

Jin L, Wessely O, Marcusson EG, Ivan C, Calin GA, Alahari SK. (2013). "Prooncogenic factors miR-23b and miR-27b are regulated by Her2/Neu, EGF, and TNF-α in breast cancer." Cancer Research **73**(9): 2884-2896.

Jin X, Wang J, Zhu L, Wang L, Dan H, Zeng X, Chen Q. (2012). "Association between-308 G/A polymorphism in TNF-α gene and lichen planus: a meta-analysis." Journal of Dermatological Science **68**(3): 127-134.

John B, Sander C, Marks DS. (2006). "Prediction of human microRNA targets." MicroRNA Protocols **342**:101-13

Johnson, C. D., et al. (2007). "The let-7 MicroRNA Represses Cell Proliferation Pathways in Human Cells." Cancer Research **67**(16): 7713-7722.

Johnson, S. M., et al. (2005). "RAS is regulated by the let-7 microRNA family." Cell **120**(5): 635-647.

Khan A, Farah CS, Savage NW, Walsh LJ, Harbrow DJ, Sugerman PB.. (2003). "Th1 cytokines in oral lichen planus." Journal of Oral Pathology & Medicine **32**(2): 77-83.

Kim, D., et al. (2020). "Anti-inflammatory roles of glucocorticoids are mediated by Foxp3+ regulatory T cells via a miR-342-dependent mechanism." Immunity **53**(3): 581-596. e585.

Kim JS, Yu SK, Lee MH, Park MG, Park E, Kim SG, Lee SY, Kim CS, Kim HJ, Chun HS, Chun SW, Kim DK.. (2013). "MicroRNA-205 directly regulates the tumor suppressor, interleukin-24, in human KB oral cancer cells." Molecules and cells **35**(1): 17-24.

Kim JW, Mori S, Nevins JR. (2010). "Myc-induced microRNAs integrate Myc-mediated cell proliferation and cell fate." Cancer Research **70**(12): 4820-4828.

Kirave P, Gondaliya P, Kulkarni B, Rawal R, Garg R, Jain A, Kalia K.. (2020). "Exosome mediated miR-155 delivery confers cisplatin chemoresistance in oral cancer cells via epithelial-mesenchymal transition." Oncotarget **11**(13): 1157-1171.

Kolarz B, Ciesla M, Dryglewska M, Rosenthal AK, Majdan M.. (2020). "Hypermethylation of the miR-155 gene in the whole blood and decreased plasma level of miR-155 in rheumatoid arthritis." PLoS ONE 15(6): e0233897.

Krenn, P. W., et al. (2016). "ILK induction in lymphoid organs by a TNFα–NF-κB–regulated pathway promotes the development of chronic lymphocytic leukemia." Cancer Research **76**(8): 2186-2196.

Kunz, M. (2013). "MicroRNAs in melanoma biology." MicroRNA Cancer Regulation: 774:103-20.

Kuo HW, Huang CY, Fu CK, Liao CH, Hsieh YH, Hsu CM, Tsai CW, Chang WS, Bau DT. (2014). "The significant association of CCND1 genotypes with gastric cancer in Taiwan." Anticancer Research **34**(9): 4963-4968.

Kumari, S., et al. (2013). "Tumor necrosis factor receptor signaling in keratinocytes triggers interleukin-24-dependent psoriasis-like skin inflammation in mice." Immunity **39**(5): 899-911.

Kurago, Z. B. (2016). "Aetiology and pathogenesis of oral lichen planus: an overview." Oral Surgery, Oral Medicine, Oral Pathology and Oral Radiology **122**(1): 72-80.

Kulkarni, M. M. (2011). "Digital multiplexed gene expression analysis using the NanoString nCounter system." Current protocols in molecular biology 94(1): 25B. 10.21-25B. 10.17.

Kuuliala K, Kuuliala A, Koivuniemi R, Oksanen S, Hämäläinen M, Moilanen E, Kautiainen H, Leirisalo-Repo M, Repo H. (2015). "Constitutive STAT3 phosphorylation in circulating CD4+ T lymphocytes associates with disease activity and treatment response in recent-onset rheumatoid arthritis." PLoS ONE **10**(9): e0137385.

Lai, M. and C. Xiao (2015). "Functional interactions among members of the miR-17–92 cluster in lymphocyte development, differentiation and malignant transformation." International Immunopharmacology **28**(2): 854-858.

Lewis BP, Burge CB, Bartel DP. (2005). "Conserved seed pairing, often flanked by adenosines, indicates that thousands of human genes are microRNA targets." Cells **120**(1): 15-20.

Lewis BP, Shih IH, Jones-Rhoades MW, Bartel DP, Burge CB. (2003). "Prediction of mammalian microRNA targets." Cell **115**(7): 787-798.

Liang L, Zhou Q, Feng L. (2021). "Decreased microRNA-155 in Behcet's disease leads to defective control of autophagy thereby stimulating excessive proinflammatory cytokine production." Arthritis Research and therapy **23**(1): 135.

Lindow M. (2011) Prediction of Targets for MicroRNAs. In: Nielsen H. (eds) RNA. Methods in Molecular Biology (Methods and Protocols), vol 703. Humana Press.

Lin, F. and Prichard, J. (2015). Handbook of practical immunohistochemistry: frequently asked questions, Springer.
Lin, J., et al. (2014). "A novel p53/microRNA-22/Cyr61 axis in synovial cells regulates inflammation in rheumatoid arthritis." Arthritis Rheumatol 66(1): 49-59.

Liu, P. N. (1990). "[Physiologic function of oncogene products: the expression of proto-oncogenes in cellular proliferation and differentiation in normal tissues and the general mechanism of their transcription]." Sheng Li Ke Xue Jin Zhan 21(2): 112-118.

Liu W, Le A, Hancock C, Lane AN, Dang CV, Fan TW, Phang JM. (2012). "Reprogramming of proline and glutamine metabolism contributes to the proliferative and metabolic responses regulated by oncogenic transcription factor c-MYC." Proceedings of the National Academy of Sciences of USA **109**(23): 8983-8988.

Liu X, Yu J, Jiang L, Wang A, Shi F, Ye H, Zhou X. (2009). "MicroRNA-222 regulates cell invasion by targeting matrix metalloproteinase 1 (MMP1) and manganese superoxide dismutase 2 (SOD2) in tongue squamous cell carcinoma cell lines." Cancer Genomics Proteomics **6**(3): 131-139.

Liu Z, Long X, Chao C, Yan C, Wu Q, Hua S, Zhang Y, Wu A, Fang W. (2014). "Knocking down CDK4 mediates the elevation of let-7c suppressing cell growth in nasopharyngeal carcinoma." BMC Cancer **14**(1): 274.

Liu J, Zhang C, Zhao Y, Feng Z. (2017). "MicroRNA control of p53." Journal of Cellular Biochemistry **118**(1): 7-14.

Liu F, Wu J, Ye F.. (2015). "Expression of miRNA-155 and miRNA-146a in peripheral blood mononuclear cells and plasma of oral lichen planus patients." Zhonghua kou qiang yi xue za zhi= Zhonghua kouqiang yixue zazhi= Chinese journal of stomatology 50(1): 23-27.

Lopez-Rincon A, Mendoza-Maldonado L, Martinez-Archundia M, Schönhuth A, Kraneveld AD, Garssen J, Tonda A(2020). "Machine Learning-Based Ensemble Recursive Feature Selection of Circulating miRNAs for Cancer Tumor Classification." Cancers (Basel) **12**(7): 1785.

Lovat F, Fassan M, Sacchi D, Ranganathan P, Palamarchuk A, Bill M, Karunasiri Met al. (2018). "Knockout of both miR-15/16 loci induces acute myeloid leukemia." Proceedings of the National Academy of Sciences 115(51): 13069-13074.

Lu LF, Boldin MP, Chaudhry A, Lin LL, Taganov KD, Hanada T, Yoshimura A, Baltimore D, Rudensky AY. (2010). "Function of miR-146a in controlling Treg cell-mediated regulation of Th1 responses." Cells **142**(6): 914-929.

Lu MC, Yu CL, Chen HC, Yu HC, Huang HB, Lai NS. (2014). "Increased miR-223 expression in T cells from patients with rheumatoid arthritis leads to decreased insulin-like growth factor-1-mediated interleukin-10 production." Clinical & Experimental Immunology **177**(3): 641-651.

Lu R, Zhang J, Sun W, Du G, Zhou G. (2015). "Inflammation-related cytokines in oral lichen planus: an overview." Journal of Oral Pathology & Medicine **44**(1): 1-14.

Ma F, Xu S, Liu X, Zhang Q, Xu X, Liu M, Hua M, Li N, Yao H, Cao X. (2011). "The microRNA miR-29 controls innate and adaptive immune responses to intracellular bacterial infection by targeting interferon-γ." Nature immunology **12**(9): 861-869.

Ma H, Wu Y, Yang H, Liu J, Dan H, Zeng X, Zhou Y, Jiang L, Chen Q. (2016). "MicroRNAs in oral lichen planus and potential miRNA–mRNA pathogenesis with essential cytokines: a review." Oral Surgery, Oral Medicine, Oral Pathology and Oral Radiology **122**(2): 164-173.

MacFarlane, L.A. and Murphy, P. R (2010). "MicroRNA: biogenesis, function and role in cancer." Current Genomics **11**(7): 537-561.

Magaki S, Hojat SA, Wei B, So A, Yong WH. (2019). "An Introduction to the Performance of Immunohistochemistry." Methods Mol Biol **1897**: 289-298.

Mahesh, G. and R. Biswas (2019). "MicroRNA-155: a master regulator of inflammation." Journal of Interferon & Cytokine Research **39**(6): 321-330.

Makeyev, E. V. and T. Maniatis (2008). "Multilevel regulation of gene expression by microRNAs." Science **319**(5871): 1789-1790.

Mali, S. B. (2015). "Review of STAT3 (Signal Transducers and Activators of Transcription) in head and neck cancer." Oral Oncology **51**(6): 565-569.

Matson JP, House AM, Grant GD, Wu H, Perez J, Cook JG.. (2019). "Intrinsic checkpoint deficiency during cell cycle re-entry from quiescence." J Cell Biol 218(7): 2169-2184.

Matthews JB, Scully CM, Potts AJ. (1984). "Oral lichen planus: an immunoperoxidase study using monoclonal antibodies to lymphocyte subsets." British Journal of Dermatology **111**(5): 587-595.

Mattsson C, Jontell M, Bergenholtz G, Heyden M, Dahlgren UI.. (1998). "Distribution of interferon-y mRNA-positive cells in oral lichen planus lesions." Journal of Oral Pathology & Medicine **27**(10): 483-488.

Mazzarella N, Femiano F, Gombos F, De Rosa A, Giuliano M. (2006). "Matrix metalloproteinase gene expression in oral lichen planus: erosive vs. reticular forms." Journal of the European Academy of Dermatology and Venereology **20**(8): 953-957.

Mazzoccoli L, Robaina MC, Bacchi CE, Soares Lima SC, Klumb CE. (2019). "miR-29 promoter and enhancer methylation identified by pyrosequencing in Burkitt lymhoma cells: Interplay between MYC and miR-29 regulation." Oncology Reports **42**(2): 775-784.

.

Mg, D. M. (2019). "microrna-222 and microrna-203 signatures in oral squamous cell carcinoma: potential role in progression and as therapeutic targets." Oral surgery, Oral medicine, Oral pathology and Oral Radiology **128**(1): e81.

Min SK, Jung SY, Kang HK, Park SA, Lee JH, Kim MJ, Min BM.. (2017). "Functional diversity of miR-146a-5p and TRAF6 in normal and oral cancer cells." International Journal of Oncology **51**(5): 1541-1552.

Mineta H, Borg A, Dictor M, Wahlberg P, Wennerberg J. (1997). "Correlation between p53 mutation and cyclin D1 amplification in head and neck squamous cell carcinoma." Oral Oncology 33(1): 42-46.

Mitamura Y, Nunomura S, Furue M, Izuhara K. (2020). IL-24: A new player in the pathogenesis of pro-inflammatory and allergic skin diseases. Allergology International.;**69**(3):405-411.

Mohseni YR, Saleem A, Tung SL, Dudreuilh C, Lang C, Peng Q., et al. (2021). "Chimeric antigen receptor-modified human regulatory T cells that constitutively express IL-10 maintain their phenotype and are potently suppressive." European Journal of Immunology **51**(10): 2522-2530.

Momen-Heravi F, Trachtenberg AJ, Kuo WP, Cheng YS. (2014). "Genomewide study of salivary microRNAs for detection of oral cancer." Journal of dental research 93(7_suppl): 86S-93S.

Monticelli S, Ansel KM, Xiao C, Socci ND, Krichevsky AM, Thai TH, Rajewsky N, Marks DS, Sander C, Rajewsky K, Rao A, Kosik KS.. (2005). "MicroRNA profiling of the murine hematopoietic system." Genome Biology **6**(8): R71.

Morita Y, Masters EA, Schwarz EM, Muthukrishnan G. (2021). "Interleukin-27 and its diverse effects on bacterial infections." Frontiers in Immunology **12**: 1752.

Mozaffari HR, Sharifi R, Sadeghi M. (2016). "Prevalence of oral lichen planus in diabetes mellitus: A meta-analysis study." Acta Informatica Medica **24**(6): 390-393

Mulholland EJ, Green WP, Buckley NE, McCarthy HO. (2019). "Exploring the Potential of MicroRNA Let-7c as a Therapeutic for Prostate Cancer." Molecular Therapy Nucleic Acids **18**: 927-937.

Nowwarote, N. and T. Osathanon (2017). "Dysregulation of Notch signalling related genes in oral lichen planus." Asian Pacific Journal of Tropical Biomedicine **7**(7): 666-669.

Nygaard, G. and G. S. Firestein (2020). "Restoring synovial homeostasis in rheumatoid arthritis by targeting fibroblast-like synoviocytes." Nature Reviews. Rheumatology **16**(6): 316-333.

O'Connell RM, Taganov KD, Boldin MP, Cheng G, Baltimore D. (2007). "MicroRNA-155 is induced during the macrophage inflammatory response." Proceedings of the National Academy of Sciences USA **104**(5): 1604-1609.

O'Donnell KA, Wentzel EA, Zeller KI, Dang CV, Mendell JT. (2005). "c-Myc-regulated microRNAs modulate E2F1 expression." Nature **435**(7043): 839-843.

O'Connor KS, Ahlenstiel G, Suppiah V, Schibeci S, Ong A, Leung R, van der Poorten D, Douglas MW, Weltman MD, Stewart GJ, Liddle C, George J, Booth DR. (2014). "IFNL3 mediates

interaction between innate immune cells: Implications for hepatitis C virus pathogenesis." Innate immunity **20**(6): 598-605.

Oh HM, Yu CR, Golestaneh N, Amadi-Obi A, Lee YS, Eseonu A, Mahdi RM, Egwuagu CE. (2011). "STAT3 protein promotes T-cell survival and inhibits interleukin-2 production through up-regulation of Class O Forkhead transcription factors." Journal of Biological Chemistry **286**(35): 30888-30897.

Ørom, U. A. and A. H. Lund (2010). "Experimental identification of microRNA targets." Gene 451(1): 1-5.

Panneerselvam J, Srivastava A, Muralidharan R, Wang Q, Zheng W, Zhao L, Chen A, Zhao YD, Munshi A, Ramesh R. (2014). "IL-24 modulates the high mobility group (HMG) A1/miR222 /AKT signaling in lung cancer cells." Oncotarget **7**(43):70247-70263

Parolini S, Santoro A, Marcenaro E, Luini W, Massardi L, Facchetti F, Communi D, Parmentier M, Majorana A, Sironi M, Tabellini G, Moretta A, Sozzani S. (2007). "The role of chemerin in the colocalisation of NK and dendritic cell subsets into inflamed tissues." Blood **109**(9): 3625-3632.

Pauley KM, Cha S, Chan EK. (2009). "MicroRNA in autoimmunity and autoimmune diseases." Journal of Autoimmunity **32**(3-4): 189-194.

Peláez, N. and R. W. Carthew (2012). "Biological robustness and the role of microRNAs: a network perspective." Current topics in Developmental Biology 99: 237-255.

Peng J, Liu H, Liu C. (2017). "MiR-155 Promotes Uveal Melanoma Cell Proliferation and Invasion by Regulating NDFIP1 Expression." Technology in Cancer Research and Treatment **16**(6): 1160-1167.

Peng, Y. and C. M. Croce (2016). "The role of MicroRNAs in human cancer." Signal Transduction and Targeted Therapy 1(1): 15004.

Peterson SM, Thompson JA, Ufkin ML, Sathyanarayana P, Liaw L, Congdon CB.. (2014). "Common features of microRNA target prediction tools." Frontiers in Genetics **5**: 23.

Pereira AC, Dias do Carmo E, Dias da Silva MA, Blumer Rosa LE. (2012). "Matrix metalloproteinase gene polymorphisms and oral cancer." Journal Clinical and Experimental Dentistry **4**(5): e297-301.

Petes C, Odoardi N, Plater SM, Martin NL, Gee K. (2018). "IL-27 amplifies cytokine responses to Gram-negative bacterial products and Salmonella typhimurium infection." Scientific Reports **8**(1): 1-13.

Pezelj-Ribaric S, Prso IB, Abram M, Glazar I, Brumini G, Simunovic-Soskic M. (2004). "Salivary levels of tumour necrosis factor-α in oral lichen planus." Mediators of Inflammation **13**(2): 131-133.

Piccinni MP, Lombardelli L, Logiodice F, Tesi D, Kullolli O, Biagiotti R, Giudizi M, Romagnani S, Maggi E, Ficarra G.. (2014). "Potential pathogenetic role of Th17, Th0, and Th2 cells in erosive and reticular oral lichen planus." Oral Diseases **20**(2): 212-218.

Portt L, Norman G, Clapp C, Greenwood M, Greenwood MT. (2011). "Anti-apoptosis and cell survival: A review." Biochimica et Biophysica Acta (BBA) - Molecular Cell Research 1813(1): 238-259.

Qiu LL, Zhang XG, Chen G, Dang YW, Huang ZG, Li MX, Liang Y, Huang SN, Tang XZ, Chen XX, Wei HY, Wu HY.. (2020). "Clinical Significance of the Interleukin 24 mRNA Level in Head and Neck Squamous Cell Carcinoma and Its Subgroups: An In Silico Investigation." Journal of Oncology 2020: 7042025.

Quillet A, Saad C, Ferry G, Anouar Y, Vergne N, Lecroq T, Dubessy C. (2020). "Improving bioinformatics prediction of microRNA targets by ranks aggregation." Frontiers in Genetics **10:** 1330.

Ramos-Vara JA, Kiupel M, Baszler T, Bliven L, Brodersen B, Chelack B, Czub S, Del Piero F, Dial S, Ehrhart EJ, Graham T, Manning L, Paulsen D, Valli VE, West K. (2008). "Suggested guidelines for immunohistochemical techniques in veterinary diagnostic laboratories." Journal of Veterinary Diagnostic Investigation **20**(4): 393-413.

Rebane, A. and C. A. Akdis (2013). "MicroRNAs: Essential players in the regulation of inflammation." Journal of Allergy and Clinical Immunology **132**(1): 15-26.

Rhodes A, Jasani B, Balaton AJ, Miller KD. (2000). "Immunohistochemical demonstration of oestrogen and progesterone receptors: correlation of standards achieved on in house tumours with that achieved on external quality assessment material in over 150 laboratories from 26 countries." Journal ofCclinical Pathology **53**(4): 292-301.

Salvi V, Gianello V, Tiberio L, Sozzani S, Bosisio D. (2019). "Cytokine targeting by miRNAs in autoimmune diseases." Frontiers in Immunology: 10-15.

Sampson VB, Rong NH, Han J, Yang Q, Aris V, Soteropoulos P, Petrelli NJ, Dunn SP, Krueger LJ. (2007). "MicroRNA let-7a down-regulates MYC and reverts MYC-induced growth in Burkitt lymphoma cells." Cancer Research **67**(20): 9762-9770.

Santoro A, Majorana A, Bardellini E, Gentili F, Festa S, Sapelli P, Facchetti F.. (2004). "Cytotoxic molecule expression and epithelial cell apoptosis in oral and cutaneous lichen planus." American Journal of Clinical Pathology **121**(5): 758-764.

Santoro A, Majorana A, Roversi L, Gentili F, Marrelli S, Vermi W, Bardellini E, Sapelli P, Facchetti F. (2005). "Recruitment of dendritic cells in oral lichen planus." The Journal of Pathology:**205**(4): 426-434.

Scheicher R, Hoelbl-Kovacic A, Bellutti F, Tigan AS, Prchal-Murphy M, Heller G, Schneckenleithner C, Salazar-Roa M, Zöchbauer-Müller S, Zuber J, Malumbres M, Kollmann K, Sexl V. (2015). "CDK6 as a key regulator of hematopoietic and leukemic stem cell activation." Blood **125**(1): 90-101.

Scully C, Eisen D, Carrozzo M. (2000). "Management of oral lichen planus." American Journal of Clinical Dermatology **1**(5): 287-306.

Segura S, Rozas-Muñoz E, Toll A, Martín-Ezquerra G, Masferrer E, Espinet B, Rodriguez M, Baró T, Barranco C, Pujol RM. (2013). "Evaluation of MYC status in oral lichen planus in patients with progression to oral squamous cell carcinoma." British Journal of Dermatology **169**(1): 106-114.

Seno K, Ohno J, Ota N, Hirofuji T, Taniguchi K. (2013). "Lupus-like oral mucosal lesions in mercury-induced autoimmune response in Brown Norway rats." BMC immunology **14**(1): 1-10.

Shang Y, Smith S, Hu X. (2016). "Role of Notch signaling in regulating innate immunity and inflammation in health and disease." Protein & Cell **7**(3): 159-174.

Shenouda, S. K. and S. K. Alahari (2009). "MicroRNA function in cancer: oncogene or a tumor suppressor?" Cancer Metastasis Rev 28(3-4): 369-378.

Shen Z, Du G, Zhou Z, Liu W, Shi L, Xu H. (2016). "Aberrant expression of interleukin-22 and its targeting micro RNA s in oral lichen planus: a preliminary study." Journal of Oral Pathology & Medicine 45(7): 523-527.

Shen Z, Gao X, Ma L, Zhou Z, Shen X, Liu W. (2014). "Expression of Foxp3 and interleukin-17 in lichen planus lesions with emphasis on difference in oral and cutaneous variants." Archives of Dermatological Research **306**(5): 441-446.

Shi W, Yang J, Li S, Shan X, Liu X, Hua H, Zhao C, Feng Z, Cai Z, Zhang L, Zhou D.. (2015). "Potential involvement of miR-375 in the premalignant progression of oral squamous cell carcinoma mediated via transcription factor KLF5." Oncotarget **6**(37): 40172.

Shimoyama T, Horie N, Kato T, Kaneko T, Komiyama K. (2000). "Helicobacter pylori in oral ulcerations." Journal of Oral Science **42**(4): 225-229.

Simpson, L. J. and K. M. Ansel (2015). "MicroRNA regulation of lymphocyte tolerance and autoimmunity." The Journal of Clinical Investigation **125**(6): 2242-2249.

Siponen M, Huuskonen L, Läärä E, Salo T. (2010). "Association of oral lichen planus with thyroid disease in a Finnish population: a retrospective case-control study." Oral Surgery, Oral Medicine, Oral Pathology, Oral Radiology, and Endodontology **110**(3): 319-324.

Sklavounou A, Chrysomali E, Scorilas A, Karameris A. (2000). "TNF-α expression and apoptosis-regulating proteins in oral lichen planus: a comparative immunohistochemical evaluation." Journal of Oral Pathology & Medicine **29**(8): 370-375.

Smolarz B, Durczyński A, Romanowicz H, Szyłło K, Hogendorf P.. (2022). "miRNAs in Cancer (Review of Literature)." International Journal of Molecular Sciences **23**(5): 2805.

Song J, Ouyang Y, Che J, Li X, Zhao Y, Yang K, Zhao X, Chen Y, Fan C, Yuan W. (2017). "Potential value of miR-221/222 as diagnostic, prognostic, and therapeutic biomarkers for diseases." Frontiers in Immunology **8**: 56.

Song X, Jin Y, Yan M, Zhang Y, Chen B. (2019). "MicroRNA-342-3p functions as a tumor suppressor by targeting LIM and SH3 protein 1 in oral squamous cell carcinoma." Oncology Letters **17**(1): 688-696.

Stagakis E, Bertsias G, Verginis P, Nakou M, Hatziapostolou M, Kritikos H, Iliopoulos D, Boumpas DT. (2011). "Identification of novel microRNA signatures linked to human lupus disease activity and pathogenesis: miR-21 regulates aberrant T cell responses through regulation of PDCD4 expression." Annals of the Rheumatic Diseases **70**(8): 1496-1506.

Stark A, Brennecke J, Bushati N, Russell RB, Cohen SM. (2005). "Animal MicroRNAs confer robustness to gene expression and have a significant impact on 3′ UTR evolution." Cells Journal **123**(6): 1133-1146.

Sugerman PB, Savage NW, Walsh LJ, Zhao ZZ, Zhou XJ, Khan A, Seymour GJ, Bigby M. (2002). "The pathogenesis of oral lichen planus." Critical Review in Oral Biology and Medicine **13**(4): 350-365.

Sun S, Sun P, Wang C, Sun T. (2014). "Downregulation of microRNA-155 accelerates cell growth and invasion by targeting c-myc in human gastric carcinoma cells." Oncology Report **32**(3): 951-956.

Suvarna C, Chaitanya NC, Ameer S, Mannava H, Bontala P, Alyami JS, Samreen H, Kondapaneni J. (2020). "A comparative evaluation on the effect of oral zinc 50 mg with or without 0.1% triamcinolone orabase on oral lichen planus." International Journal of Applied and Basic Medical Research **10**(1): 54.

Tai MC, Kajino T, Nakatochi M, Arima C, Shimada Y, Suzuki M, Miyoshi H, Yatabe Y, Yanagisawa K, Takahashi T. (2015). "miR-342-3p regulates MYC transcriptional activity via direct repression of E2F1 in human lung cancer." Carcinogenesis **36**(12): 1464-1473.

Taganov KD, Boldin MP, Chang KJ, Baltimore D. (2006). "NF-κB-dependent induction of microRNA miR-146, an inhibitor targeted to signaling proteins of innate immune responses." Proceedings of the National Academy of Sciences **103**(33): 12481-12486.

Tao JH, Cheng M, Tang JP, Liu Q, Pan F, Li XP. (2017). "Foxp3, regulatory T cell, and autoimmune diseases." Inflammation **40**(1): 328-339.

Tao XA, Li CY, Xia J, Yang X, Chen XH, Jian YT, Cheng B. (2009). "Differential gene expression profiles of whole lesions from patients with oral lichen planus." Journal of Oral Pathology & Medicine **38**(5): 427-433.

Tao Y, Ai R, Hao Y, Jiang L, Dan H, Ji N, Zeng X, Zhou Y, Chen Q. (2019). "Role of miR-155 in immune regulation and its relevance in oral lichen planus (Review)." Experimental and Therapeutic Medicine **17**(1): 575-586.

Thomas DW, Stephens P, Stephens M, Patten DW, Lim SH. (1997). "T-cell receptor Vβ usage by lesional lymphocytes in oral lichen planus." Journal of Oral Pathology & Medicine **26**(3): 105-109.

Thongprasom K, Dhanuthai K, Sarideechaigul W, Chaiyarit P, Chaimusig M. (2006). "Expression of TNF-α in oral lichen planus treated with fluocinolone acetonide 0.1%." Journal of Oral Pathology & Medicine **35**(3): 161-166.

Thongprasom K, Prapinjumrune C, Carrozzo M.. (2013). "Novel therapies for oral lichen planus." Journal of Oral Pathology & Medicine **42**(10): 721-727.

Tili E, Michaille JJ, Croce CM. (2013). "MicroRNAs play a central role in molecular dysfunctions linking inflammation with cancer." Immunology Review **253**(1): 167-184.

Tomankova T, Petrek M, Gallo J, Kriegova E.. (2012). "MicroRNAs: emerging regulators of immune-mediated diseases." Scandinavian Journal of Immunology **75**(2): 129-141.

Uma Maheswari TN, Nivedhitha MS, Ramani P.Expression profile of salivary micro RNA-21 and 31 in oral potentially malignant disorders.Braz Oral Res. 2020 Feb 10;34:e002.

Vahabi M, Blandino G, Di Agostino S. (2021). "MicroRNAs in head and neck squamous cell carcinoma: a possible challenge as biomarkers, determinants for the choice of therapy and targets for personalized molecular therapies." Translational Cancer Research **10**(6): 3090.

Valente G, Pagano M, Carrozzo M, Carbone M, Bobba V, Palestro G, Gandolfo S. (2001). "Sequential immunohistochemical p53 expression in biopsies of oral lichen planus undergoing malignant evolution." Journal of Oral Pathology & Medicine **30**(3): 135-140.

Valenti MT, Deiana M, Cheri S, Dotta M, Zamboni F, Gabbiani D, Schena F, Dalle Carbonare L, Mottes M.. (2019). "Physical exercise modulates miR-21-5p, miR-129-5p, miR-378-5p, and miR-188-5p expression in progenitor cells promoting osteogenesis." Cells Journal **8**(7): 742.

Van der Meij, E. and Van der Waal, I. (2003). "Lack of clinicopathologic correlation in the diagnosis of oral lichen planus based on the presently available diagnostic criteria and suggestions for modifications." Journal of Oral Pathology & Medicine **32**(9): 507-512.

Visone R, Rassenti LZ, Veronese A, Taccioli C, Costinean S, Aguda BD, Volinia S, Ferracin M, Palatini J, Balatti V, Alder H, Negrini M, Kipps TJ, Croce CM. (2009). "Karyotype-specific microRNA signature in chronic lymphocytic leukemia." Blood **114**(18): 3872-3879.

Waggott D, Chu K, Yin S, Wouters BG, Liu FF, Boutros PC. (2012). "NanoStringNorm: an extensible R package for the pre-processing of NanoString mRNA and miRNA data." Bioinformatics 28(11): 1546-1548.

Wallden B, Storhoff J, Nielsen T, Dowidar N, Schaper C, Ferree S, Liu S, Leung S, Geiss G, Snider J, Vickery T, Davies SR, Mardis ER, Gnant M, Sestak I, Ellis MJ, Perou CM, Bernard PS, Parker JS. (2015). "Development and verification of the PAM50-based Prosigna breast cancer gene signature assay." BMC Medical Genomics 8(1): 54.

Walton LJ, Macey MG, Thornhill MH, Farthing PM. (1998). "Intra-epithelial subpopulations of T lymphocytes and Langerhans cells in oral lichen planus." Journal of Oral Pathology & Medicine **27**(3): 116-123.

Wan J, Yang X, Ren Y, Li X, Zhu Y, Haddock AN, Ji B, Xia L, Lu N. (2019). "Inhibition of miR-155 reduces impaired autophagy and improves prognosis in an experimental pancreatitis mouse model." Cell Death and Disease **10**(4): 303.

Wang F, Zhang S, Jeon R, Vuckovic I, Jiang X, Lerman A, Folmes CD, Dzeja PD, Herrmann J. (2018). "Interferon gamma induces reversible metabolic reprogramming of M1 macrophages to sustain cell viability and pro-inflammatory activity." EBioMedicine **30**: 303-316.

Wang, J.Z. and Zhao, B.H. (2021). "MiR-23b-3p functions as a positive factor for osteoporosis progression by targeting CCND1 in MC3T3-E1 cells." In Vitro Cellular & Developmental Biology - Animal **57**(3): 324-331.

Wang KC, Nguyen P, Weiss A, Yeh YT, Chien HS, Lee A, Teng D, Subramaniam S, Li YS, Chien S. (2014). "MicroRNA-23b regulates cyclin-dependent kinase-activating kinase complex through cyclin H repression to modulate endothelial transcription and growth under flow." Arteriosclerosis, Thrombosis and Vascular Biology **34**(7): 1437-1445.

Wang, L.-J. and H.-Q. Cai (2020). "Let-7b downgrades CCND1 to repress osteogenic proliferation and differentiation of MC3T3-E1 cells: An implication in osteoporosis." The Kaohsiung Journal of Medical Sciences **36**(10): 775-785.

Wang QM, Huang XY, Guan WQ. (2022). "Expressions of Interleukin-27 in Oral Lichen Planus, Oral Leukoplakia, and Oral Squamous Cell Carcinoma." Inflammation: 1-16.

Wang Y, Feng T, Duan S, Shi Y, Li S, Zhang X, Zhang L.. (2020). "miR-155 promotes fibroblast-like synoviocyte proliferation and inflammatory cytokine secretion in rheumatoid arthritis by targeting FOXO3a." Experimental and Therapeutic Medicine **19**(2): 1288-1296.

Wang F, Zhang S, Jeon R, Vuckovic I, Jiang X, Lerman A, Folmes CD, Dzeja PD, Herrmann J. (2018). "Interferon gamma induces reversible metabolic reprogramming of M1 macrophages to sustain cell viability and pro-inflammatory activity." EBioMedicine **30**: 303-316.

Wissink EM, Smith NL, Spektor R, Rudd BD, Grimson A. (2015). "MicroRNAs and their targets are differentially regulated in adult and neonatal mouse CD8+ T cells." Genetics **201**(3): 1017-1030.

Wolff AC, Hammond ME, Hicks DG, Dowsett M, McShane LM, Allison KH, Allred DC, Bartlett JM, Bilous M, Fitzgibbons P, Hanna W, Jenkins RB, Mangu PB, Paik S, Perez EA, Press MF, Spears PA, Vance GH, Viale G. (2014). "Recommendations for human epidermal growth factor receptor 2 testing in breast cancer: American Society of Clinical Oncology/College of American Pathologists clinical practice guideline update." Archives of Pathology and Laboratory Medicine **138**(2): 241-256.

Wong HR, Lindsell CJ, Lahni P, Hart KW, Gibot S.. (2013). "Interleukin-27 as a sepsis diagnostic biomarker in critically ill adults." Shock (Augusta, Ga.) **40**(5): 382-386

Wu D, Talbot CC Jr, Liu Q, Jing ZC, Damico RL, Tuder R, Barnes KC, Hassoun PM, Gao L. (2016). "Identifying microRNAs targeting Wnt/β-catenin pathway in end-stage idiopathic pulmonary arterial hypertension." Journal of Molecular Medicine (Berl) **94**(8): 875-885.

Wu R, Zeng J, Yuan J, Deng X, Huang Y, Chen L, Zhang P, Feng H, Liu Z, Wang Z, Gao X, Wu H, Wang H, Su Y, Zhao M, Lu Q. (2018). "MicroRNA-210 overexpression promotes psoriasis-like inflammation by inducing Th1 and Th17 cell differentiation." The Journal of Clinical Investigation **128**(6): 2551-2568.

Wu YY, Lai HF, Huang TC, Chen YG, Ye RH, Chang PY, Lai SW, Chen YC, Lee CH, Liu WN, Dai MS, Chen JH, Ho CL, Chiu YL. (2021). "Aberrantly reduced expression of miR-342-5p contributes to CCND1-associated chronic myeloid leukemia progression and imatinib resistance." Cell Death and Disease **12**(10): 908.

Xiao L, Li X, Mu Z, Zhou J, Zhou P, Xie C, Jiang S. (2020). "FTO Inhibition Enhances the Antitumor Effect of Temozolomide by Targeting MYC-miR-155/23a Cluster-MXI1 Feedback Circuit in Glioma." Cancer Research **80**(18): 3945-3958.

Xu C, Ren G, Cao G, Chen Q, Shou P, Zheng C, Du L, Han X, Jiang M, Yang Q, Lin L, Wang G, Yu P, Zhang X, Cao W, Brewer G, Wang Y, Shi Y.. (2013). "miR-155 Regulates Immune Modulatory Properties of Mesenchymal Stem Cells by Targeting TAK1-binding Protein 2*." Journal of Biological Chemistry **288**(16): 11074-11079.

Xu, J. and Lin, D. I. (2018). "Oncogenic c-terminal cyclin D1 (CCND1) mutations are enriched in endometrioid endometrial adenocarcinomas." PLoS ONE **13**(7): e0199688.

Yadahalli, R., et al. (2021). "Micro RNA as a potential biomarker in Oral Leukoplakia -A Review." European Journal of Translational and Clinical Medicine **7**: 2020.

Yamamoto, T. and T. Osaki (1995). "Characteristic cytokines generated by keratinocytes and mononuclear infiltrates in oral lichen planus." Journal of Investigative Dermatology **104**(5): 784-788.

Yang L, Boldin MP, Yu Y, Liu CS, Ea CK, Ramakrishnan P, Taganov KD, Zhao JL, Baltimore D. (2012). "miR-146a controls the resolution of T cell responses in mice." Journal of Experimental Medicine **209**(9): 1655-1670.

Yao R, Ma YL, Liang W, Li HH, Ma ZJ, Yu X, Liao YH. (2012). "MicroRNA-155 modulates Treg and Th17 cells differentiation and Th17 cell function by targeting SOCS1." **7**(10):e46082

Yin J, Zhao J, Hu W, Yang G, Yu H, Wang R, Wang L, Zhang G, Fu W, Dai L, Li W, Liao B, Zhang S. (2017). "Disturbance of the let-7/LIN28 double-negative feedback loop is associated with radio- and chemo-resistance in non-small cell lung cancer." PLoS ONE **12**(2): e0172787.

Yoshizawa, J. M. and Wong, D. T. (2013). "Salivary microRNAs and oral cancer detection." MicroRNA Protocols: 313-324.

Yu JJ, Ruddy MJ, Wong GC, Sfintescu C, Baker PJ, Smith JB, Evans RT, Gaffen SL. (2007). "An essential role for IL-17 in preventing pathogen-initiated bone destruction: recruitment of neutrophils to inflamed bone requires IL-17 receptor–dependent signals." Blood **109**(9): 3794-3802.

Zhang A, Wang K, Zhou C, Gan Z, Ma D, Ye P, Sun Y, Wu J, Huang X, Ren L, Deng P, Wu C, Yue Z, Ding X, Chen J, Xia J. (2017). "Knockout of microRNA-155 ameliorates the Th1/Th17 immune response and tissue injury in chronic rejection." The Journal of Heart and Lung Transplantation **36**(2): 175-184.

Zhan M, Qu Q, Wang G, Liu YZ, Tan SL, Lou XY, Yu J, Zhou HH. (2013). "Let-7c inhibits NSCLC cell proliferation by targeting HOXA1." Asian Pac Journal of Cancer Prevention **14**(1): 387-392. Asian Pacific journal of cancer prevention: APJCP.

Zhang J, Zhang J, Pang X, Chen Z, Zhang Z, Lei L, Xu H, Wen L, Zhu J, Jiang Y, Cui Y, Chen G, Wang X. (2021). "MiR-205–5p suppresses angiogenesis in gastric cancer by downregulating the expression of VEGFA and FGF1." Experimental Cell Research **404**(2): 112579.

Zhang H, Hao Y, Yang J, Zhou Y, Li J, Yin S, Sun C, Ma M, Huang Y, Xi JJ. (2011). "Genome-wide functional screening of miR-23b as a pleiotropic modulator suppressing cancer metastasis." Nature communications **2**: 554.

Zhang L, Wu H, Zhao M, Lu Q. (2020). "Identifying the differentially expressed microRNAs in autoimmunity: a systemic review and meta-analysis." Autoimmunity **53**(3): 122-136.

Zhang Y, Lin X, Zhang L, Hong W, Zeng K. (2018). "MicroRNA-222 regulates the viability of fibroblasts in hypertrophic scars via matrix metalloproteinase 1." Experimental and Therapeutic Medicine **15**: 1803 - 1808.

Zhao, L. and Y. Zhang (2015). "miR-342-3p affects hepatocellular carcinoma cell proliferation via regulating NF-κB pathway." Biochemical and Biophysical Research Communications **457**(3): 370-377.

Zhong Y, Zhang X, Chong Wl. (2022). "Interleukin-24 Immunobiology and Its Roles in Inflammatory Diseases." International Journal of Molecular Sciences **23**(2): 627.

Zhou F, Chen J, Zhao KN. (2013). "Human papillomavirus 16-encoded E7 protein inhibits IFN-γ-mediated MHC class I antigen presentation and CTL-induced lysis by blocking IRF-1 expression in mouse keratinocytes." Journal of General Virology **94**(11): 2504-2514.

Zhou H, Huang X, Cui H, Luo X, Tang Y, Chen S, Wu L, Shen N. (2010). "miR-155 and its star-form partner miR-155* cooperatively regulate type I interferon production by human plasmacytoid dendritic cells." Blood **116**(26): 5885-5894.

Zhu S, Pan W, Song X, Liu Y, Shao X, Tang Y, Liang D, He D, Wang H, Liu W, Shi Y, Harley JB, Shen N, Qian Y. (2012). "The microRNA miR-23b suppresses IL-17-associated autoimmune inflammation by targeting TAB2, TAB3 and IKK-α." Nature Medicine **18**(7): 1077-1086.

Zhu Y, Skogerbø G, Ning Q, Wang Z, Li B, Yang S, Sun H, Li Y. (2012). "Evolutionary relationships between miRNA genes and their activity." BMC Genomics 13: 718.

Appendix (1)

Summary of abnormal miRNAs expression in OLP analysed by microarray/RNA-seq

miRNA	Expression	Country	N	Sources	Reference
miR-1	Upregulated	China	9	Tissue	(Chen, Du et al., 2017)
miR-4521	Upregulated	China	9	Tissue	(Chen, Du et al., 2017)
miR-335	Upregulated	China	9	Tissue	(Chen, Du et al., 2017)
miR-150	Upregulated	China	9	Tissue	(Chen, Du et al., 2017)
miR-146b	Upregulated	China	9	Tissue	(Chen, Du et al., 2017)
miR-146a	Upregulated	Iran	40	PBMC	(Ahmadi-Motamayel1 et al., 2017)
miR-100	Upregulated	China	9	Tissue	(Chen, Du et al., 2017)
miR-411	Upregulated	China	9	Tissue	(Chen, Du et al., 2017)
miR-142	Upregulated	China	9	Tissue	(Chen, Du et al., 2017)
miR-31	Upregulated	China	9	Tissue	(Chen, Du et al., 2017)
miR-423	Upregulated	China	9 22	Tissue PBMC	(Chen, Du et al., 2017) (Wang et al., 2019)
miR-1307	Upregulated	China	9	Tissue	(Chen, Du et al., 2017)
miR-3184	Upregulated	China	9	Tissue	(Chen, Du et al., 2017)
miR-4483	Upregulated	China	9	Tissue	(Chen, Du et al., 2017)
miR-206	Upregulated	China	9	Tissue	(Chen, Du et al., 2017)
miR-340	Upregulated	China	9	Tissue	(Chen, Du et al., 2017)
miR-504	Upregulated	China	9	Tissue	(Chen, Du et al., 2017)
miR-142	Upregulated	China	9	Tissue	(Chen, Du et al., 2017)
miR-26b	Upregulated	China	9	Tissue	(Chen, Du et al., 2017)
miR-27a	Upregulated	China	9	Tissue	(Chen, Du et al., 2017)
miR-146a	Upregulated	China	9	Tissue	(Chen, Du et al., 2017)

miR-218	Upregulated	China	9	Tissue	(Chen, Du et al., 2017)
miR-941	Upregulated	China	9	Tissue	(Chen, Du et al., 2017)
miR-499a	Upregulated	China	9	Tissue	(Chen, Du et al., 2017)
miR-874	Upregulated	China	9	Tissue	(Chen, Du et al., 2017)
miR-27a	Upregulated	China	9	Tissue	(Chen, Du et al., 2017)
miR-7	Upregulated	China	9	Tissue	(Chen, Du et al., 2017)
miR-143	Upregulated	China	9	Tissue	(Chen, Du et al., 2017)
miR-185	Upregulated	China	9	Tissue	(Chen, Du et al., 2017)
miR-484	Upregulated	China	9	Tissue	(Chen, Du et al., 2017)
miR-511	Upregulated	China	9	Tissue	(Chen, Du et al., 2017)
miR-629	Upregulated	China	9	Tissue	(Chen, Du et al., 2017)
miR-3182	Upregulated	China	9	Tissue	(Chen, Du et al., 2017)
miR-548	Upregulated	China	9	Tissue	(Chen, Du et al., 2017)
miR-30c	Upregulated	China	9	Tissue	(Chen, Du et al., 2017)
miR-139	Upregulated	China	9	Tissue	(Chen, Du et al., 2017)
miR-128	Upregulated	China	9	Tissue	(Chen, Du et al., 2017)
miR-125a	Upregulated	China	9	Tissue	(Chen, Du et al., 2017)
miR-125b	Upregulated	China	5	Saliva	(Di Stasio et al., 2019)
miR-126	Upregulated	China	9	Tissue	(Chen, Du et al., 2017)
miR-148b	Upregulated	China	9	Tissue	(Chen, Du et al., 2017)
miR-660	Upregulated	China	9	Tissue	(Chen, Du et al., 2017)
miR-509	Upregulated	China	9	Tissue	(Chen, Du et al., 2017)
miR-203a	Upregulated	China Italy	9 5	Tissue Saliva	(Chen, Du et al., 2017) (Di Stasio et al., 2019)
miR-144	Upregulated	China	9	Tissue	(Chen, Du et al., 2017)
miR-126	Upregulated	China	9	Tissue	(Chen, Du et al., 2017)

miR-374a	Upregulated	China	9	Tissue	(Chen, Du et al., 2017)
miR-335	Upregulated	China	9	Tissue	(Chen, Du et al., 2017)
miR-34b	Upregulated	China	22	Tissue	(Shi, Yang et al., 2015)
miR-155	Upregulated	Germany China Iran China	7 9 40 22	Tissue Tissue PBMC PBMC	(Gassling, Hampe et al., 2013) (Chen, Du et al., 2017) (Ahmadi-Motamayel1 et al., 2017) (Wang et al., 2019)
miR-133a	Upregulated	China China	3 9	Tissue Tissue	(Zhang, Liu et al., 2012) (Chen, Du et al., 2017)
miR-133b	Upregulated	China	22	PBMC	(Wang et al., 2019)
Let-7i	Upregulated	Germany China	7 9	Tissue Tissue	(Gassling, Hampe et al. 2013) (Chen, Du et al., 2017)
miR-877	Upregulated	China	22	Tissue	(Shi, Yang et al. 2015)
miR-21-3p	Upregulated	China	22	Tissue	(Shi, Yang et al. 2015)
miR-135	Upregulated	China	22 9	Tissue Tissue	(Shi, Yang et al., 2015) (Chen, Du et al., 2017)
miR-205	Upregulated	China	22	Tissue	(Shi, Yang et al., 2015)
miR-21-5p	Upregulated	China Italy	22 5	Tissue Saliva	(Shi, Yang et al., 2015) (Di Stasio et al., 2019)
miR-944	Upregulated	China	22	Tissue	(Shi, Yang et al., 2015)
miR-34b	Upregulated	China	22	Tissue	(Shi, Yang et al., 2015)
miR-877	Upregulated	China	22	Tissue	(Shi, Yang et al., 2015)
miR-223	Upregulated	China	22	PBMC	(Wang et al., 2019)
miR-186	Upregulated	China	22	PBMC	(Wang et al., 2019)
miR-181a	Upregulated	China	22	PBMC	(Wang et al., 2019)
miR-455	Upregulated	China	22	PBMC	(Wang et al., 2019)

	Downregulated	China	9	Tissue	Chen, Du et al., 2017)
miR-375	Upregulated Downregulated	China China China	22 3 22	PBMC Tissue Tissue	(Wang et al., 2019) (Zhang, Liu et al., 2012) (Shi, Yang et al. 2015)
miR-923	Upregulated Downregulated	China Germany	3 7	Tissue Tissue	(Zhang, Liu et al., 2012) (Gassling, Hampe et al. 2013)
miR-210	Upregulated Downregulated	China China	22 3	Tissue Tissue	(Shi, Yang et al., 2015) (Zhang, Liu et al., 2012)
miR-203	Upregulated Downregulated	China China	22 3	Tissue Tissue	(Shi, Yang et al. 2015) (Zhang, Liu et al., 2012)
Let-7a,7c	Downregulated	China	3	Tissue	(Zhang, Liu et al., 2012)
miR-30b	Downregulated	Germany China	7 22	Tissue	(Gassling, Hampe et al., 2013) (Shi, Yang et al., 2015)
miR-342	Downregulated	Germany	7	Tissue	(Gassling, Hampe et al., 2013)
miR-204	Downregulated	China China	3 9	Tissue Tissue	(Zhang, Liu et al., 2012) (Chen, Du et al., 2017)
miR-200a,b,c	Downregulate	China	3	Tissue	(Zhang, Liu et al., 2012)
miR-205	Downregulated	Germany China	7 9	Tissue Tissue	(Gassling, Hampe et al., 2013) (Chen, Du et al., 2017)
miR-4492	Downregulated	China	9	Tissue	Chen, Du et al., 2017)
miR-4532	Downregulated	China	9	Tissue	Chen, Du et al., 2017)
miR-3960	Downregulated	China	9	Tissue	Chen, Du et al., 2017)
miR-96	Downregulated	China	9	Tissue	Chen, Du et al., 2017)
miR-182	Downregulated	China	9	Tissue	Chen, Du et al., 2017)
miR-152	Downregulated	China	9	Tissue	Chen, Du et al., 2017)
miR-195	Downregulated	China	9	Tissue	Chen, Du et al., 2017)
miR-141	Downregulated	China	9	Tissue	Chen, Du et al., 2017)

miR-3195	Downregulated	China	9	Tissue	Chen, Du et al., 2017)
miR-3196	Downregulated	China	9	Tissue	Chen, Du et al., 2017)
miR-3656	Downregulated	China	9	Tissue	Chen, Du et al., 2017)
miR-5787	Downregulated	China	9	Tissue	Chen, Du et al., 2017)
miR-7977	Downregulated	China	9	Tissue	Chen, Du et al., 2017)
miR-148a	Downregulated	China	9	Tissue	Chen, Du et al., 2017)
miR-187	Downregulated	China	9	Tissue	Chen, Du et al., 2017)
miR-134	Downregulated	China	9	Tissue	Chen, Du et al., 2017)
miR-4497	Downregulated	China	9	Tissue	Chen, Du et al., 2017)
miR-4508	Downregulated	China	9	Tissue	Chen, Du et al., 2017)
miR-944	Downregulated	China	9	Tissue	Chen, Du et al., 2017)
miR-7975	Downregulated	China	9	Tissue	Chen, Du et al., 2017)
miR-23a	Downregulated	China	9	Tissue	Chen, Du et al., 2017)
miR-4516	Downregulated	China	9	Tissue	Chen, Du et al., 2017)
miR-4516	Downregulated	China	9	Tissue	Chen, Du et al., 2017)
miR-202	Downregulated	China	9	Tissue	Chen, Du et al., 2017)
miR-138	Downregulated	China	9	Tissue	Chen, Du et al., 2017)
miR-183	Downregulated	China	9	Tissue	Chen, Du et al., 2017)
miR-365a	Downregulated	China	9	Tissue	Chen, Du et al., 2017)
miR-493	Downregulated	China	9	Tissue	Chen, Du et al., 2017)
miR-193b	Downregulated	China	9	Tissue	Chen, Du et al., 2017)
miR-656	Downregulated	China	9	Tissue	Chen, Du et al., 2017)
miR-664a	Downregulated	China	9	Tissue	Chen, Du et al., 2017)
miR-6510	Downregulated	China	9	Tissue	Chen, Du et al., 2017)
miR-99a	Downregulated	China	9	Tissue	Chen, Du et al., 2017)

miR-199a	Downregulated Downregulated	China China	9 22	Tissue PBMC	Chen, Du et al., 2017) (Wang et al., 2019)
miR-27b	Downregulated	China	9	Tissue	Chen, Du et al., 2017)
miR-148	Downregulated	China	9	Tissue	Chen, Du et al., 2017)
miR-127	Downregulated	China	9	Tissue	Chen, Du et al., 2017)
miR-136	Downregulated	China	9	Tissue	Chen, Du et al., 2017)
miR-376	Downregulated	China	9	Tissue	Chen, Du et al., 2017)
miR-497	Downregulated	China	9	Tissue	Chen, Du et al., 2017)
miR-455	Downregulated	China	9	Tissue	Chen, Du et al., 2017)
miR-27a-b	Downregulated	China	3	Tissue	(Zhang, Liu et al., 2012)
miR-92	Downregulated	China	22	PBMC	(Wang et al., 2019)
miR-564	Downregulated	China	22	PBMC	(Wang et al., 2019)
miR-1304	Downregulated	China	22	PBMC	(Wang et al., 2019)
miR-296	Downregulated	China	22	PBMC	(Wang et al., 2019)
miR-346	Downregulated	China	22	PBMC	(Wang et al., 2019)
miR-19a	Downregulated	China	22	PBMC	(Wang et al., 2019)
miR-122	Downregulated	China	22	PBMC	(Wang et al., 2019)